STABILISING AN ISLANDED NUCLEAR POWER PLANT WITH A HIGH-ENERGY RESISTOR

A DISSERTATION SUBMITTED TO THE FACULTY OF
ENGINEERING AND BUILT ENVIRONMENT OF
THE UNIVERSITY OF CAPE TOWN
IN FULFILMENT OF THE REQUIREMENTS FOR
THE DEGREE OF DOCTOR OF PHILOSOPHY

Peter Lilje October 2009

Supervisor: Prof. A. Petroianu

Dedicated to my wife, Esther and my two boys, Timon and Stefan

List of Contents

Figures

Tables

List of Symbols

Nomenclature

A	Multiplier used in turbine model
$A_g, A_{sat}, B_g, B_{sat}$	Constants used in describing the generator saturation characteristic
a, b, c, d	Constants in Model 2
CVP	Control valve position
e	Stator voltage
e_d, e_q	d- and q-axis components of stator voltage
f_n	Nominal frequency (50 Hz)
E_{fd}	Field voltage (in exciter per unit system)
H	Shaft inertia constant
IVP	Intercept valve position
i	Stator current
i_d, i_q	d- and q-axis components of stator current
i_{fd}	Current in the d-axis rotor winding representing the field winding
i_{1d}, i_{1q}, i_{2q}	Damper winding currents
K_A	Excitation system gain
K_D	Mechanical damping constant
K_e	Stabilising controller gain
K_{sd}, K_{sq}	Saturation constants (average slop of saturation characteristic)
K_{sdi}, K_{sqi}	Saturation constants (slope of saturation characteristic)
K_{vnl}	Incremental slope of the non-linear valve characteristic
K_2, K_3, K_7, K_8, K_9	Constants in Model 2 (which is developed in Chapter 3)
k	Constant in the calculation of the multiplier, A
L_{ad} (X_{ad})	Mutual inductance (reactance) between the d-axis windings (stator and rotor

	windings)
L_{aq} (X_{aq})	Mutual inductance (reactance) between the q-axis windings (stator and rotor windings)
L_{adsi}, L_{aqsi} (X_{adsi}, X_{aqsi})	Incremental mutual inductances (reactances) in d- and q-axis
L_{ads}, L_{aqs} (X_{ads}, X_{aqs})	Saturated mutual inductances (reactances) in d- and q-axis
L_{adu} (X_{adu})	Unsaturated value of d-axis mutual inductance (reactance)
$L_{ffd}, L_{11d}, L_{11q}, L_{22q}$ $(X_{ffd}, X_{11d}, X_{11q}, X_{22q})$	Self-inductances (reactances) of rotor windings
L_l	Leakage inductance of the stator circuits
R_a, R_{fd}	Armature resistance, field resistance
R_E	External resistance of high-energy resistor
R_{1d}, R_{1q}, R_{2q}	Damper winding resistances
r, r_c	Pressure ratio, critical pressure ratio
P_m	Mechanical power
p_{drop}	Pressure drop across the valve at full load with the valve fully open
p_{IP}	Pressure at the inlet to the intermediate-pressure turbine
p_R	Pressure at the reheater outlet
T_e	Electromagnetic torque, i.e. air-gap torque
T_m	Mechanical torque
T'_{do}	d-axis axis open-circuit transient time constant
T''_{do}	d-axis axis open-circuit subtransient time constant
T_{kd}	d-axis damper winding time constant
T'_{qo}	q-axis open-circuit transient time

	constant
T''_{qo}	q-axis open-circuit subtransient time constant
T_A, T_B, T_C	Excitation system time constants
T_3	Field-circuit time constant in seconds
ω	Rotational speed
ω_n	Rated rotational speed
ω_{ref}	Reference speed
X_{Td}, X_{Tq}	Total d- and q-axis reactances
δ_i	Initial internal machine angle
δ	Rotor angle relative to infinite bus
ψ_d, ψ_q	d- and q-axis stator flux linkages
ψ_{ad}, ψ_{aq}	d- and q-axis magnetizing flux linkges
ψ_{fd}	Field flux linkage
$\psi_{1d}, \psi_{1q}, \psi_{2q}$	Flux linkages of rotor circuits
ψ_m	Magnetising flux linkages

Subscripts

In addition to the subscripts used in the above variables, the subscript o is used to denote an initial value.

Operators and transfer functions

j	Complex operators
p	Operator d/dt
s	Laplace operator (complex frequency)
Δ	Small signal
$G_{ex}(s)$	Linear transfer function of excitation system

Acronyms and abbreviations

AGC	Automatic Generation Control
AVR	Arbeitsgemeinschaft Versuchsreaktor
EPRI	Electric Power Research Institute
HTR	High-Temperature Reactor
IEEE	Institute of Electrical and Electronics Engineers
PBMR	Pebble Bed Modular Reactor
PWR	Pressurised Water Reactor
PWRS	Power Systems
SR	Stabilising resistor
SC	Stabilising controller

Chapter 1 Introduction

Humanity is faced with significant challenges with respect to its sources of energy. These challenges include ever increasing demand for electrical power, rising energy costs and the need to protect the environment. The available technologies each have a unique mix of advantages and disadvantages. The technologies may be compared in terms of cost, operating characteristics, effect on the environment, human safety etc. One advantage of nuclear power is the lack of carbon dioxide emissions, and a disadvantage is that the consequences of human error can be extremely severe. Engineers in the nuclear industry constantly seek methods of enhancing the safety of nuclear power plants.

The safety of a conventional nuclear power plant depends on the cooling of its reactor. During normal operation, the energy conversion process removes decay heat[1], and hence cools the reactor. A pressurised water reactor (PWR) has two steam cycles – the first cycle removes heat from the reactor and passes it onto the steam that drives the turbine. In a CANDU reactor there is only one steam cycle. The steam that removes heat from the reactor drives the turbine.

If the generator of a nuclear plant is disconnected from the power system the plant's control system releases control rods into the reactor. These rapidly reduce the rate of nuclear fission and hence the heat produced. The steam flow to the turbine is reduced and diverted to a condenser. Excess heat is dissipated to the atmosphere. It is vital that the plant's cooling water system functions correctly to ensure the continued cooling of the reactor. It is also vital that the steam flow though the turbine reduces rapidly so as to prevent the shaft speed from exceeding its design limits.

[1] Decay heat is the heat released as a result of radioactive decay. The energy of the alpha, beta and gamma radiation is converted into thermal energy - the movement of atoms.

A disconnection of the generator from the power system is initiated by the plant's protection equipment. A disturbance within the power system may be so severe that power plants must be disconnected from the power system to prevent damage. The protection system responds to both failures within the power plant and failures within the power system. Some power plants have the capability of islanding, i.e. reaching a new stable operating point following the disconnection from the power system.

Inserting the control rods into the reactor has an important negative consequence: It leads to a dramatic increase in the concentration of by-products within the reactor, which absorb neutrons. The process is called "reactor poisoning". Xenon 135 is the most important by-product because of its large cross-section for absorbing neutrons. Unless the reactor power can be raised significantly reactor poisoning will lead to an extended shutdown period – possibly some days.

The Pebble Bed Modular Reactor (PBMR) is a nuclear power plant being developed in South Africa. The main advantage of the PBMR over other nuclear plants is its safety – there is no risk of a meltdown, even in the event of a total loss of reactor cooling. It is foreseen that production units will deliver up to 180 MW to the power system (the output of the prototype unit will be lower).

The PBMR thermodynamic cycle is known as the Brayton cycle. Helium gas is heated in the reactor and drives the turbine. During normal operation, power control is achieved through the operation of control valves, which divert the flow of gas past the turbine.

Eskom, the public utility of South Africa and investor in the PBMR development project, requires that the PBMR be capable of islanding. The designers had difficulty in meeting this requirement. They showed that, if the plant was disconnected from the power system, the plant would have to be shut down to prevent the shaft speed from exceeding its maximum allowable limit. The designers exhausted all possibilities to reduce the speed over-shoot (for instance by

maximising the operating rates of the control valves). Despite this, the speed could not be limited below 140 % through the action of the control valves. At such high speeds the centrifugal forces within the rotating components could lead to mechanical failure, i.e. the destruction of the plant and the release of contaminated gas. The speed could only be limited to safe levels through the activation of the shutdown valves. Operation would then be discontinued, i.e. the plant would not island. The levels of Xenon 135 would rise, which would delay a re-start.

The PBMR designers investigated the inclusion of a high-energy resistor in the plant's control devices. When the plant is disconnected from the power system the resistor, hereafter referred to as the stabilising resistor (SR), would be connected to the generator terminals. As long as the SR remains in service the generator develops a braking torque, which opposes an acceleration of the shaft. The author's task was to investigate the feasibility of such a SR. He investigated the construction, layout and costs of high-energy resistors. In this document he investigates the stability of the islanded PBMR plant. He considers the transition of the PBMR plant from normal operation to islanded operation, as well as operation during the islanded period. The investigation includes analyses in the frequency-domain as well as the time-domain. Results obtained from the software package DIgSILENT *PowerFactory* are verified using MATLAB SimPowerSystems.

The author shows that the SR limits the maximum shaft speed, as required. However, depending on the rating of the SR and the turbine characteristics, the plant may become unstable a few seconds after islanding. For these situations, the author proposes that an additional controller is used in conjunction with the SR. The controller is hereafter referred to as the stabilising controller (SC).

The thesis is motivated not only by the PBMR project. The concept of the SR could be applied to conventional nuclear power plants, namely to reduce to risk of a shaft over-speed, to improve the probability of successful islanding, and to reduce reactor poisoning.

Nuclear safety is determined, amongst many other criteria, by the number and reliability of power sources available to supply the cooling water system. If the plant has the capability of islanding then the generator can be counted as one such power source. If the use of a SR improves the islanding performance of a nuclear power plant then this will improve the plant's nuclear safety.

1.1 History of high-temperature reactors[2]

In the 1960s German engineers researched and developed a high-temperature nuclear reactor (HTR) at the Jülich Research Centre in Germany. They subsequently built a prototype reactor, which operated from 1966 to 1988. The reactor generated 40 MW thermal power and 15 MW electrical power. The reactor was decommissioned for political reasons in 1988. By that time all the planned research experiments had been completed. The reactor was called the AVR (Arbeitsgemeinschaft Versuchsreaktor - co-operation prototype reactor).

In conventional nuclear plants the maximum temperature of the reactor has to be limited for safety reasons. If the temperature is too high the fuel produces additional heat, which causes a further increase in temperature. This may lead to a thermal instability, i.e. a meltdown. During operation the energy conversion process removes the decay heat from the reactor. If the reactor is shut down an alternative cooling system removes the heat from the reactor. The failure of that cooling system may lead to a catastrophic nuclear accident.

The main advantage of the AVR prototype reactor is that a core meltdown is not possible. The decay heat produced by the fuel decreased with an increase in temperature. This characteristic is known as the "negative temperature coefficient of reactivity" and prevents the possibility of thermal instability. Achieving the

[2] The information presented in this section is from the PBMR company.

negative temperature characteristic requires that the fuel elements operate at relatively high temperatures. The AVR used spherical fuel elements, which contained the nuclear fuel particles. The nuclear fuel particles were coated with ceramic and graphite.

The inherent nuclear safety of the AVR was demonstrated during a public safety test, when the flow of coolant through the reactor core was stopped. There was no need to insert the control rods to ensure that the reactor would remain in a safe state.

The AVR was used to test different designs of fuel elements, fuel loading systems and safety systems. In spite of the test programmes the AVR produced power for 70% of its life. During its 22 years of operation, the design proved the superior behaviour of the coated particle fuel concept.

The German engineers continued with the construction of a 300 MWe (750 MWt) Thorium High-Temperature Reactor (THTR), which operated between 1985 and 1988. The THTR was a first-of-its-kind production plant intended to demonstrate that its subsystems could be maintained with a reasonable effort and had a high availability. The THTR-300 was intended as the frontrunner of a commercial design, namely the HTR-500.

Based on the experience gained from the AVR and the THTR, ABB (previously Brown Boveri and ASEA) and Siemens developed further HTRs. These two groups later combined to form Hochtemperatur Reaktorbau GmbH.

Prior to the fall of the Berlin wall in 1989 Siemens negotiated orders for several reactors from the then East German government, the USSR and a large German chemical company. After the reunification of East Germany with West Germany all negotiations for the Siemens reactors were discontinued. Siemens subsequently decided to stop further work. At the same time, the West German government came under pressure to close existing nuclear plants. The HTR research reactors were the first to be closed, since these had no significant impact on German power

generation. In the years that followed, the collapse of the USSR and the reunification of Germany placed constraints on the further development of reactors.

1.2 The Pebble Bed Modular Reactor (PBMR)[3]

In the 1990s Eskom, the electricity utility of South Africa, embarked on a project to develop a HTR called the Pebble Bed Modular Reactor (PBMR). Eskom accelerated the development by acquiring the right to access the Siemens HTR engineering database.

The Pebble Bed Modular Reactor (PBMR) is based on the high-temperature reactor technology developed in Germany.

The PBMR differs from previous HTRs in that it uses only one gas cycle. Previous HTRs included a heat exchanger that transferred the energy from the coolant gas to steam, which then powered the turbine. The PBMR eliminates the heat exchanger. The turbine is driven by the reactor coolant gas.

The PBMR plant uses the inert gas helium as a reactor cooling gas. The helium is heated to approximately 900^{o}C in the reactor. The thermodynamic cycle is a closed cycle, known as a Brayton cycle. The plant's turbines operate at a higher temperature than conventional turbines. The PBMR uses turbine technology advances that have been made since the 1980s, namely the increase in temperature that the gas turbine materials can withstand. Eliminating the heat exchanger brings about cost savings and an increase in efficiency.

The PBMR has many advantages compared to conventional power plants. The design of the fuel particles limits the maximum temperature that the fuel can reach so that a meltdown cannot occur. The PBMR plant does not have the emissions

[3] The information presented in this section is from the PBMR company.

problems of fossil fuel fired power plants. By constructing a "demonstration plant" near Cape Town in South Africa, the PBMR investors intend to prove that the plant offers a cost-competitive alternative to other power plants.

In the PBMR plant the flow of gas through the turbine is not controlled through in-line valves, but through by-pass valves. This is due to the unavailability of suitable in-line valves on the market. The control valves and emergency shutdown valves are of the bypass type. The opening of these valves diverts the gas flow away from the turbine.

The designers of the PBMR found that the response of power to a change in control valve position is relatively slow. A sudden loss of electrical load leads to an increase in turbine speed above the tripping value (130%). The turbine protection operates to prevent mechanical damage. It activates emergency shutdown valves, which stops the thermodynamic cycle. To ensure that the PBMR could sustain operation after a disconnection from the power system, the PBMR designers proposed the SR.

The concept of the SR is depicted in Figure 1-1. In the event of a sudden disconnection of the plant from the external power system, the SR is connected to the generator terminals. The number of SR stages that are switched in depends on the power that the generator initially delivered to the power system. The SR power should be a little lower than the produced power, so that some reserve mechanical power is available for speed regulation. For example, the SR rating could be 175 MW, so that 5 MW of reserve power is available if the plant initially delivered 180 MW. The power dissipated by the SR determines the maximum shaft speed. The difference between the initial power and the SR power causes a change in the reactor's operating temperature. Therefore, the SR rating is determined either by the gas temperature or by the maximum speed.

The turbine control system (governor) regulates the shaft speed (and therefore the electrical frequency). The governor would, of course, also act if no SR were

connected to the generator. However, the SR reduces the demand on the mechanical system. The plant continues to operate until it is resynchronised to the network.

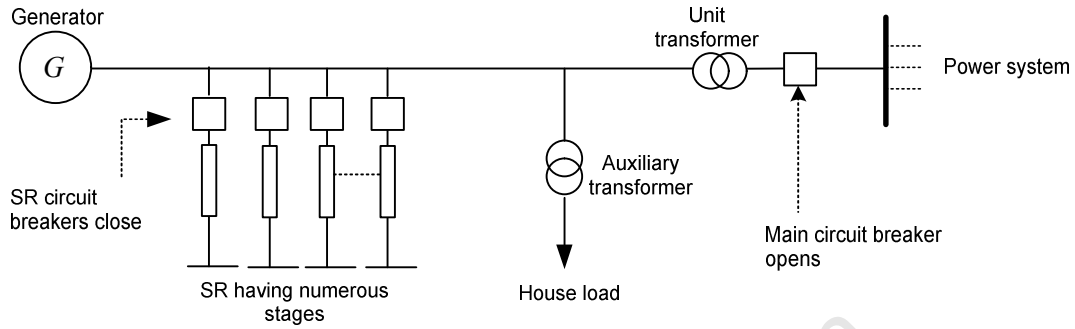

Figure 1-1: Layout of the PBMR plant's electrical system

Medium voltage resistors capable of dissipating hundreds of megawatts are available commercially. PBMR liaised with the Italian company Microelettrica, who proposed a resistor that is constructed of stainless steel elements. The resistor would be cooled by natural airflow. The final rating had not yet been decided at the time of the investigation. A resistor rated at 100 MW (continuous), cooled by natural airflow and constructed of stainless steel elements, occupies a space of approximately 30 m x 30 m x 2½ m. The cost such a resistor, including busbars and circuit breakers, amounts to approximately € 2.5 million.

1.3 Objectives

The goal of this thesis is to investigate the stability of the islanded PBMR power plant. The investigation shall consider the transition to the islanded state as well as operation within the islanded state for a period of up to 20 seconds.

The main objectives of the thesis are as follows:

- to investigate, using both frequency-domain and time-domain techniques, the stability of the islanded plant under small disturbances,
- to investigate, using time-domain techniques, the stability of the plant under large disturbances.

1.4 Methodology

The author investigated the stability of the islanded PBMR plant under both small disturbances and large disturbances. He decided to use both frequency-domain analysis techniques and time-domain analysis techniques, in order to gain a thorough understanding of the plant's stability. He further decided to use two software programmes for simulations to reduce the possibility of calculation errors. Throughout the investigation he researched the topics of stability, control and modelling. Based on this research and on the insight that he gained in the process he modified his models and, where necessary, repeated earlier analyses.

A detailed description of the methodology follows. It refers to Figure 1-2, which represents the structure of the PBMR plant model. The nuclear reactor is excluded from the model, because the author assumes that the gas pressure from the reactor does not vary over the time period investigated.

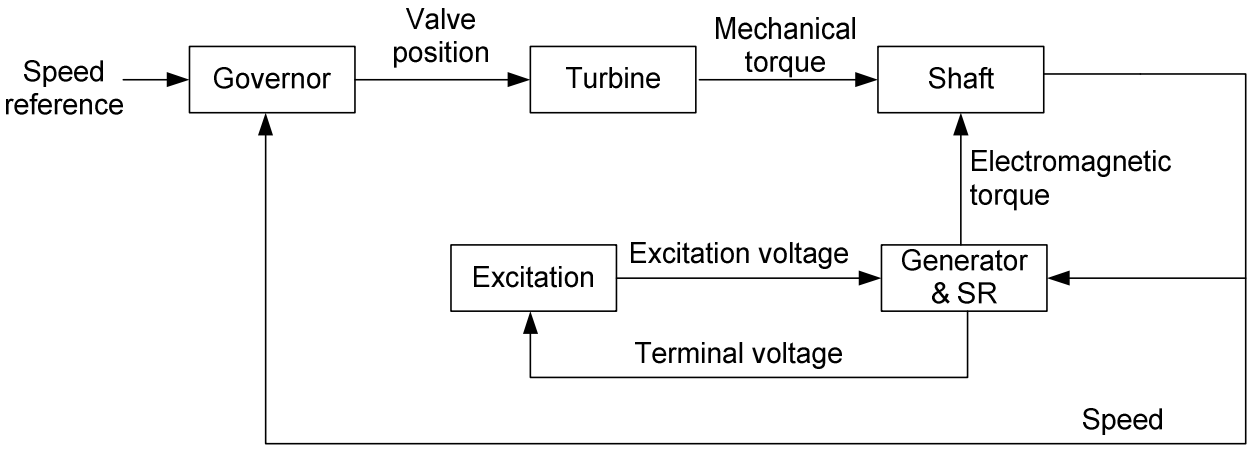

Figure 1-2: Structure of the PBMR plant model

The description of the methodology also refers to Table 1-1, which lists the main steps undertaken by the author. Analyses in the frequency-domain include eigenvalues calculations and the construction of Bode plots. Analyses in the time-domain include numerical integration of differential equations. The disturbances considered in the time-domain analyses are listed in Table 1-2.

Table 1-1: Summary of analyses

Step No.	Step Description	Power System Analysis Software	Notes on model	Finding
1	Response to small disturbances; frequency-domain; neglecting governor and generator	None	Model 1, i.e. constant voltage source and shaft (1st order), and SR	-Unstable -Turbine type has significant effect on damping
2	Response to small disturbances; frequency-domain and time-domain; considering generator and excitation system, neglecting governor and turbine	None	Model 2 - generator including shaft (2nd order), SR, excitation system, but excluding governor and turbine	-Unstable -Turbine type has significant effect on damping -Software packages' models use saturated inductances, not incremental inductances
		DIgSILENT *PowerFactory*	Generator including shaft (6th order), SR and excitation system	
		MATLAB SimPowerSystems	Generator including shaft (8th order), SR and excitation system	
3	Response to small disturbances; frequency-domain and time-domain; considering generator, excitation system, governor and turbine	None	As in Step 2, but including governor and turbine	-Stable, i.e. governor stabilises the plant -Large phase lag due to instability of 'inner loop' -Turbine type has significant effect on damping -Damper windings have no significant effect on damping
		DIgSILENT *PowerFactory*		
		MATLAB SimPowerSystems		

Step No.	Description	Power System Analysis Software	Notes on model	Finding
4	Response to large disturbances; time-domain; considering generator and excitation system, governor and turbine	DIgSILENT *PowerFactory* MATLAB SimPowerSystems	As in Step 2, but including governor and turbine	-Unstable in case of torque machine, stable in case of power machine -Important aspects are SR rating and valve operating rates -Damper windings and initial reactive power have significant effect on stability
5	Response to small disturbances, frequency-domain and time-domain, considering generator and excitation system, governor, turbine and SC	DIgSILENT *PowerFactory* MATLAB SimPowerSystems None	As in Step 2, but including SC	-SC significantly increases damping -SC and governor act in unison
6	Response to large disturbances, time-domain, considering generator and excitation system, governor, turbine and SC	DIgSILENT *PowerFactory* MATLAB SimPowerSystems	As in Step 2, but including governor, turbine and SC	-Stable, even in case of torque machine (due to SC)

Table 1-2: List of simulated disturbances in the analyses of Table 1-1

Step No.	Description	Simulated disturbance in the time-domain analyses
1	Response to small disturbances, frequency-domain , neglecting governor and generator	-Not applicable (no time-domain analyses)
2	Response to small disturbances; frequency-domain and time-domain; considering generator and excitation system, neglecting governor and turbine	-Temporary torque disturbance of 0.05 p.u., 0.10 s -Constant torque disturbance of 0.01 p.u.
3	Response to small disturbances, frequency-domain and time-domain, considering generator, excitation system, governor and turbine	- Step changes in speed reference of 0.002 p.u. -Change in active power of 2 MW
4	Response to large disturbances, time-domain, considering generator and excitation system, governor and turbine	-Short-circuit at the plant's high-voltage terminals, followed after 120 ms by the disconnection of plant from power system and, after 80 ms, by the connection of a 175 MW SR (the plant initially operates at 180 MW, 0.9 power factor leading) -The same initial conditions and fault, but the connection of an 85 MW SR instead of an 175 MW SR
5	Response to small disturbances, frequency-domain and time-domain, considering generator and excitation system, governor, turbine and SC	-As in (3)
6	Response to large disturbances, time-domain, considering generator and excitation system, governor, turbine and SC	-As in (4)

In Step 1 the author investigates the stability of the plant without governor under small disturbances. This system may also be referred to as the 'inner loop'. He used the model structure shown in Figure 1-3. He excludes the characteristics of the

excitation system and dynamics of the generator, i.e. he assumes that the generator behaves as a constant voltage source. He models the SR as a constant resistance.

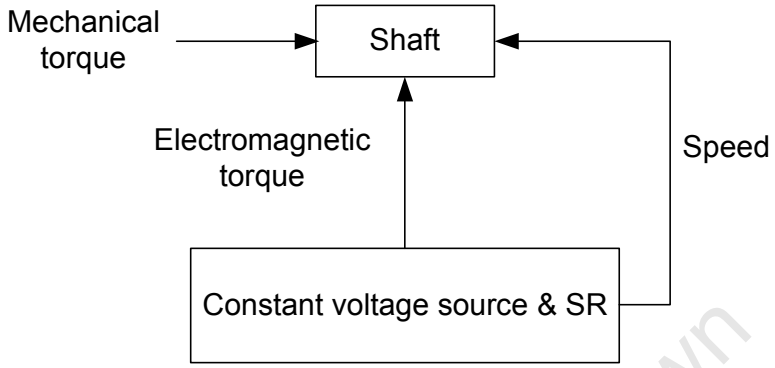

Figure 1-3: Structure of model used in Step 1

The author developed a transfer function for the relationship between shaft speed and mechanical torque. The transfer function has a positive real pole, hence the author concluded that the inner-loop is unstable – an increase in speed leads to a decrease in electromagnetic torque, which causes a further increase in speed. Likewise, a decrease in speed leads to an increase in electromagnetic torque. Unlike the electrical system of a normal power system the electrical system investigated in here does not have a self-regulating characteristic, i.e. the load power does not vary with frequency. For a constant generator terminal voltage the power is constant.

In later analyses the author considers the variation of mechanical torque due to the action of the governor. Before continuing with such analyses he questioned whether the mechanical torque could vary in response to speed changes without any governor action. The 'natural' relationship between a turbine's mechanical torque and speed refers to the relationship between torque and speed under constant gas pressure and valve positions. It is not clear from the literature what the true characteristics of this natural relationship are, especially with respect to speed excursions beyond ±5 %. Experts implicitly assume one of two characteristics: either the mechanical torque is independent of speed or the mechanical power is independent of speed. The author introduces the terms 'torque machine' and 'power machine' to distinguish between

two characteristics. He considers both turbine types in his investigation. This topic is discussed in more detail in Chapter 2.

The finding that the inner loop is unstable is based on the assumption that the turbine is a torque machine. In Step 1 the author also considers the case of a power machine. He finds that, if mechanical torque varies with speed as it does in a power machine, the system is on the verge of instability. A power machine has a stabilising characteristic: An increase (decrease) in shaft speed leads to a decrease (increase) in mechanical torque. This characteristic could be termed a mechanical self-regulating characteristic.

For subsequent analyses the author needed models of the generator, excitation system, turbine and governor. He used the software packages DIgSILENT *PowerFactory* and MATLAB SimPowerSystems, which both have built-in synchronous machine models. He implemented models for the excitation system, turbine and governor, and linked these to the built-in synchronous machine models.

The author used the same models for analyses in the time-domain and frequency-domain. The two software packages include functions for the calculation of eigenvalues. These functions use numerical techniques to linearise models. The author also linearised the model of the PBMR plant analytically. He calls the linearised model 'Model 2'. Model 2 includes the equations for the generator, excitation system, turbine and governor. The author used Model 2 for special investigations described below, which cannot be done using the software packages' generator models. Some additional comments on various models follow before continuing the discussion of Step 2.

The built-in synchronous machine models of DIgSILENT *PowerFactory* and MATLAB SimPowerSystems are of 8th order (one differential equation for the field winding, one for the damper winding in the d-axis, two for the damper windings in

the q-axis, two for the stator flux transients and two for the shaft[4]). In DIgSILENT *PowerFactory* the model is reduced automatically to 6th-order (by neglecting the stator flux transients) if the user performs eigenvalues calculations or if he executes a time-domain simulation of the 'RMS' type. The generator model within Model 2 is of 2nd-order – it includes the differential equations representing the shaft dynamics and field-winding dynamics, but not those of the damper windings and transformer voltage terms. The generator models of both software packages, as well as the generator model developed by the author, include core saturation. The modelling parameters were obtained from MITSUBISHI, the company that designed PBMR's generator.

The author derived a model of PBMR's static excitation system using the recommendations of IEEE [17]. He used typical parameters, as defined in the literature [24], since the final parameters for the PBMR plant were not yet available.

At the time of investigating the SR the PBMR turbine model was at an early stage of development and no proper documentation was available for it. The PBMR plant is neither a conventional steam turbine nor a conventional gas turbine. The author chose to use turbine and governor models of a conventional steam turbine and governor. This decision is supported by the author's view that the concept of the SR may also be applied to a conventional nuclear plant. The turbine and governor models are taken from IEEE [21]. The author obtained typical model parameters from the literature [24].

The author did not model the house-load separately. The power consumed by the house-load is only about 2 % of the generator rating.

In Step 2, the author continues the investigation into the stability of the plant without governor (i.e. the inner loop) under small disturbances. He uses the model

[4] The models of both software programmes include two states for the shaft, namely speed and load angle.

structure shown in Figure 1-4. The model includes the characteristics of the generator, excitation system, turbine and governor, as described above. The author confirms, by means of eigenvalue calculations, that the plant without governor is unstable and that the turbine type has a significant effect on the damping.

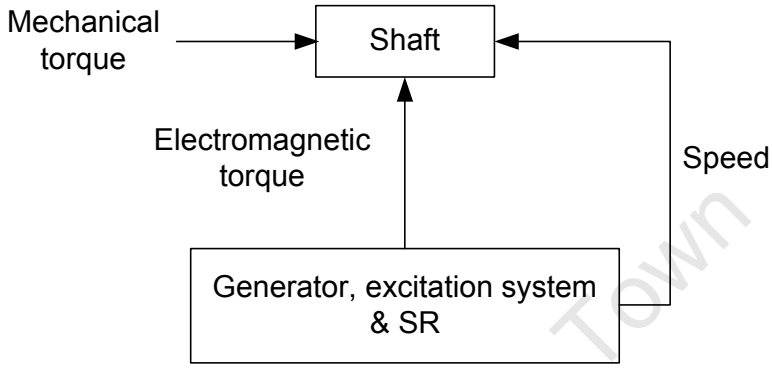

Figure 1-4: Structure of model used in Step 2

The eigenvalues of Model 2 (i.e. the analytically linearised model) differ significantly from the eigenvalues of the models implemented in the software programmes (i.e. the numerically linearised models). The author found the reason for the difference to lie in the method of modelling the magnetising inductances. The linearised models from the software packages are based on 'saturated inductances', whereas Model 2 is based on 'incremental inductances' (these terms are explained in Chapter 2). The method of modelling saturation may be important, since there is no significant damping from the damper windings. The author confirmed the instability by means of time-domain analyses.

In Step 3 the author investigates the stability of the plant (including governor) under small disturbances. He uses the model structure shown in Figure 1-2. He does analyses in the frequency-domain using the linearised models from the software packages as well as Model 2. In addition, he does analyses in the time-domain using the software packages – he simulates a change in the speed reference of 0.2 %. Such a change in speed reference could occur prior to re-synchronisation. He also

investigates the response of the plant to a 2 MW change in active power. Such a change in power could be due to switching within the house-load.

There is close agreement between the results from the two software packages and the hand-calculations. The results of all analyses show that the system is stable with respect to small disturbances, irrespective of the turbine type (power machine or torque machine). Therefore, the governor overcomes the instability of the inner loop. The turbine type has a significant effect on the system's damping. The method of modelling magnetising inductances (saturated or incremental) has no significant effect on the system's damping. The damper windings decrease the damping, but the decrease is not significant.

In Step 4 the author simulates a disturbance and the subsequent islanding of the power plant. He selected the disturbance to be a three-phase fault at the high-voltage side of the transformer. Such a fault represents a severe condition, since no power is exported to the grid during the fault.

The author uses the two software packages to investigate the stability of the plant under large disturbances. He uses the model structure shown in Figure 1-5. He simulates the plant's response to the following events: A short-circuit on the high-voltage side of the transformer at time 0 s, the disconnection of the plant from the power system at time 120 ms, and the connection of the SR at time 200 ms. The author considers both a 175 MW SR and an 85 MW SR. He investigates the effect of the level of reactive power prior to the disconnection from the power system, the effect of the damper windings, and the effect of the valve opening rate.

The author finds that a SR rating of 175 MW limits the maximum speed to 112 %, whereas a rating of 85 MW SR limits the maximum speed to 130 %. He concludes that the SR rating should be in the range 85-175 MW, and considers both ratings in all further analyses (he also returns to previous analyses and repeats them for both SR ratings). The author also finds that the highest speed occurs if the generator is initially under-excited.

From the time-domain analyses the author finds that the plant with the 175 MW SR is unstable. He finds that the instability is due to the destabilising relationship between electromagnetic torque and shaft speed (as observed in Steps 1 and 2).

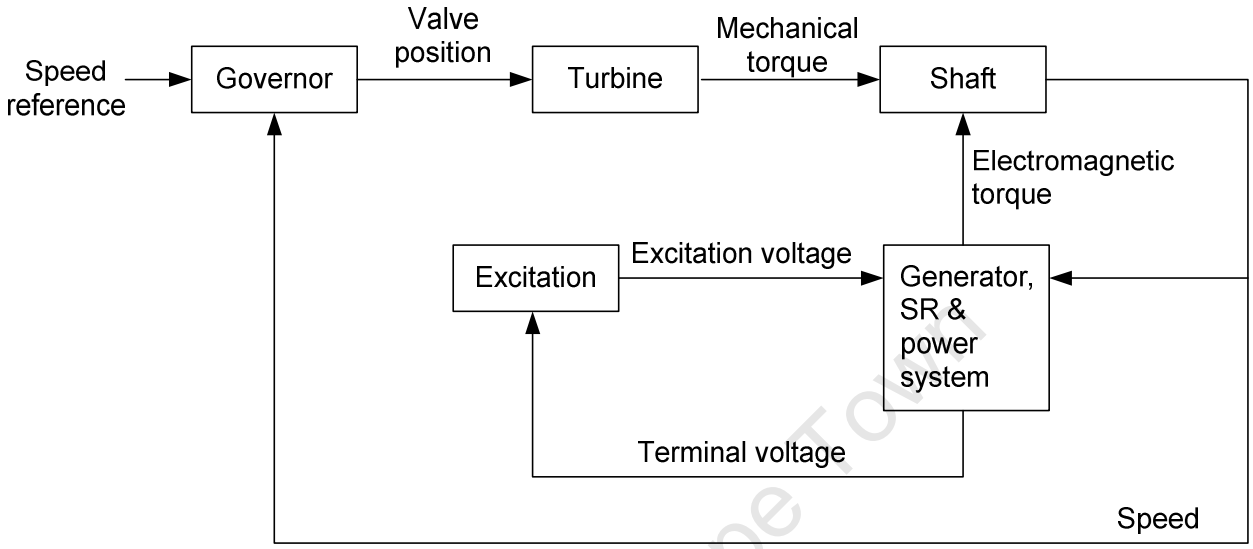

Figure 1-5: Structure of model used in Step 4

The author proposes a stabilising controller (SC) to improve the plant's stability, especially the stability under large disturbances. The SC changes the excitation in response to speed changes, similarly to a power system stabiliser (PSS). The change in excitation causes a change in terminal voltage, which causes a change in power and hence a change in electromagnetic torque. The change in torque is such as to oppose the change in speed. The SC differs from a conventional PSS in its purpose. A PSS improves the rotor-angle stability of a generator in a multi-machine power system, and the SC improves the frequency stability of a single, islanded generator.

In Step 5 the author investigates the stability of the plant, including the SC, under small disturbances. He uses the model structure shown in Figure 1-6. The author shows, by means of analyses in the frequency-domain and the time-domain, that the SC significantly improves the system's damping.

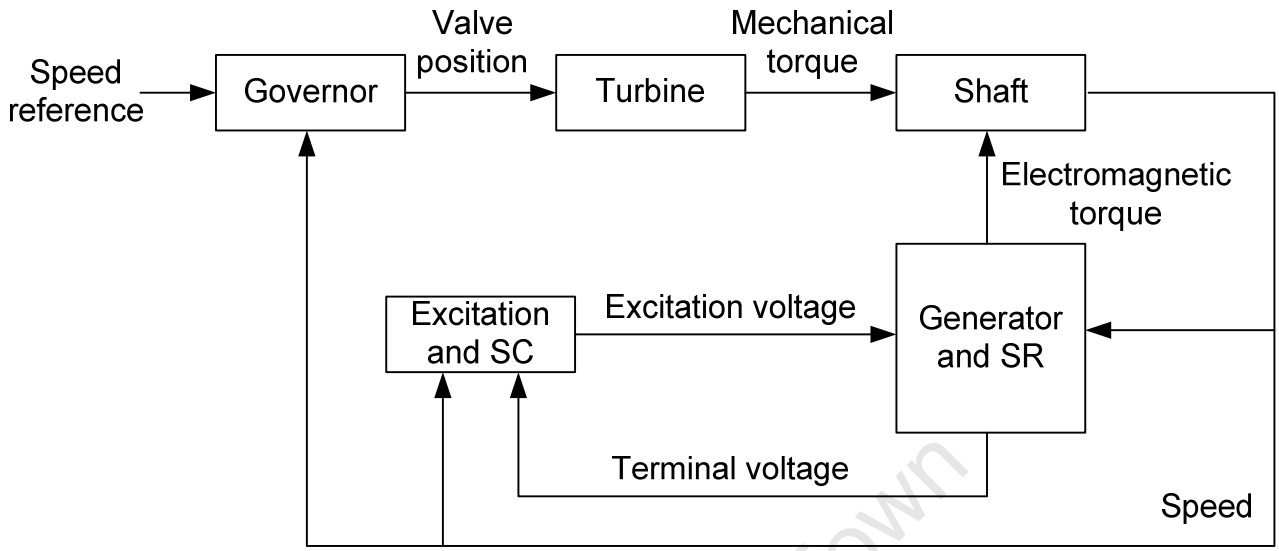

Figure 1-6: Structure of model used in Step 5

In Step 6 the author repeats the investigation into the stability of the complete plant, including the SC, under large disturbances. He uses the model structure shown in Figure 1-7. He finds that the PBMR plant remains stable, i.e. the SC supplements the SR and improves the plant's stability.

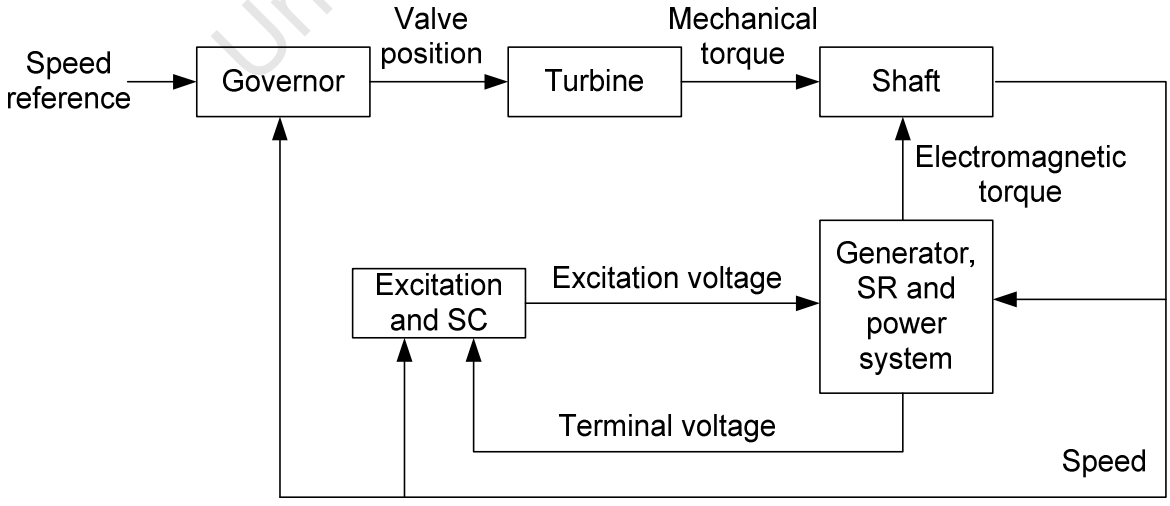

Figure 1-7: Structure of model used in Step 6

1.5 Document overview

Chapter 2 provides on overview of the literature that is relevant to this thesis. Models of the main components of the PBMR plant are discussed.

Chapter 3 discusses the implementation of the PBMR model in the software packages DIgSILENT *PowerFactory* and MATLAB SimPowerSystems. The chapter includes the derivation of Model 1, as well as a summary of the derivation of Model 2 (the full derivation of Model 2 is contained in an appendix).

Chapter 4 contains the stability analyses of the PBMR plant under small disturbances, i.e. Steps 1-3 and 5 in Table 1-1. The analyses are done in both the frequency-domain and the time-domain. The author explains the instability of the inner loop. He shows that the governor stabilises the plant. He also shows how the plant's stability improves due to the SC.

Chapter 5 contains the stability analyses of the PBMR plant under large disturbances, i.e. Steps 4 and 6 in Table 1-1. The analyses are done in the time-domain. The author shows that the SR limits the shaft speed below the tripping value, but that the plant may become unstable depending on certain factors (such as the SR rating). He shows that additional control, in the form of the SC, ensures that the plant remains stable following the connection of the SR.

Chapter 6 contains the conclusions of the thesis. It summarises the contributions made by the author and makes recommendations about further research.

Appendix A contains the modelling parameters used in the calculations. Appendix B contains the full derivation of Model 2. Appendix C and Appendix D contain the block diagrams of the models used in MATLAB SimPowerSystems and DIgSILENT *PowerFactory*. Brief descriptions of the block diagrams are included.

Appendix E and F contain simulation results, which are referenced in Chapters 4 and 5.

Chapter 2 Literature review

This chapter includes a definition of power system stability, and its categorisation into rotor-angle stability, frequency stability and voltage stability. Even though this thesis is about frequency stability this chapter cites some references related to rotor-angle stability. This is because the author applied techniques commonly used in the assessment and enhancement of rotor-angle stability. Chapter 3 cites the literature relevant to the modelling of power plant components. It covers the special modelling topics of turbine type (torque machine and power machine) and generator magnetising inductances (saturated and incremental).

2.1 Power system stability

The IEEE [12] defines power system stability as the ability of an electric power system, for a given initial operating condition, to regain a state of equilibrium after being subjected to physical disturbances, with most system variables bounded so that practically the entire system remains intact. Classifying stability into categories facilitates its understanding. The IEEE proposes a classification of power system stability based on the following considerations:

a. the physical nature of the resulting mode of instability as indicated by the main system variable in which instability can be observed;

b. the size of the disturbance considered, which influences the method of calculation and prediction of stability; and

c. the devices, processes, and the time span that must be taken into consideration in order to assess stability.

The categories (and subcategories) of power system stability are shown in Figure 2-1.

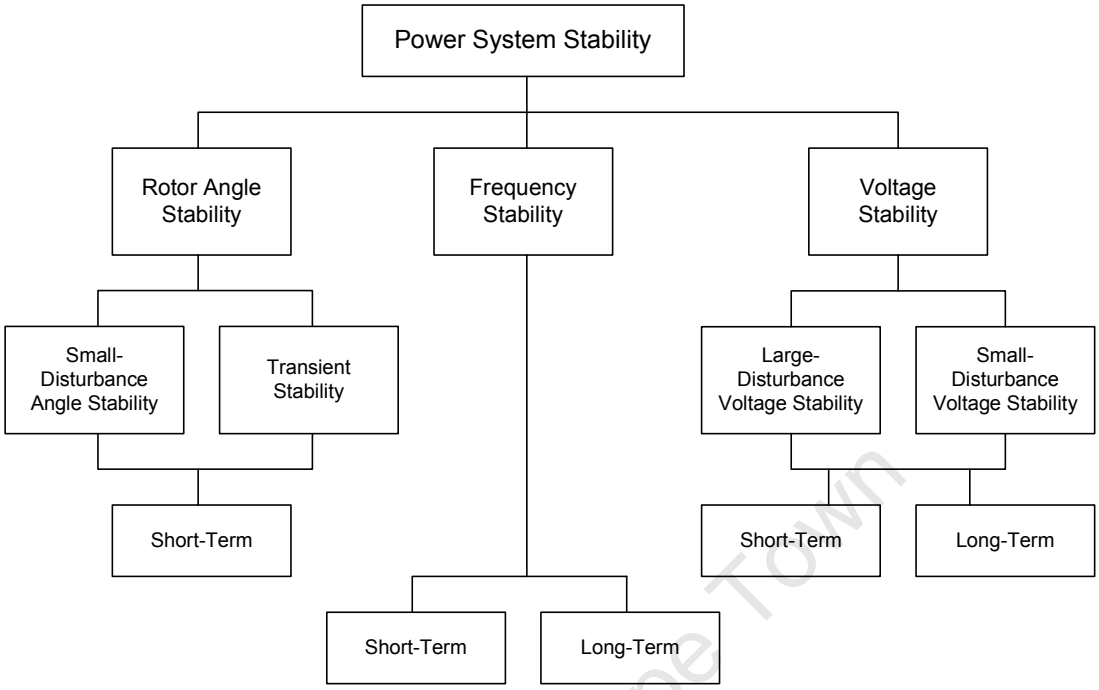

Figure 2-1: Classification of power system stability

"Rotor Angle Stability" refers to the ability of synchronous machines of an interconnected power system to remain in synchronism after being subjected to a disturbance. It reflects the ability of each synchronous machine in the system to maintain or restore equilibrium between electromagnetic torque and mechanical torque. Instability occurs in the form of increasing angular swings of some generators leading to their loss of synchronism with other generators.

The sub-category "Small-disturbance rotor angle stability" (or "small-signal rotor angle stability") is the ability of the power system to maintain synchronism under small disturbances. The disturbances are sufficiently small so that linearising the system equations is permissible for purposes of analysis. The time frame of interest is usually in the order of 10 to 20 seconds following the disturbance.

The sub-category "Large-disturbance rotor angle stability" (or "transient stability") is the ability of the power system to remain in synchronism when subjected to a severe disturbance. The resulting system response involves large excursions of generator

rotor angles and is described by the non-linear power-angle relationship. The time frame of interest is usually 3 to 5 seconds following the disturbance. For the investigation of power system stability under large disturbances the non-linear relationships between variables cannot be neglected - linearising is not acceptable.

"Frequency stability" refers to the ability of a power system to maintain steady frequency following a severe system disturbance, which results in a significant imbalance between generation and load. It reflects the power system's ability to maintain or restore equilibrium between system generation and load. Instability occurs in the form of sustained frequency swings leading to tripping of generating units and/or loads. The characteristic times of the processes and devices that are activated during frequency excursions will range from fractions of seconds to several minutes. Frequency stability may thus be a short-term or a long-term phenomenon.

"Voltage stability" refers to the ability of a power system to maintain steady voltages at all buses in the system after being subjected to a disturbance. It reflects the power system's ability to maintain/restore equilibrium between reactive load demand and supply in the power system. Instability occurs in the form of a progressive fall or rise of voltages of some buses.

The sub-category "Large-disturbance voltage stability" refers to the system's ability to maintain steady voltages following large disturbances such as system faults, loss of generation or circuit contingencies.

The sub-category "Small-disturbance voltage stability" refers to the system's ability to maintain steady voltages when subjected to small perturbations such as incremental changes in system load.

In voltage stability of the study period of interest may extend from a few seconds to tens of minutes. Therefore voltage stability may either be a short-term or a long-term phenomenon.

The analyses in this thesis show that shaft speed is the main variable in which instability can be observed. The author investigates the response of the PBMR plant

to both small and large disturbances. He studies the plant's stability for up to 20 s after a disturbance. Therefore, this thesis is about the short-term frequency stability of the islanded PBMR plant.

2.1.1 Rotor angle stability

The following sections cover the topic of rotor angle stability under small disturbances and large disturbances.

2.1.1.1 Rotor angle stability under small disturbances

Stability with respect to small disturbances can be assessed from the roots of a model's characteristic equation, i.e. the eigenvalues of the models' state matrix [1, 24]. The calculation of eigenvalues requires that the model be approximated by a set of linear differential equations. Therefore, the equations of the power system are linearised at a chosen operating point, i.e. the set of non-linear differential equations is approximated by a set of linear differential equations.

The stability of the system can be assessed from the following criteria:

- When the eigenvalues have negative real parts, the system is asymptotically stable, i.e. when subjected to a small disturbance about an equilibrium point it remains within a small region surrounding the equilibrium point and returns to the state as time increases.

- When at least one of the eigenvalues has a positive real part, the system is unstable.

- When the eigenvalues have real parts equal to zero, it is not possible to say whether the system is stable or unstable.

- Real eigenvalues indicate non-oscillatory modes of response. A positive real eigenvalue indicates aperiodic instability, whilst a negative real eigenvalue indicates decaying modes. Complex eigenvalues occur as conjugate pairs. Each pair corresponds to an oscillatory mode [30].

Engineers use linear power system models to calculate eigenvalues. They make use of software packages, which derive linear models numerically. Before such software packages were available engineers developed linear models analytically [7, 23, 24]. Kundur presents the derivation of a linear model of a single machine-infinite bus. The author adapted and applied the procedure to derive a linear model of the PBMR plant. He used the linear model not to assess rotor angle stability, but frequency stability. He refers to the model as Model 2.

2.1.1.1.1 Power system stabiliser

A power system stabiliser (PSS) is an effective means of increasing the damping of small-signal oscillations. It is an additional control loop that responds to rotor speed oscillations and modulates the output of the excitation system [1, 24]. The inputs to the stabiliser are normally rotor speed, generator output power, frequency, or a combination of these signals. The output is normally added to the voltage reference of the excitation system. A PSS typically responds to frequencies in the range 0.1 – 3 Hz. The result is a variation in the generator's electrical torque, which dampens the oscillation.

The author proposes SC, which is similar to a conventional PSS. The SC responds to speed deviations. Its output is added to the voltage reference of the excitation system. Whereas a PSS improves the rotor angle stability of a machine connected to a multi-machine power system, the SC improves the frequency stability of a single machine that is islanded from the power system. The SC responds to frequencies lower than 0.1 Hz.

2.1.1.2 Rotor angle stability under large disturbances (transient stability)

Engineers typically use time-domain simulation in order to assess the transient stability of a power system. In time-domain simulation, the non-linear system equations are solved using numerical integration techniques. The models of the power system elements include the non-linear characteristics that are relevant for the analysis. Examples of such non-linear characteristics are generator saturation,

the relationship between steam valve position and flow area, the limitation of signals within control systems.

The author uses time-domain simulation to assess the frequency stability of the islanded PBMR plant. His models include non-linear characteristics such as turbine valves and saturation.

2.1.1.2.1 Turbine fast-valving

A severe fault in a power system may cause a generator, or a group of generators, to accelerate with respect to the remaining power system. The increase in load angle of the generator, or group of generators, may be such that the generator(s) become(s) unstable. A fast reduction in the mechanical power reduces the acceleration of the shaft. The fast reduction in mechanical power is achieved using the technique of fast-valving. This technique refers to the activation of a special closing mechanism, which leads to significantly shorter closing times than normal closing times. The intermediate- and low-pressure turbine sections typically produce 70% of the total turbine power. Hence fast-valving technology is normally applied to the intercept valves, which control the steam flow to the intermediate- and low-pressure turbine sections. Complete valve closure may be achieved in 0.08 to 0.4s. Compared to generator-tripping (see paragraph 2.1.1.2.3), fast-valving has the advantage that the generators remain connected to the power system. The literature reports on the experience of turbine fast-valving [20, 25, 26, 27].

Fast-valving is not the topic of this thesis. The author studied the turbine models used in fast-valving investigations. Kundur used turbine models having the structure recommended by the IEEE [21], but differing in two respects: He used higher valve closing rates and he considered the effects of valve choking[5]. In Chapter 3 the author shows how he included the effects of valve choking into the turbine model used in his investigations.

[5] Valve choking refers to a limitation in flow through a valve if a high pressure ratio exists across the valve.

2.1.1.2.2 Dynamic braking

Dynamic braking refers to the insertion of a load that dissipates active power during a transient. The load replaces some of the load that has been 'lost' to the generators as a result of the fault. Dynamic braking limits the acceleration of the generators. Dynamic braking has to date been applied only to hydraulic machines [5, 10, 18, 32].

Reference [32] presents an application of dynamic braking at the Bonneville Power Administration's Chief Joseph Substation. A 1400 MW, 230 kV resistor is connected to the transmission system. The paper presents the need for and the benefits of dynamic braking. The control system and the resistor's physical and electrical properties are described. Phase-plane diagrams are used to derive a suitable switching strategy for the case of a single-machine infinite-bus system. The resistor switch is closed in the event of a sudden power decrease and a simultaneous decrease in bus voltage. The resistor remains connected for a fixed time of half a second.

Ellis studied various means of improving the transient stability of the Peace River 500 kV transmission system [10]. The means included the application of series compensation of transmission lines, reducing transformer reactances, increasing machine inertias, reducing generator reactances, increasing exciter ceiling voltages, and utilising dynamic braking. A dynamic brake, rated at 600 MW, 138kV offered the most effective single means of improving transient stability. The authors considered different loading conditions, resistor ratings and switching times.

Dynamic braking appears to be directly relevant to the topic of this thesis, since it is about the connection of a high-power resistor to a power plant. However, the author did not apply the knowledge of dynamic braking in his investigations. The control systems used in dynamic braking are not applicable, since they are designed to improve rotor angle stability and not frequency stability. The resistor technology is not applicable, since dynamic braking resistors dissipate very little energy compared to the SR.

2.1.1.2.3 Generator disconnection

References [3] and [27] provide information on the experience of generator tripping as a means of improving transient stability. The disconnection of generators following a fault reduces the accelerating power. The reduction in accelerating power limits the increase in load angle. Since generating units can be tripped rapidly, generator disconnection is a very effective means of improving transient stability.

The disconnected generators may be shut down and restarted or, if they have the capability, they may be tripped to house-load. As discussed in 2.2, full power is restored more quickly if the machines are islanded (i.e. tripped to house-load) rather than shut down. Both options cause thermal stress of the mechanical plant, including shaft fatigue. Power plant islanding is discussed in section 2.2.

2.1.2 Frequency stability

Kundur discusses the theory of frequency stability [24]. He focuses on the determination of steady-state frequency. The steady-state frequency is determined by the characteristics of the load, the governors and the Automatic Generation Control system (AGC).

Power system loads include a variety of electrical devices. The electrical power of some loads, such as lighting and heating loads, does not vary with frequency. The electrical power of motor loads does vary with frequency. The variation of the total load with frequency gives the power system a self-regulating characteristic – the electrical power of the load decreases (increases) with a decrease (increase) in frequency. The load's frequency-dependence dampens the response of frequency to disturbances. Typical values are 1 – 2 %, i.e. a 1 % change in frequency leads to a 1 – 2% change in load.

A power plant that supplies an isolated load may have an isochronous governor. This governor controls the frequency to a reference value, e.g. nominal frequency.

Kundur presents linear models of governors (first-order) and turbines (first-order and second-order). He uses a first-order model for the remainder of the power system. He represents the electrical system (generation and load) by a constant.

The author uses linear models to investigate the frequency stability of the islanded PBMR plant. He includes detailed models of the electrical system. This allows him to investigate the importance of saturation modelling, the effect of the damper windings, the effect of the house-load and the interaction between the governor and the SC.

Anderson [1] also uses linear models to investigate frequency stability. His models include the generator (first-order) and excitation system (first-order) in addition to the turbine and governor (together first-order). He does categorise stability into frequency stability and rotor-angle stability.

2.2 Power plant islanding

Major power system disturbances can cause power systems to break up into islands. A special case of islanding is 'unit islanding', also referred to as 'trip to house-load'. This refers to the continued operation of a power plant following its disconnection from the power system. The disconnection from the power system is initiated by the plant's protection systems. It occurs to prevent a shutdown as a result of voltage and frequency excursions. To be capable of unit islanding the power plant needs to reduce its output power quickly and to sustain operation at the reduced output power [34].

The IEEE provides guidelines for enhancing the response of thermal power plants to partial load rejections [19]. In summary, these guidelines comprise:

1. the ability to quickly reduce turbine input power (using, for example, steam bypass systems);

2. the ability to limit turbine speed below the trip level, and the ability of the over-speed controls to discriminate between load rejections and transient system disturbances such as transmission line faults; and

3. the ability of vital auxiliaries to continue operation in spite of voltage and frequency variations experienced during partial load rejections.

The capability of unit islanding is specified as a requirement in many grid codes [6, 29, 33] and is sometimes categorised as an ancillary service. The grid codes typically require that power plant be capable of islanding for up to 2 hours. The Czech Grid Code emphasises the high demands that islanding has on a unit's regulation capabilities. Power plant designers pay special attention to ensure that power plants can reduce active power output quickly and sustain operation thereafter.

2.3 High-power resistors

Section 1.2 provides some basic characteristics of the high-energy resistor designed for the PBMR company by Microelettrica.

The company Avron[6] in the United States markets forced air-cooled resistors. Resistors are used for dynamic braking of cranes and locomotives, to load emergency diesel generators and uninterruptible power supplies etc. The resistor elements are made from a Nickel Chrome alloy. Resistor banks are made up of modules, each dissipating up to 7 MW. The banks do not include transformers – they are designed to operate either at low voltage (e.g. 400 V) or medium voltage, (e.g. 11 kV or 13.8

[6] The information about the company's products was obtained from the internet, http://www.avtron.com.

kV). The banks can be constructed to dissipate hundreds of megawatts on a continuous basis.

Section 2.1.1.2.2 discusses the application of a resistor to improve the transient stability of a group of generators in a power system. In this example of dynamic braking the resistor operates at high-voltage, i.e. the voltage of the transmission system. The resistor is large (physically) due to insulation requirements.

EPRI studied the feasibility of a resistor as a means of damping shaft torsional oscillations [11]. Such damping is especially important in series compensated transmission systems, where subsynchronous resonance phenomena occur. EPRI's report studies braking resistors rated at up to 850 MW (and less than 30 kV). The resistors are connected and disconnected using bang-bang control for a period of up to 2 seconds. The report cites a resistor used in the "Magnetohydrodynamic High Enthalpy Demonstration Experiment" by the Arnold Air Development Centre. The resistor, which has been decommissioned due to the completion of the experiment, was capable of dissipating 25 MW for up to 30 seconds. The brake occupied a space of 56 m^2. It consisted of stainless electrodes immersed in untreated water to a depth of 0.90 m.

2.4 Modelling

This section presents the models of the following power plant components: synchronous machine (or generator), excitation system, turbine, governor and shaft.

The section on the synchronous machine includes the topic of saturation modelling, and specifically the difference between saturated inductances and incremental inductances.

The section on the turbine defines the terms "torque machine" and "power machine", as mentioned in Chapter 1.

2.4.1 Synchronous machine

The generator of the PBMR plant is a round rotor synchronous machine, rated at 180 MW, 13.2 kV.

The mathematical modelling of synchronous machines is discussed in an IEEE guide [13] as well as numerous textbooks, e.g. [1, 23, 24]. The model equations contain inductance terms that depend on the angle of the rotor with respect to the stationary reference frame. Since the angle varies with time, these inductance terms vary with time. The resulting set of equations is difficult to solve. To simplify the machine equations, the stator equations are written in a rotating reference frame, called the 'dq0 reference frame'. In this reference frame, the mathematical equations have constant inductances.

A commonly used model includes equations representing the field winding, one damper winding in the d-axis and one damper winding in the q-axis. The IEEE labels a model "Model 2.1". Such a model is represented by the following equations (equations in the zero sequence are not shown, since these are only required in the study of unbalanced operation):

$$\begin{aligned} e_d &= p\psi_d - \psi_q\omega - R_a i_d \\ e_q &= p\psi_q + \psi_d\omega - R_a i_q \end{aligned} \tag{2.1}$$

$$\begin{aligned} \psi_d &= -(L_{ad} + L_l)i_d + L_{ad}i_{fd} + L_{ad}i_{1d} \\ \psi_q &= -(L_{aq} + L_l)i_q + L_{aq}i_{1q} + L_{aq}i_{2g} \\ \psi_{fd} &= L_{ffd}i_{fd} + L_{f1d}i_{1d} - L_{ad}i_d \\ \psi_{1d} &= L_{f1d}i_{fd} + L_{11d}i_{1d} - L_{ad}i_d \\ \psi_{1q} &= L_{11q}i_{1q} + L_{aq}i_{2q} - L_{aq}i_q \\ \psi_{2q} &= L_{aq}i_{1q} + L_{22q}i_{2q} - L_{aq}i_q \end{aligned} \tag{2.2}$$

$$E_{fd} = \left[\frac{1}{\omega_n} \cdot \frac{d\psi_{fd}}{dt} + \omega_n R_{fd} i_{fd} \right] \cdot \frac{L_{adu}}{R_{fd}}$$

$$\begin{aligned} 0 &= p\psi_{1d} + R_{1d} i_{1d} \\ 0 &= p\psi_{1q} + R_{1q} i_{1q} \\ 0 &= p\psi_{2q} + R_{2q} i_{2q} \end{aligned} \tag{2.3}$$

$$T_e = \psi_{ad} \cdot i_q - \psi_{aq} \cdot i_d \tag{2.4}$$

$$2H \cdot \frac{d\omega}{dt} + K_D w = T_m - T_e \tag{2.5}$$

where the symbols are defined in the section titled 'List of Symbols'.

'Standard parameters' are defined in the literature, which describe the effective reactances as seen from the terminals of the machine during sustained, transient and subtransient conditions. The standard parameters also include time constants, which describe the rate of decay of voltages and currents. Manufacturers typically specify the characteristics of the machine in terms of the standard parameters $X_d, X'_d, X''_d, X_q, X'_q, X''_q, X_l, T'_{do}, T''_{do}, T'_{qo}, T''_{qo}$ and R_a. The resistances and inductances in (2.1) to (2.3) are calculated from these parameters.

The parameters L_{ad} and L_{aq} vary with the level of magnetic saturation in the synchronous generator. Figure 2-2 shows the open-circuit saturation characteristic of a synchronous generator.

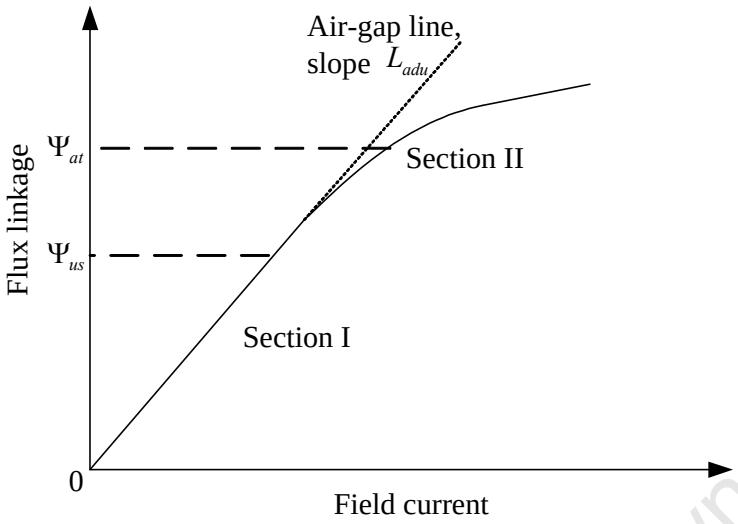

Ψ_{at} Flux linkage ψ_d with the generator in open circuit

Ψ_{us} Flux linkage in the linear (unsaturated) section I

L_{adu} Unsaturated value of L_{ad} , i.e. slope in section I

Figure 2-2: Saturation characteristic

The saturation characteristic consists of an (approximately) linear section I and a non-linear section II. In section I L_{ad} is given by its unsaturated value L_{adu}. A variety of equations can be used to represent L_{ad} in the non-linear section II. For example L_{ad} can be calculated using the exponential function below, where A_{sat}, B_{sat}, K_{sd} and K_{sq} are constants.

$$\begin{aligned} \psi_{at} &= L_{adu} i_{fd} - A_{sat} e^{B_{sat}(\psi_{at} - \psi_{us})} \\ L_{ad} &= K_{sd} * L_{adu} \\ K_{sd} &= \frac{\psi_{at}}{\psi_{at} + A_{sat} e^{B_{sat}(\psi_{at} - \psi_{us})}} \end{aligned} \tag{2.6}$$

$$\begin{aligned} K_{sq} &= K_{sd} \\ L_{aq} &= K_{sq} * L_{aqu} \end{aligned} \tag{2.7}$$

For the purpose of 'small signal analyses' (i.e. analyses of stability under small disturbances), the equations representing the synchronous machine model are linearised. The transformer voltage terms $p\psi_d$ and $p\psi_q$ in equations (2.1) are neglected, to be consistent with the practice of neglecting power system network transients. In addition, the effects of speed variations in the stator voltage equations (2.1) are sometimes neglected, i.e. ω is set to 1.0 p.u. This is acceptable if the speed is very close to the normal 50 Hz. In the study of isolated power systems the frequency may deviate significantly from the normal 50 Hz, and it may not be acceptable to neglect the effect of speed variations.

A distinction is made in the literature between saturated mutual inductances and incremental mutual inductances. In the study of stability under small disturbances (i.e. 'small signal analyses') the permeability of the generator iron can be considered constant relative to changes in flux density. However, as a result of the hysteretic nature of iron, the permeability for small disturbances is different from that for steady-state operation. Therefore, the inductances differ from the steady-state constants L_{ad} and L_{aq}. The inductances for small-signal analyses are approximated using the slope of the saturation characteristic at the initial operating point. In Figure 2-3 the 'saturated inductance' L_{ads} is the average slope of the saturation characteristic, whereas the 'incremental inductance' L_{aqsi} is the slope at the operating point. The saturated inductances are used to calculate the initial voltages, currents, flux linkages and angles. The incremental inductances are used to calculate the variation of voltages, currents, flux linkages and angles.

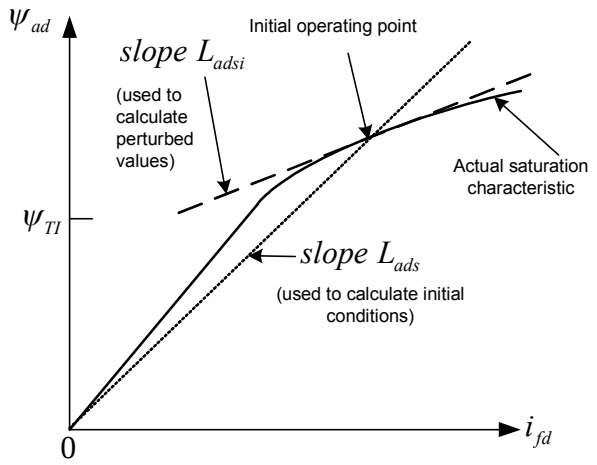

Figure 2-3: Saturated inductance L_{ads} and incremental inductance L_{adsi}

According to the IEEE, the method of modelling magnetising inductances (saturated or incremental) has a relatively minor effect on analyses of oscillating frequencies in the range 0.5 Hz to 10 Hz. The parameters representing the characteristics of the damper windings are the important factors in the study of such oscillating frequencies.

In his investigation of the stability of the islanded PBMR plant under small disturbances, the author found the oscillating frequency to be less than 0.5 Hz, and the effect of the damper windings to be unimportant. Therefore he distinguishes between saturated inductances and incremental inductances.

The coefficient K_D in equation (2.8) represents mechanical damping due to, for example, bearing friction. It excludes electromechanical damping, which is due to the generator. Such damping is included in the calculation of electromechanical torque, T_e.

2.4.2 Excitation system

The PBMR plant has a static excitation system, whose structure is shown in Figure 2-4.

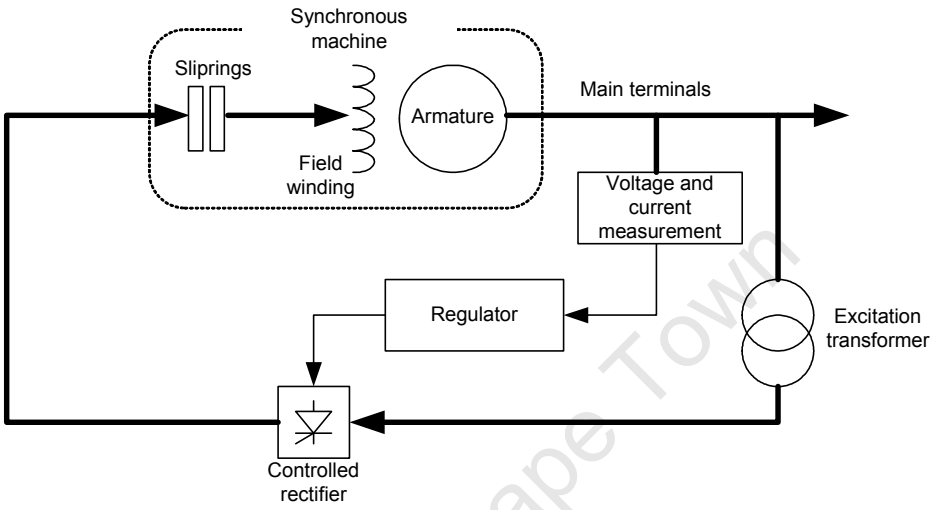

Figure 2-4: Structure of a static excitation system

The IEEE recommends that the model ST1A is used to represent a static excitation system [15, 16]. Figure 2-5 represents the model ST1A together with some simplifications: Not shown are the inputs for the under-excitation limiter and over-excitation limiter – the author did not include these in his investigation. Also, the author used only one lag-lead circuit (the IEEE model allows for two such circuits as well as a rate-feedback circuit).

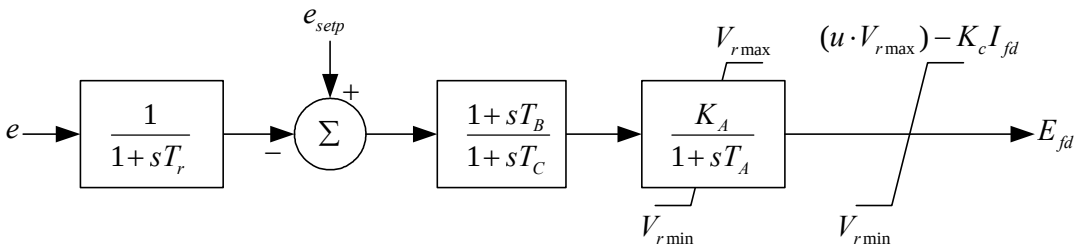

e_{setp}	Reference voltage	T_A	Excitation system time constant
e	Generator terminal voltage	K_C	Commutation loss constant
T_r	Transducer time constant	$V_{r\max}$	Maximum output at rated voltage
$T_{B,C}$	Compensator time constants	$V_{r\min}$	Minimum output at rated voltage
K_A	Excitation system gain	E_{fd}	Output (field voltage)

Figure 2-5: Excitation system model

2.4.3 Turbine

In the investigation into the stability of the islanded PBMR plant, the author used the model of a steam turbine rated at 180 MW. He assumed a turbine having three sections (high-pressure, intermediate-pressure and low-pressure), as shown in Figure 2-6.

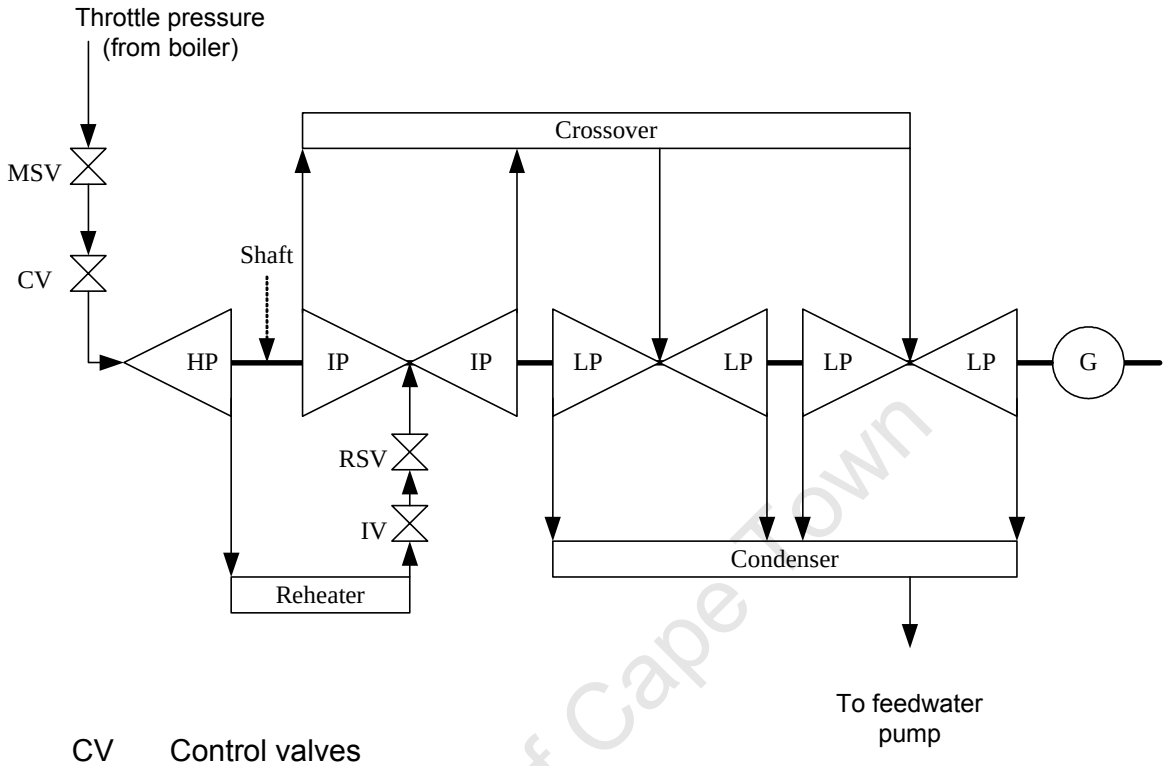

CV	Control valves
G	Generator
HP	High-pressure turbine section
IP	Intermediate-pressure turbine section
IV	Intercept valves
LP	Low-pressure turbine section
MSV	Main stop valves
RSV	Reheater stop valves

Figure 2-6: Structure of a single-reheat tandem-compound turbine

The control valves adjust the steam flow through the turbine. Fast output power reductions are achieved by closing the intercept valves and/or control valves. The main stop valves and the reheater stop valves are used for emergency tripping.

Each turbine section has a number of stages (or rows) of blades. The torque of each section is the sum of the torques of each turbine stage. The torque of each stage is a function of stage efficiency and pressure difference across that stage.

The IEEE provides guidelines for the modelling of steam turbines [21]. Additional information about the derivation of these models is given in [24]. The torque of each turbine section is approximated as being proportional to the steam flow rate through that section. The non-linear effect of the reheater safety valves is represented using a saturation element. The following valve characteristics are represented:

1. For both the control and intercept valves, the non-linear relationship between valve position and valve opening, or 'flow area', is represented.

2. For the intercept valve, the maximum flow rate, or 'critical flow rate', is represented [4].

The maximum rates of valve opening and valve closing are included in the governor model, and not in the turbine model (see section 2.4.4).

The critical flow rate of the intercept valve is modelled using the multiplier, A. During normal operation the multiplier has a value of 1.0. Severe disturbances may lead to the temporary closure, and the re-opening of the intercept valve. The multiplier temporarily drops below 1.0. The following equations are used to calculate the multiplier.

$$A = \begin{cases} \dfrac{\sqrt{r^{2/k} - r^{(k+1)/k}}}{\sqrt{r_c^{\,2/k} - r_c^{\,(k+1)/k}}} & if \quad r < r_c \\ 1 \quad if \quad r \geq r_c \end{cases} \tag{2.8}$$

$$r = \frac{p_{IP}}{p_R}\left(1 - p_{drop}\right)$$

where

p_{IP}, p_R are the pressures at the intermediate-pressure section and reheater

r is the pressure ratio

r_c is the critical pressure ratio

k is a constant

Critical flow rate is considered in Chapter 5.

Figure 2-7 shows a model of the steam turbine having the configuration of Figure 2-6 [21, 24].

The output of the turbine model is a signal representing mechanical torque, i.e. at constant valve positions and inlet conditions the turbine torque is independent of speed. According to the literature the torque-speed relationship of unregulated machines is not known with certainty. The IEEE [14] states that the power of the steam turbine is likely to be independent of speed. To model such a machine, the output torque T_m in Figure 2-7 should be replaced by power, P_m. Kundur [24] presents a derivation of the turbine model, which shows no relationship between the torque (of the unregulated machine) and the speed.

The IEEE states that the torque-speed relationship of an unregulated combustion turbine is not apparent. Reference [31] provides an equation for a gas turbine's torque as a function of speed. According to that equation the torque increases (decreases) with a reduction (increase) in speed. However, the torque/ speed dependence is not such that the power is independent of speed.

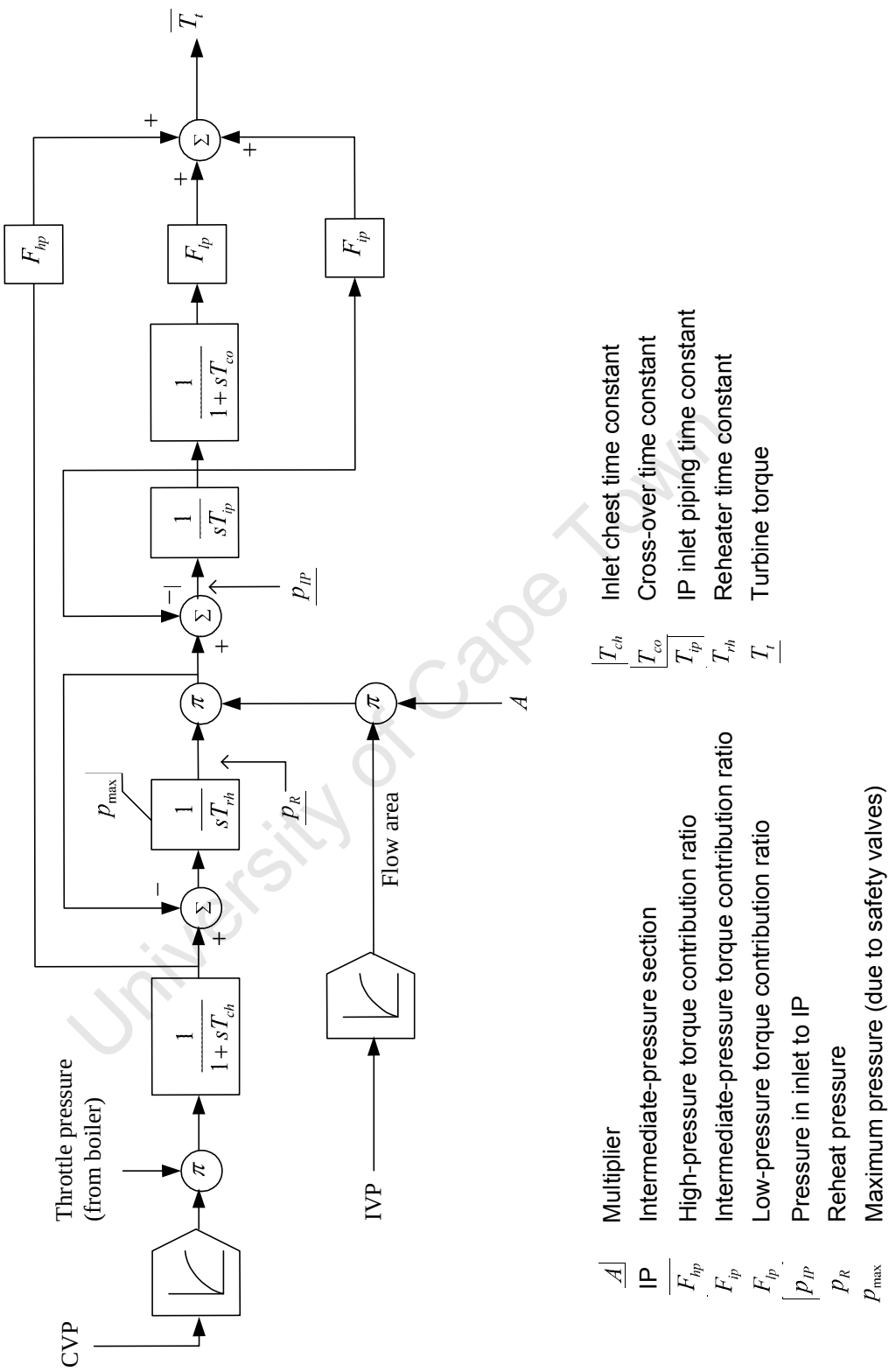

Figure 2-7: Steam turbine model

The IEEE [14] explains how the damping term in the swing equation should be selected to represent different torque-speed relationships. It recommends that analysts investigate how the swing equation is implemented in their software packages. If the turbine is not modelled, then some software packages treat the torque as constant, whereas others treat the power as constant. Reference [22] investigates the effect of these two cases on the electromechanical modes of a generator.

The author introduces the terms 'torque machine' and 'power machine' with reference to Figure 2-8. In the case of a 'torque machine', the torque of the unregulated machine does not vary in response to small speed changes. In a 'power machine' the torque increases (decreases) in response to a small speed decrease (increase), such that the power does not vary with changes in speed. Therefore, in a power machine the torque responds such as to counteract a change in speed, even without the action of the governor.

The action of the governor modifies the turbine's torque/ speed relationship. Figure 2-9 shows that the turbine torque increases (decreases) in response to a small speed decrease (increase). This is true for both the torque machine and the power machine. The torque/ speed characteristic of the power machine has a higher slope than that of the torque machine.

The two turbine types – torque machine and power machine – bound the turbine characteristics mentioned by the IEEE. The author performs his investigations assuming a torque machine, since this yields more conservative results. He repeats some analyses assuming a power machine, and shows that the relationship between the turbine's torque and speed is important to the plant's stability.

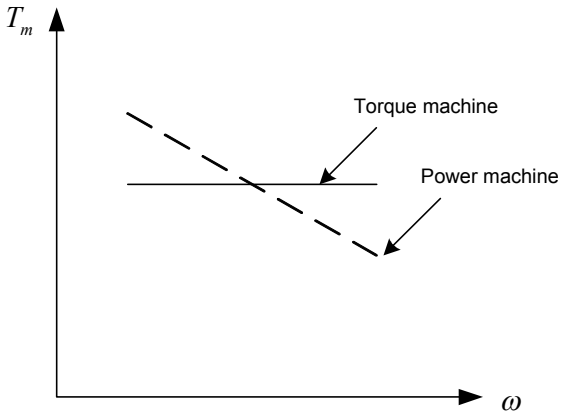

Figure 2-8: Torque-speed relationship of unregulated turbine

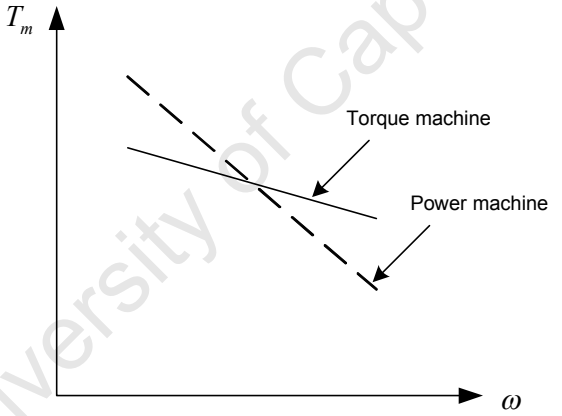

Figure 2-9: Torque-speed relationship of regulated turbine

2.4.4 Governor

The author selected a governor model that is compatible with the steam turbine model.

The IEEE provides governor models [21], and Kundur discusses numerous governors of different technologies [24]. The turbine control system measures the generator

load and the shaft speed. Its outputs determine the positions of the control valves and intercept valves.

Figure 2-10 shows the model of an electro-hydraulic governor. The governor has the gain K_G In steady-sate conditions the intercept valves are fully open due to the valve opening bias, IVOB. During islanding conditions the integrator T_I is switched on. It ensures that the steady-state speed equals the reference value, ω_{ref}, even if the load reference does not exactly match the actual load. If the speed exceeds the maximum $\omega_{\max}$ then the valves are closed at their maximum rates.

The characteristics of the servomotors are included in the turbine control system model. The valve opening and closing rates are determined by the parameters $L_{C1,}L_{C2,}L_{I1}$ and L_{I2}. The effect of the non-linear feedback circuits is to compensate for the non-linear relationship between valve position and valve opening.

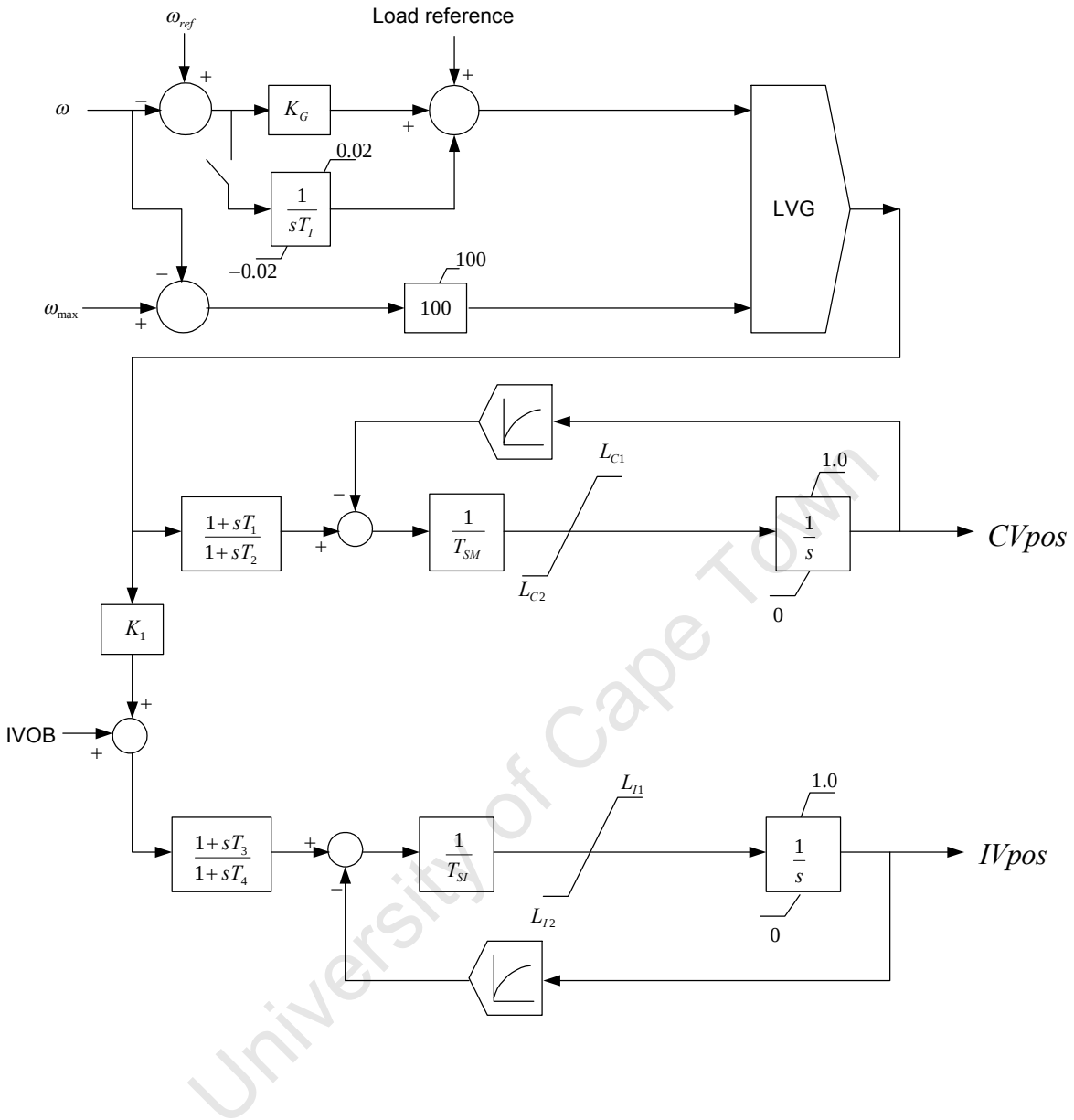

Figure 2-10: Governor model

2.4.5 Stabilising resistor

The author modelled the SR using Ohm's law. The reactance and capacitance was neglected – according to the resistor manufacturer AVTRON the inductive reactance and the capacitive reactance each amount to less than 0.5 % of the resistance. The author also neglected the change in resistance due to a change in temperature. The

maximum operating temperature is reached several minutes after energising the SR, whereas the stability studies cover only the first 20 s of operation.

The author represented the SR using the following equation:

$$P_E = \frac{e^2}{R_E} \tag{2.9}$$

where

P_E is the electrical power supplied to the SR

e is the generator terminal voltage

R_e is the SR resistance

Chapter 3 Development of PBMR Plant Models

The author uses a few different models in the investigation of the PBMR plant's stability. For the analyses in the time-domain he uses models that he developed in the software programmes DIgSILENT *PowerFactory* and MATLAB SimPowerSystems. For the analyses in the frequency-domain he uses the software packages to derive linear models (the software packages use numerical techniques for this). He also uses linear models that he developed by hand - Model 1 and Model 2.

This chapter discusses the models that were developed using the software packages, as well as the models developed by hand.

3.1 Models developed by the author using software packages

The author used the synchronous machine models included in the software packages DIgSILENT *PowerFactory* and MATLAB SimPowerSystems. For the excitation system, turbine and governor he constructed models using DIgSILENT Simulation Language (DSL) and MATLAB Simulink.

Additional information on the models of the generator, excitation system, turbine and governor is presented below.

3.1.1 Generator and stabilising resistor

The software packages' generator models are in accordance with "Model 2.1" of the IEEE [13]. The generator models of both software packages include the transformer voltage terms $p\psi_d$ and $p\psi_q$. However, these terms are omitted from the model of

DIgSILENT *PowerFactory* if the user selects to perform a study of electromechanical transients rather than electromagnetic transients. In this software package the transformer voltage terms are always neglected if the user performs an eigenvalues calculation. The model linearization functions of the two software packages do not fix the speed at 1.0 p.u. in the stator voltage equations.

In both software packages the signal representing the input from the turbine represents mechanical power. Therefore, if the turbine is a torque machine, as discussed in Chapter 2, the output of the turbine model must be multiplied by rotational speed before being passed to the generator model.

The generator model of DIgSILENT *PowerFactory* has a quadratic function to represent core saturation, as shown in equation (3.1). The function is derived from the constants $S_{1.0}$ and $S_{1.2}$, which are entered by the user. The model in MATLAB SimPowerSystems has a polynomial function, which is derived from an array of co-ordinates of the saturation characteristic entered by the user. It is not clear from the manuals of the two software packages whether their linearization functions make any adjustments to the magnetising inductances, i.e. whether the linear models are based on saturated inductances or incremental inductances. The author investigates this further in Chapter 4.

$$K_{sd} = \begin{cases} \dfrac{\psi_m}{\psi_m + B_g(\psi_m - A_g)^2} & if\ \psi_m > A_g \\ 0 & if\ \psi_m \le A_g \end{cases} \tag{3.1}$$

with

$$\begin{aligned} \psi_m &= \sqrt{(\psi_d^2 + x_l i_d)^2 + (\psi_q^2 + x_l i_q)^2} \\ x_l &= 2\pi f_n L_l \\ A_g &= \frac{1.2 - \sqrt{1.2 \cdot S_{1.2}/S_{1.0}}}{1.0 - \sqrt{1.2 \cdot S_{1.2}/S_{1.0}}} \\ B_g &= \frac{S_{1.0}}{\left(1 - A_g\right)^2} \end{aligned} \tag{3.2}$$

where

K_{sd} is a saturation coefficient

ψ_m is the magnetizing flux linkage

ψ_d, ψ_q are the flux linkages in the d- and q-axes

x_l is the leakage reactance

L_l is the leakage inductance

f_n is the nominal frequency

A_g, B_g are constants

The author uses a per unit system in which 1.0 p.u. field voltage is that field voltage required for rated stator voltage on the air-gap line. This is also the per unit system of the generator model in DIgSILENT *PowerFactory*. However, the per unit system of MATLAB SimPowerSystems differs from this – 1.0 p.u. field voltage is the field voltage required for rated stator voltage on the non-linear saturation characteristic. The author considered this difference in the development of the excitation system model.

The author also chose a per unit system in which 1.0 per unit power is equal to the generator's rated apparent power. This is also the per unit system of MATLAB SimPowerSystems. In DIgSILENT *PowerFactory*, however, different per unit systems are used for electrical power and mechanical power – 1.0 per unit electrical power equals the generator's rated apparent power, but 1.0 per unit mechanical power equals the generator's rated active power, i.e. rated apparent power multiplied by rated power factor. The author considered this difference in the development of the turbine model.

Both software packages include models for resistor, in which the relationship between voltage and current is represented by Ohm's law.

3.1.2 Excitation system, turbine and governor

Chapter 2 presents the models of the excitation system, turbine and governor. Appendix C and Appendix D show the implementation of these models in the two software packages. The excitation system model in MATLAB includes a gain in the output signal to compensate for the difference in the per unit systems of the two software packages' generator models, as discussed in section 3.1.1. Likewise, the turbine model in MATLAB includes a gain in the output signal to compensate for the difference in the software packages' per unit systems, as discussed in section 3.1.1.

3.2 Models developed analytically by the author

The author developed two linear models for the analyses in the frequency-domain. These are introduced with reference to Figure 3-1, which shows the structure of a linear plant model. In Figure 3-1, $\Delta CVpos$ represents the change in control valve position, and $\Delta\omega_e$ the change in speed-error.

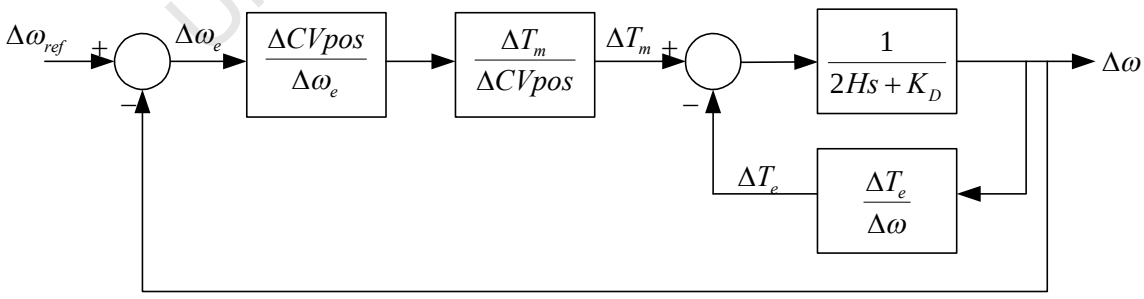

Figure 3-1: Structure of linear plant model

Model 1 includes only the transfer function $\Delta\omega/\Delta T_m$. It is based on the assumption that the generator terminal voltage is constant. The excitation system, turbine and

governor are excluded. The author uses Model 1 in Chapter 4 for some analyses of the open-loop system. It is useful to understand the instability of the 'inner loop' mentioned in section 1.4.

Model 2 is more detailed than Model 1. It includes the generator, excitation system, turbine and governor. The author uses Model 2 in Chapter 4 for analyses of both the open-loop and closed-loop system. He also uses it to develop Bode diagrams for the transfer functions $\Delta T_m / \Delta\omega$ and $\Delta T_e / \Delta\omega$ (the latter cannot be obtained directly from the software packages, because the speed signal may only be treated as an output).

The derivation of the two linear models follows.

3.2.1 Model 1

In Model 1 the generator is represented by a constant voltage source without any internal impedance. The generator power is given by:

$$P_E = \frac{e^2}{R_E} \tag{3.3}$$

where the generator terminal voltage e is constant. The SR resistance R_E is assumed to be constant, hence P_E is also constant.

The electromagnetic torque is given be:

$$T_e = \frac{P_E}{\omega} \tag{3.4}$$

Differentiating (3.4) leads to:

$$\frac{dT_e}{d\omega} = \frac{-P_E}{\omega^2} + \frac{\partial P_E}{\partial \omega} = \frac{-P_E}{\omega^2} \tag{3.5}$$

A linearized form of (3.4), at the initial operating point, is as follows:

$$\Delta T_e = \frac{-P_E}{\omega_o^2} \cdot \Delta\omega \tag{3.6}$$

Thus a small increase (decrease) in speed leads to a decrease (increase) in electromagnetic torque.

The equation of motion is as follows:

$$T_m - T_e = 2H\omega s + K_D\omega \tag{3.7}$$

Differentiating this equation yields:

$$\frac{\partial T_m}{\partial \omega} - \frac{\partial T_e}{\partial \omega} = 2Hs + K_D \tag{3.8}$$

A linearised form of (3.7), at the initial operating point, is as follows:

$$\Delta T_m - \Delta T_e = \left(2Hs + K_D\right)\Delta\omega \tag{3.9}$$

Model 1 is obtained by developing the transfer function $\Delta\omega / \Delta T_m$ using (3.6) and (3.9):

$$\frac{\Delta\omega}{\Delta T_m} = \frac{\omega_o^2/(P_E - K_D\omega_o^2)}{s \cdot 2H\omega_o^2/(P_E - K_D\omega_o^2) - 1} \tag{3.10}$$

No reference frame is defined for Model 1, since it does not use the d-q axis theory of synchronous machines.

3.2.2 Model 2

Model 2 consists of linear models of the generator, excitation system, turbine and governor.

3.2.2.1 Generator and Stabilising Resistor

The generator is represented by a 2nd order model, based on the well-known d-q axis theory of synchronous machines. According to that theory, the reference frame is

defined by the position of the rotor relative to the magnetic field of the stator. The IEEE labels such a generator representation "Model 1.0" [13]. The model includes an equation representing the field winding. It excludes equations representing the damper windings. The equations representing the generator follow:

$$\begin{aligned} e_d &= -\omega\psi_q - R_a i_d \\ e_q &= +\omega\psi_d - R_a i_q \\ e^2 &= e_d^2 + e_q^2 \end{aligned} \tag{3.11}$$

$$\begin{aligned} \psi_{ad} &= L_{ads}(-i_d + i_{fd}) = \psi_d + L_l i_d \\ \psi_{aq} &= -L_{aqs} \cdot i_q = \psi_q + L_l i_q \\ \psi_{fd} &= \psi_{ad} + L_{fd} i_{fd} \end{aligned} \tag{3.12}$$

$$\frac{d\psi_{fd}}{dt} = \omega_n \left[\frac{R_{fd}}{L_{adu}} \cdot E_{fd} - R_{fd} \cdot i_{fd} \right] \tag{3.13}$$

$$T_e = \psi_{ad} \cdot i_q - \psi_{aq} \cdot i_d \tag{3.14}$$

$$T_m - T_e = J \cdot \frac{d\omega}{dt} + K_D \cdot \omega \tag{3.15}$$

where the symbols are defined in the section 'List of symbols'.

The SR is modelled using Ohm's law:

$$\begin{aligned} e_d &= i_d R_E \\ e_q &= i_q R_E \end{aligned} \tag{3.16}$$

The author developed a linear model of the generator and SR. He followed a similar process to the one used to develop a linear model of a single machine-infinite bus [7, 8, 24]. However, he does not assume the speed to be 1.0 p.u. within the stator voltage equations – in the case of the islanded PBMR plant there is no external source that holds the speed constant. The author included the effects of core saturation. He distinguished between saturated inductances and incremental inductances. He

assumed that the same saturation characteristic applies to both the d-axis and the q-axis.

A summary of the derivation of the linear model of the generator and SR follows. The complete derivation is given in 0.

The author developed a linear form of (3.14) by differentiating it with respect to ω and ψ_{fd}. He developed expressions for the partial derivatives, in terms of $\Delta\omega$ and $\Delta\psi_{fd}$, using equations (3.11), (3.12) and (3.16). Finally, he expressed the perturbed electrical torque ΔT_e as a function of $\Delta\omega$ and $\Delta\psi_{fd}$:

$$\Delta T_e = K_{t\omega}\Delta\omega + K_{t\psi}\Delta\psi_{fd} \tag{3.17}$$

where the constants $K_{t\omega}$ and $K_{t\psi}$ depend on the initial operating point. Note that the above equation excludes the (perturbed) load angle $\Delta\delta$, since there is no synchronising torque between the generator and the external network. The generator rotor does not necessarily rotate at synchronous speed, and there is no merit in comparing the angle of the rotor to the angle of an external source.

The author developed an expression for the perturbed field flux as a function of the perturbed field voltage and perturbed shaft speed:

$$\Delta\psi_{fd} = \frac{K_{fd}}{sT_{fd}+1}\left[\Delta E_{fd} - K_{\omega f}\Delta\omega\right] \tag{3.18}$$

where $K_{fd}, K_{\omega f}$ and T_{fd} are constants, which depend on the initial operating point.

ΔE_{fd} is obtained from $G_{ex}(s)\cdot\Delta e$, where $G_{ex}(s)$ is the transfer function of the excitation system and Δe is the perturbed terminal voltage.

Δe is found by linearising equation (3.11):

$$(e_o + \Delta e)^2 = (e_{do} + \Delta e_d)^2 + (e_{qo} + \Delta e_q)^2 \tag{3.19}$$

The linearised equation is expanded and second-order terms are neglected:

$$2e_o\Delta e = 2e_{do}\Delta e_d + 2e_{qo}\Delta e_q \tag{3.20}$$

$$\Delta e = \frac{e_{do}}{e_o}\Delta e_d + \frac{e_{qo}}{e_o}\Delta e_q \tag{3.21}$$

where

e_o is the initial terminal voltage

e_d, e_q are the d- and q-axis initial terminal voltage

The author developed equations for Δe_d and Δe_q in terms of $\Delta\omega$ and $\Delta\psi_{fd}$. From these and equation (3.21), he developed an equation for Δe in terms of $\Delta\omega$ and $\Delta\psi_{fd}$:

$$\Delta e = K_{e\omega}\Delta\omega + K_{e\psi}\Delta\psi_{fd} \tag{3.22}$$

where $K_{e\omega}$ and $K_{e\psi}$ are constants, which depend on the initial operating point.

Finally, he used the same linearised form of the shaft equation as in Model 1:

$$\Delta T_m - \Delta T_e = \left(2Hs + K_D\right)\Delta\omega \tag{3.23}$$

where ΔT_m is the output of the linear turbine model.

Model 2 is shown in Figure 3-2. The figure shows the linear generator model its connection to the linear models of the excitation system, turbine and governor.

The author also developed the transfer function $\Delta\omega/\Delta T_m$ from Figure 3-2. He uses this transfer function in Chapter 4 to investigate the stability of the PBMR plant without the action of the governor.

$$\frac{\Delta\omega}{\Delta T_m} = \frac{s^2(T_{fd}T_r) + s(T_{fd} + T_r) + K_{fd}K_A K_{e\omega}}{ps^3 + qs^2 + rs + t} \tag{3.24}$$

where p, q, r and t are constants, defined as follows:

$$
\begin{aligned}
p &= 2HT_{fd}T_r \\
q &= 2H \cdot (T_{fd} + T_r) + T_{fd}T_r \cdot (K_D + K_{t\omega}) \\
r &= (K_D + K_{t\omega}) \cdot (T_{fd} + T_r) + K_{fd} \cdot (2HK_{e\psi}K_A - K_{t\psi}K_{\omega f}T_r) \\
t &= K_{fd}K_{e\psi}K_A \cdot (K_D + K_{t\omega}) - K_{t\psi}K_{fd} \cdot (K_{\omega f} + K_A K_{e\omega})
\end{aligned}
\tag{3.25}
$$

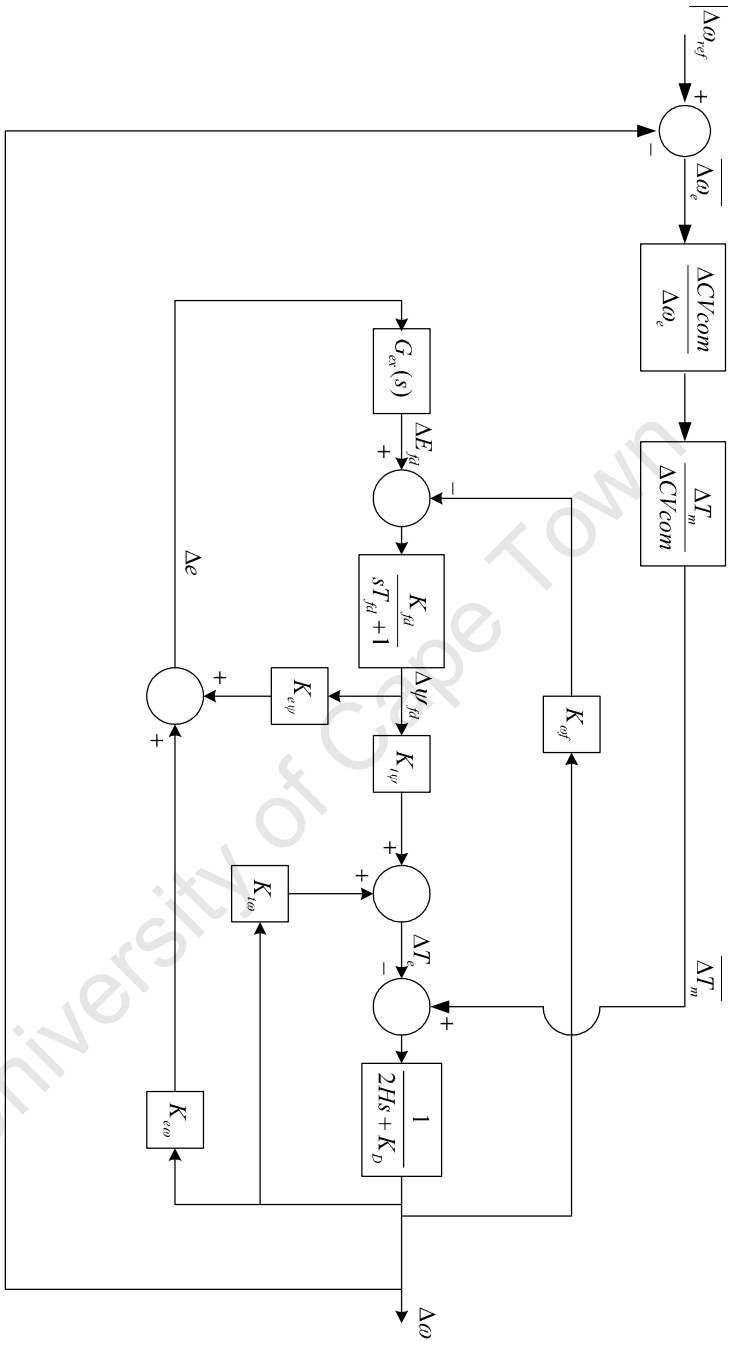

Figure 3-2: Model 2

3.2.2.2 Excitation system

The author developed a linearised model of the excitation system from the model presented in section 2.4.2. He assumed that the signals remain within their limits, i.e. he neglected the signal limits. The linearised excitation system model is given by the following transfer function:

$$G_{ex}(s) = \frac{\Delta E_{fd}}{\Delta e} = \frac{-K_A(sT_B + 1)}{(sT_r + 1)\cdot(sT_C + 1)\cdot(sT_A + 1)} \tag{3.26}$$

3.2.2.3 Turbine

The author developed a linear model of the turbine from the model presented in section 2.4.3. He neglected the signal limits and the valve choking characteristic. He developed the linear model for the conditions of 1.0 p.u. pressure from the steam generator and fully open intercept valves.

The linearization of the valve characteristic is explained with reference to Figure 3-3. The relationship between the valve's flow area and its position, at the initial operating point, is represented by the linear gain K_{vnl}.

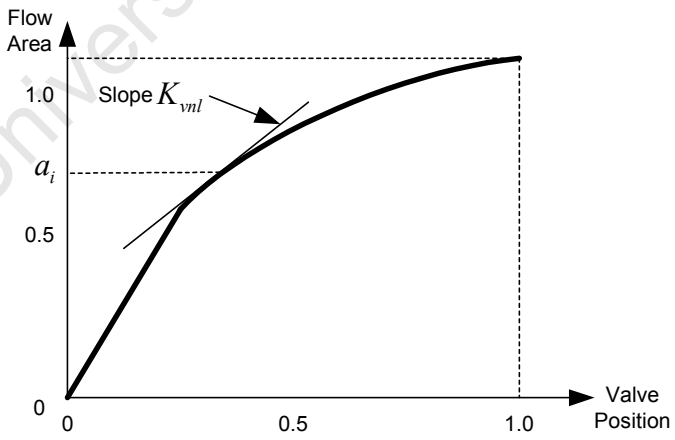

Figure 3-3: Valve characteristic

The linearised turbine model is presented in Figure 3-4.

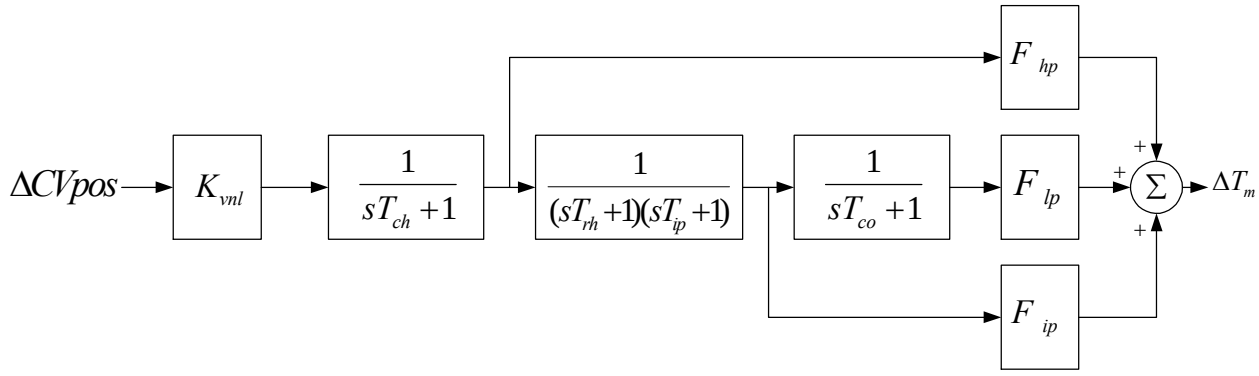

Figure 3-4: Linear turbine model ($\Delta T_m / \Delta CVpos$)

In section 3.2.2.4 it is shown that the linear governor model contains the gain $1/K_{vnl}$, i.e. the inverse of the gain K_{vnl} that appears in the linear turbine model. The non-linearity in the turbine control system compensates the non-linearity in the turbine valves. The linear models of the turbine and governor can thus be simplified by omitting the gains K_{vnl} and $1/K_{vnl}$.

3.2.2.4 Governor

The author developed a linear model of the governor from the model presented in section 2.4.4. He neglected the signal limits and the overspeed controls. As in the development the turbine model, he assumed the intercept valves to be fully open.

Figure 3-5 shows the linear governor model. The term K_{vnl} represents the feedback that compensates for the non-linear characteristic of the turbine valves. An alternative representation of the linear governor model is shown in Figure 3-6. That representation shows the gain $1/K_{vnl}$, which was mentioned in section 3.2.2.3.

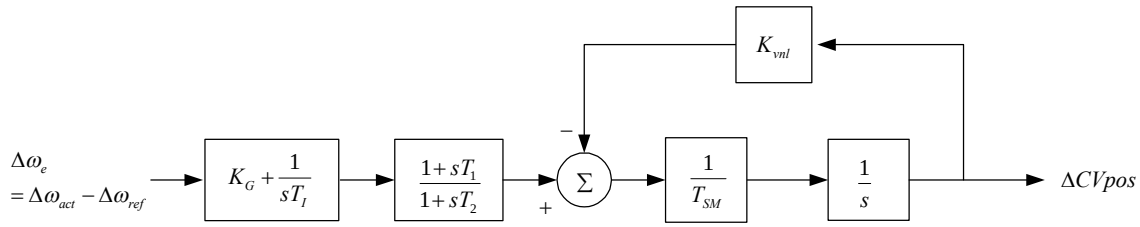

Figure 3-5: Linear governor model ($\Delta CVpos / \Delta\omega_e$)

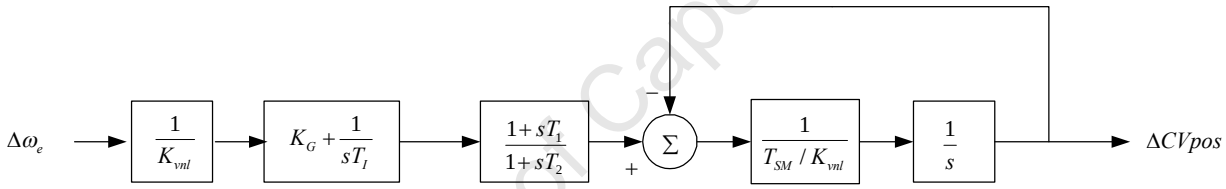

Figure 3-6: Alternative representation of linear governor model ($\Delta CVpos / \Delta\omega_e$)

Chapter 4 Stability of the power plant under small disturbances

In this chapter the author investigates the stability of the PBMR plant (also referred to as the "system") under small disturbances. The investigation considers the plant in the islanded state with the SR connected. The transition to the islanded state is investigated in Chapter 5.

The author's investigations include analyses in both the frequency- domain and the time-domain. He investigates the stability of both the open-loop system (neglecting the governor) and the closed-loop system (considering the governor). He uses the software programmes DIgSILENT *PowerFactory* and MATLAB SimPowerSystems in his analyses. For the analyses in the frequency-domain, he also uses hand-calculations based on Model 1 and Model 2.

The author shows that, without the governor, the system is unstable. The electromagnetic torque increases (decreases) in response to a speed decrease (increase). The governor stabilises the system, i.e. it counteracts the relationship between electromagnetic torque and speed.

In Chapter 5 the author shows that a large disturbance may lead to the instability of the system, and the instability is due to the relationship between electromagnetic torque and speed. The instability can be avoided through the addition of a SC. The action of the SC causes the electromagnetic torque to decrease (increase) in response to a speed increase (decrease), hence it improves the performance of the governor.

In this chapter the author describes the SC, and shows what effect it has on the stability of the PBMR plant under small disturbances.

The author investigates whether the calculated damping is affected significantly by the turbine type, the damper windings and the method of modelling the magnetising inductances – saturated inductances or incremental inductances.

4.1 Frequency-domain analysis neglecting the governor

In this section of the thesis the author shows that the system without governor is unstable. In section 4.1.1 he explains the instability using Model 1, in which the voltage across the SR is assumed to be constant, i.e. the generator field winding and excitation system are neglected.

In section 4.1.2 the author analyses the system using Model 2 as well as the models implemented in the software programmes. Therefore, he considers the generator field winding and the excitation system. He finds the system to be unstable. He compares the results obtained from the different models.

The author designs the SC to eliminate the abovementioned instability. The benefit of the SC is observed in the analyses of the closed-loop system – particularly under large disturbances.

4.1.1 Neglecting the generator and excitation system

Model 1, which is derived in Chapter 3, is represented by the following transfer function $\Delta\omega / \Delta T_m$:

$$\frac{\Delta\omega}{\Delta T_m} = \frac{\omega_o^2 /(P_E - K_D\omega_o^2)}{s \cdot 2H\omega_o^2 /(P_E - K_D\omega_o^2) - 1} \tag{4.1}$$

The model's eigenvalue is found by setting the denominator in (4.1) to zero:

$$s = \frac{P_E - K_D\omega_o^2}{2H\omega_o^2} \tag{4.2}$$

A typical value for K_D is 1 - 2%, hence $K_D \cdot \omega_o^2$ is significantly lower than the SR rating. Equation (4.2) yields a positive real value for the system's eigenvalue, indicating that the system exhibits aperiodic instability. The plant could be

described as having "negative damping", since the electromagnetic torque is such that it supports a change in speed, rather than oppose it.

The power plant's instability is caused by the response of electromagnetic torque to shaft speed. If the generator terminal voltage e is constant, the electromechanical torque is inversely proportional to the rotational speed. An increase (decrease) in speed results in a reduction (increase) in electromechanical torque, thereby causing a further increase (decrease) in speed.

Table 4-1 shows the eigenvalue of the transfer function $\Delta\omega / \Delta T_m$ at different levels of electrical power. The plant's stability deteriorates as the power level increases.

Table 4-1: Eigenvalue of Model 1

P_E (p.u.)	Eigenvalue (s^{-1})
0.850	0.1384
0.826	0.1345
0.400	0.06515

The above analysis is based on the assumption that the turbine is a 'torque machine' (as defined in section 2.4.3). In the case of a torque machine ΔT_m does not vary in response to speed changes (assuming no governor). If the turbine had been modelled as a 'power machine', then ΔT_m would be speed-dependent. The author investigated the impact of the two different turbine types.

In the case of a 'power machine' the mechanical torque varies with mechanical power according to equation (4.3):

$$T_m = \frac{P_m}{\omega} \tag{4.3}$$

A linearised form of (4.3), at the initial speed ω_o, is found from a Tailor series expansion, considering only the first-order derivative with respect to speed:

$$\Delta T_m = -\frac{P_m}{\omega_o^2}\Delta\omega \tag{4.4}$$

Therefore, an increase (decrease) in shaft speed would cause a reduction (increase) in mechanical torque. The effect of using a 'power machine' model would have been to increase the damping. This damping would counteract the negative damping due to the electrical system.

The net variation in torque, as a result of a variation in speed, is derived using equation (3.6) and equation (4.4):

$$\Delta T_m - \Delta T_e = -P_m \cdot \frac{\Delta\omega}{\omega_o^2} + P_e \cdot \frac{\Delta\omega}{\omega_o^2} \tag{4.5}$$

The mechanical power is almost equal to the electrical power – the difference is only the power dissipated in the generator stator resistance. Therefore, if the power loss of the stator is neglected, then $P_m = P_e$, and $\Delta T_m - \Delta T_e = 0$. The variation in electromagnetic torque due to a speed variation is counteracted by a variation in mechanical torque. The power plant having a power machine is on the verge of instability – its only damping is mechanical damping, $K_D \cdot \omega^2$.

The instability (or poor damping) described above occurs within the system's "inner loop", i.e. it occurs if the effect of the governor is neglected. According to [30], unstable inner loops should be avoided. They cause system's to have a relatively slow response to disturbances, and they can cause a system to be of non-minimum phase (which means that their initial response to a disturbance is in the wrong direction).

4.1.2 Considering the generator and excitation system

Model 2, which is derived in Chapter 3, includes the following transfer function:

$$\frac{\Delta\omega}{\Delta T_m} = \frac{s^2(\tau_3\tau_m) + s(\tau_3 + \tau_m) + K_3K_AK_9}{ps^3 + qs^2 + rs + t} \tag{4.6}$$

The author found the model's eigenvalues by calculating the roots of the denominator[7] in equation (4.6). One of the eigenvalues was real and positive, indicating that the system is unstable. Table 4-2 shows the value of this eigenvalue for different levels of electrical power. The table also provides a comparison to the results obtained from Model 1.

Table 4-2: Comparison of eigenvalues of Models 1 and 2 (excluding governor)

P_E (p.u.)	Eigenvalue (s^{-1})		
	Model 1	Model 2	Difference
0.850	0.1384	0.1616	14%
0.826	0.1345	0.1569	14%
0.400	0.06515	0.07172	9%

The results obtained from Model 2 are marginally poorer (in terms of stability) than the results obtained from Model 1, i.e. the system is marginally less stable than predicted using Model 1. The author considers Model 2 to be more accurate than Model 1, since it is based on fewer simplifying assumptions.

As discussed in Chapter 3, the author constructed a model of the power plant in both DIgSILENT *PowerFactory* and MATLAB SimPowerSystems. He calculated the eigenvalues of these models using the software packages. Before presenting the results, some remarks on the calculation of eigenvalues using these two software packages follow:

- *PowerFactory* calculates a numeric linear representation of the system using the QR method. From this linear representation the software calculates the eigenvalues. The calculation of eigenvalues is initiated from the program's menu [9]. It is not possible to view the matrices representing the linearised model. The

[7] The denominator of the transfer function is known as the characteristic equation.

details of the calculation processes are not disclosed to the user; hence the user cannot assess the limitations that the calculation procedure may impose.

- In MATLAB, the function 'linmod' is used to calculate the linear state-space model of the power system, which is represented graphically using the SimPowerSystems [28]. The 'linmod' function provides the state-space matrices A, B, C and D. The function 'eig' is then used to calculate the eigenvalues of the linearised model. As in the case of *PowerFactory*, the details of the calculation processes are not disclosed to the user.

From the results the author confirmed the presence of a positive real eigenvalue. He also confirmed that the plant's damping deteriorates with an increase in power. The value of positive eigenvalue, for different levels of SR power, is shown in Table 4-3. Also included in the table are the results obtained using Model 2.

Table 4-3: Eigenvalues of Model 2 and the models in the software packages (excluding governor)

P_E (p.u.)	Eigenvalue (radian. s^{-1})		
	Model 2	Model in DIgSILENT *PowerFactory*	Model in MATLAB SimPowerSystems
0.850	0.1616	0.1386	0.1348
0.826	0.1569	0.1311	0.1310
0.400	0.07172	0.06349	0.06388

The results obtained from the models implemented in DIgSILENT and in MATLAB are in close agreement, but differ from the results obtained from Model 2. The author investigated the cause of the difference, and concluded that the software packages use 'saturated inductances' and not incremental inductances. He observed that, if Model 2 is adapted to use saturated inductances, the eigenvalue closely matches the results from the models of the software packages. This is shown in Table 4-4.

Table 4-4: Effect of different mutual inductances on stability (excluding governor)

P_E (p.u.)	Eigenvalue (radian. s^{-1})	
	Model 2 (with incremental inductances)	Model 2 (with saturated inductances)
0.850	0.1616	0.1354
0.826	0.1569	0.1316
0.400	0.07172	0.0640

The eigenvalues of the models implemented in the two software packages are almost identical to the eigenvalues of Model 1. This is despite the fact that the models implemented in the software packages are significantly more detailed than Model 1. The results obtained from Model 2 are more pessimistic than the ones obtained from Model 1. If the linearization of the model's equations considers the non-linearity of the magnetising inductance, then the results are more pessimistic than if the non-linearity is not considered. The non-linearity of the magnetising inductance has a destabilising effect on the power plant, when it is subjected to small disturbances.

4.1.3 Introducing the stabilising controller

For the case where the turbine is a torque machine, the inner loop (i.e. the plant without governor) is unstable. Therefore, for the plant to be stable the governor has to oppose the instability of the inner loop. The governor can be tuned to dampen the speed in response to many disturbances, but its effectiveness is limited by the instability of the inner loop. The counteraction between the outer loop (i.e. governor control) and the inner loop may lead to non-linear limit cycles. Also, the governor's output may saturate, in which case it no longer counteracts the unstable inner loop. Considering the uncertainty in the turbine's torque/ speed relationship, the author proposes to modify the inner loop so as to 'remove' the instability. The author proposes a stabilising controller (SC), which modifies the relationship between speed

and electromagnetic torque, as explained below. The SC stabilises the inner loop, thereby reducing the burden on the governor in controlling the speed.

The SC is introduced by revisiting the derivation of Model 1. As explained in Chapter 3, Model 1 was developed from the following simplified equation for electromagnetic torque:

$$T_e = \frac{e^2}{\omega R_E} \tag{4.7}$$

In the development of Model 1 it was assumed that the generator terminal voltage e is constant. The linear model was derived by differentiating equation (4.7) with respect to ω, and not with respect to e.

If equation (4.7) is differentiated with respect to both ω and e (i.e. regarding e as variable), the result is as follows:

$$\frac{dT_e}{d\omega} = \frac{\partial T_e}{\partial e}\cdot\frac{\partial e}{\partial \omega} + \frac{\partial T_e}{\partial \omega}\cdot\frac{\partial \omega}{\partial \omega} = \frac{2e}{\omega R_E}\cdot\frac{\partial e}{\partial \omega} - \frac{e^2}{\omega^2 R_E}\cdot\frac{\partial \omega}{\partial \omega} \tag{4.8}$$

From this equation, the author obtained the linearised form of (4.7) at the initial terminal voltage e_o and speed ω_o:

$$\Delta T_e = \frac{-e_o^2}{\omega_o^2 R_E}\Delta\omega + \frac{2e_o}{\omega_o R_E}\Delta e \tag{4.9}$$

According to equation (4.9) either a change in shaft speed or a change in terminal voltage will cause a change in electromagnetic torque. Hence the torque can be changed by changing the generator terminal voltage. More specifically, the generator voltage can be controlled in response to a speed change, so that the net change in electromagnetic torque opposes the speed change.

The condition of $\Delta T_e = 0$ is achieved if the two terms on the right of equation (4.9) are equal in magnitude and opposite in sign. Such a counteraction of the two torque

components occurs if the generator terminal voltage changes in response to speed according to equation (4.10).

$$\Delta e = \frac{e_o}{2\omega_o}\Delta\omega \tag{4.10}$$

If the voltage varies in response to a speed change according to (4.10) then $\Delta T_e / \Delta\omega = 0$.

The author proposes a SC, similar to a conventional power system stabiliser, which causes the generator voltage to vary in response to a speed change. The SC, and its interface to the excitation system, is depicted in Figure 4-1. The gain K_e can be adjusted so that an increase (decrease) in shaft speed causes an increase (decrease) in electromagnetic torque, i.e. $\Delta T_e / \Delta\omega > 0$. The output of the stabilising controller is limited so that the controller does not cause the generator voltage to exceed design limits (typically $\pm 5\%$). A high-pass filter ensures that, in a steady-state condition, the output of the stabilising controller is zero. Therefore, the steady-state speed is determined by the governor. The SC is active only whilst the generator is islanded from the external network, otherwise it is disconnected.

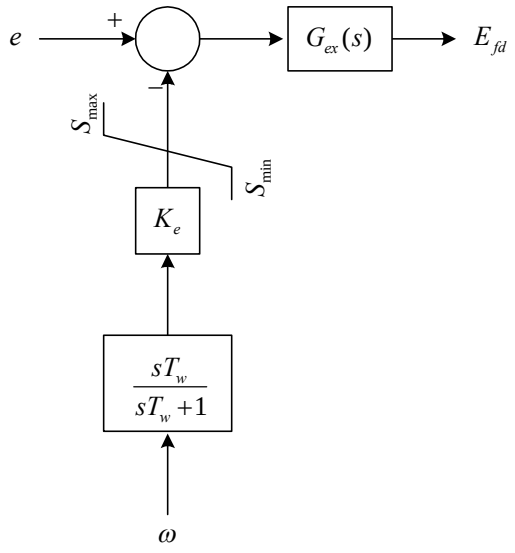

Figure 4-1: Stabilising controller (SC)

A linear model of the SC is shown in Figure 4-2. The author uses this model in the frequency-domain analyses of this chapter.

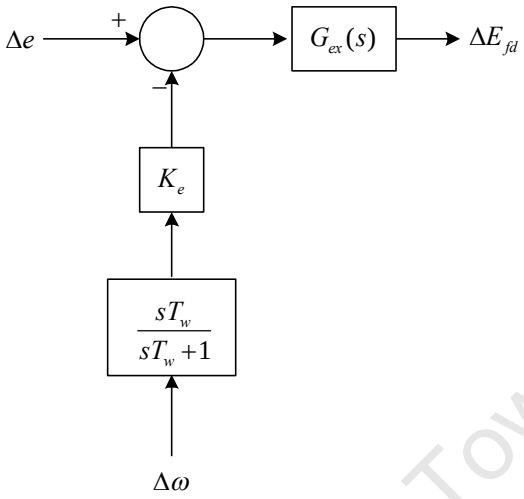

Figure 4-2: Linear model of stabilising controller (SC)

The similarities and differences between the proposed SC and a conventional PSS are as follows:

1. A PSS is used to improve rotor-angle stability, whereas the SC is used to improve frequency stability. Therefore, the two differ in purpose.
2. A PSS is used in a multi-machine power system, whereas the SC is applicable to a single-machine system.

The above derivation of the SC ignores the effects of the generator field winding, the damper windings, saturation and the excitation system. Despite this, the SC effectively increases the system's damping, as subsequent sections of this chapter will show. In Chapter 5, the author shows that the SC greatly improves the stability of the plant under large disturbances.

Table 4-5 shows the effect on the damping if the plant includes a SC with a gain of 2.0 p.u. The SC increases the damping significantly. The damping is still marginally negative despite the SC. This is due to the effect of the washout filter within the SC.

Table 4-5: Effect of SC on stability (excluding governor)

P_E (p.u.)	Eigenvalue (radian. s^{-1})	
	Without SC	With SC
0.826	0.1311	0.0144
0.600	0.0639	0.0126

An investigation into the torsional modes of the shaft, and the possibility of exciting such modes through the SC, was not the scope of the thesis. Potential problems with torsional modes can be addressed through careful selection of the location of the speed measurement device along the shaft length and through the addition of notch filters in the SC.

4.2 Frequency-domain analysis considering the governor

In the following paragraphs the author considers the effect of the governor on the stability of the plant under small disturbances. He uses Model 2 as well as the models implemented in the software programmes. He compares the eigenvalues of the different models.

In section 4.2.1 the author investigates the stability of the plant without the SC. He shows that the governor stabilises the plant. He assesses the effect on damping of the two different turbine types – torque machine and power machine. He also assesses the importance of using incremental inductances as opposed to saturated inductances in the equations describing the synchronous machine.

In section 4.2.2 the author investigates the stability of the plant with the SC. He assesses the effectiveness of the SC using detailed models of the generator (recall that the design of the SC is based on Model 1, which excludes the equations for the describing the generator field winding and the excitation system).

The analyses of section 4.2 are based on a SR rating of 175 MW (0.826 p.u.). Additional analyses, in which a rating of 85 MW (0.4 p.u.) is considered, are presented in section 4.5.

4.2.1 Excluding the stabilising controller

The author proposes a value for the governor gain that causes the system's gain margin to exceed 10 dB, and the phase margin to exceed 30 °. A gain margin of 16.0 dB and a phase margin of 32.7° are achieved using a gain of $K_G = 25$. Figure 4-3 shows the Bode diagrams of the open-loop transfer function $\Delta\omega / \Delta\omega_e$.

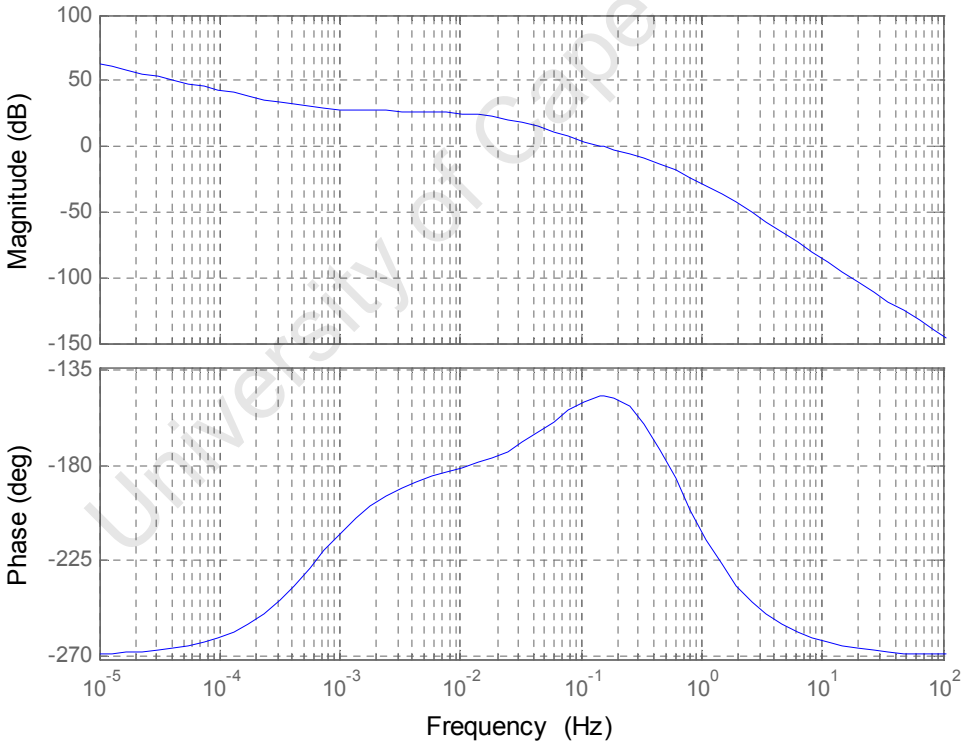

Figure 4-3: Bode diagrams of $\Delta\omega / \Delta\omega_e$ (excluding SC)

Even though the governor stabilises the power plant the Bode plots show an undesirable characteristic, namely that the phase lag is very large (-270° to 180° at low frequencies). The large phase lag is due to the poor damping of the "inner loop",

as discussed in section 4.1.1 (it is shown in section 4.1.3 that the SC significantly reduces this phase lag).

Table 4-6 shows the results of the five 'slowest modes' that are observed in the state $\Delta\omega$, as obtained from Model 2 and from the models implemented in the software programmes, where 'slow' is a measure of the proximity of the eigenvalue to the origin (a complete list of eigenvalues is included in Appendix E). All eigenvalues have negative real parts, confirming that the system is stable. The two oscillatory modes have the frequencies 0.12 Hz and 0.11 Hz. There is a close correlation between the results obtained from the models implemented in the two software packages.

Table 4-6: Eigenvalues of Model 2 and models in software packages (including governor, excluding SC)

	Eigenvalues (s^{-1})		
No.	Model 2	Model implemented in DIgSILENT *PowerFactory*	Model implemented in MATLAB SimPowerSystems
1,2	-0.4241 ± j0.7657	-0.4506 ± j0.7666	-0.4466 ± j0.7677
3,4	-1.600 ± j0.6916	-1.582 ± j0.7666	-1.574 ± j0.6707
5	-5.262	-5.252	-5.235

Model 2 yields a lower damping of the eigenvalues 1 and 2 than the models implemented in the software programmes (the difference is about 5 %). The author found this difference to be related to saturation modelling. The difference is not due to the fact that Model 2 excludes the equations of the damper windings, whereas these equations are included in the models of the software programmes. Therefore, the damper windings do not have a significant effect on the frequency stability of the islanded PBMR plant, subjected to small disturbances.

Table 4-7 shows the effect of using saturated inductances, as opposed to incremental inductances, on the five slowest eigenvalues of Model 2. If saturated inductances are

used then the calculated damping of the slowest modes is marginally better than if incremental inductances are used.

Table 4-7: Effect of different inductances on damping (including governor)

	Incremental inductances		Saturated inductances		Difference
No.	Eigenvalues (s^{-1})	Damping ratio	Eigenvalues (s^{-1})	Damping ratio	Damping ratio
1,2	-0.4241 ± j0.7657	0.485	-0.4513 ± j0.7654	0.508	4.7%
3,4	-1.600 ± j0.6916	0.918	-1.581 ± j0.6952	0.915	0.33%
5	-5.262	-	-5.272	-	-

4.2.2 Including the stabilising controller

The effect of the SC on the transfer function $\Delta T_e / \Delta\omega$ is shown in Figure 4-5. Without a SC the transfer function has a phase lag of 180° over a wide frequency range (up to about 0.10 Hz). It is this phase lag that causes the instability of the inner loop, as discussed in section 4.1. The SC reduces the phase lag between 0.001 Hz and 10 Hz considerably. The phase lag of 180° at a frequency of 10^{-4} Hz is due to the high-pass filter in the SC. The high-pass filter effectively disables the SC in steady-state conditions. The steady-state speed is determined by the governor, and is not influenced by the SC.

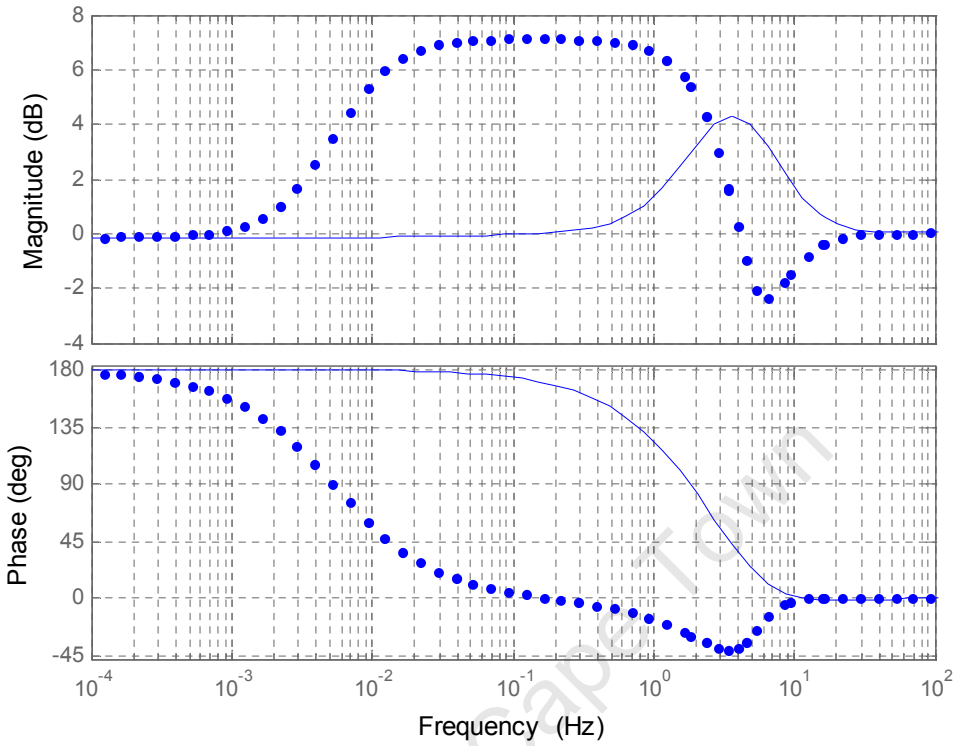

\- Without stabilising controller
* With stabilising controller

Figure 4-4: Bode diagrams of $\Delta T_e / \Delta\omega$

The author analysed the transfer function $\Delta\omega / \Delta\omega_e$, including the SC. He modified Model 2 to include the SC, as shown in Figure 4-5.

Figure 4-6 shows the Bode diagram of the transfer function $\Delta\omega / \Delta\omega_e$, without and with SC. The SC reduces the phase lag. The gain margin is 18.2 dB and the phase margin is 64.7°. The SC increases the phase margin by 32.0°.

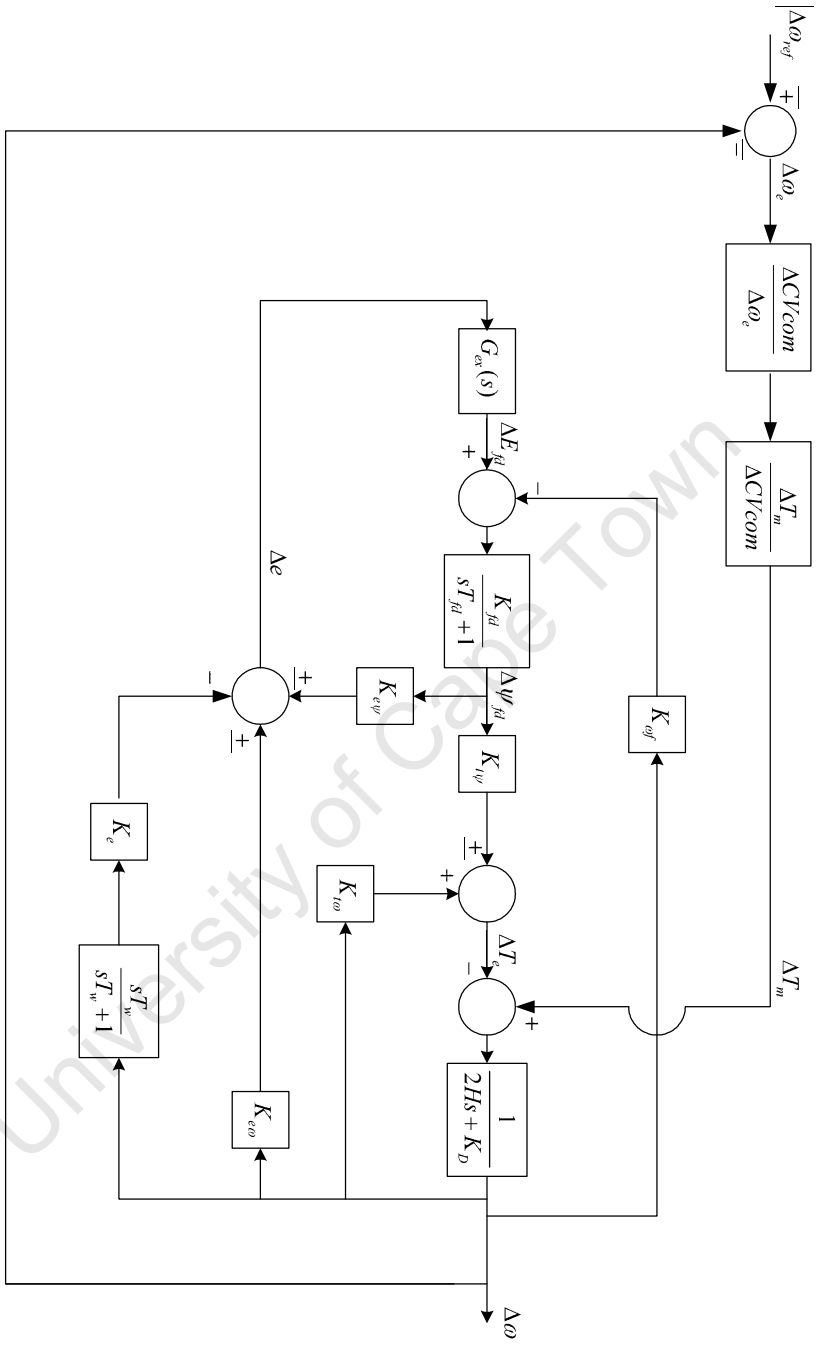

Figure 4-5: Model 2 modified to include the SC

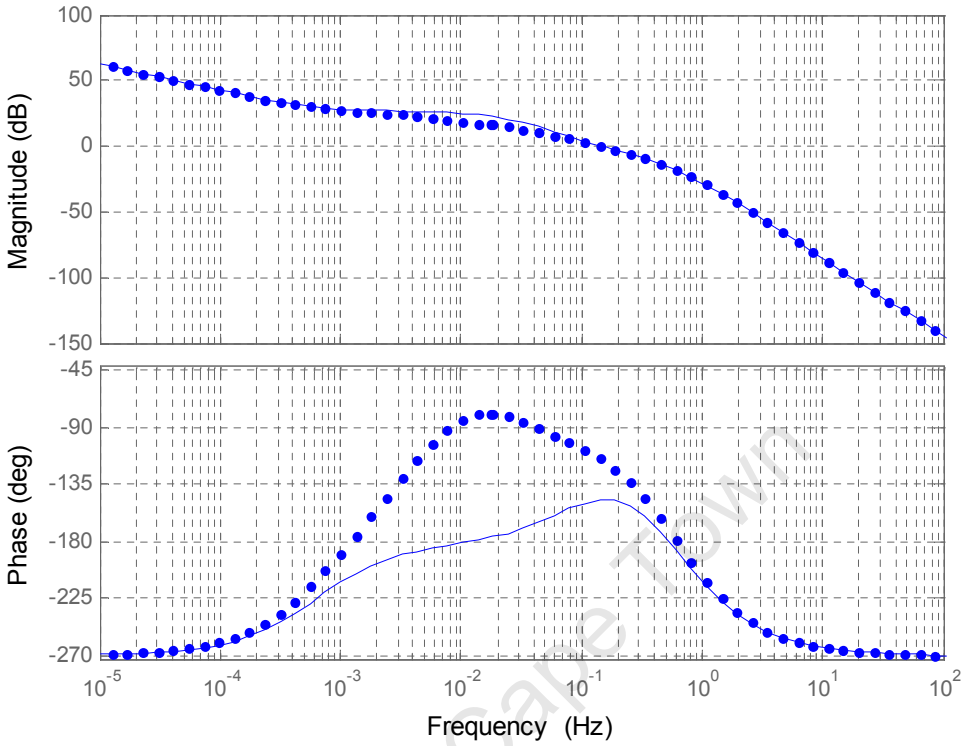

\- Without stabilising controller
* With stabilising controller

Figure 4-6: Bode diagrams of $\Delta\omega/\Delta\omega_e$ (including SC)

Table 4-8 shows the eigenvalue with the lowest damping for the system without SC and with SC. The SC increases the damping of the system in response to small disturbances by 74 %.

Table 4-8: Effect of SC on damping (including governor)

Without stabilising controller		With stabilising controller		Difference
Eigenvalues (s^{-1})	Damping ratio	Eigenvalues (s^{-1})	Damping ratio	Damping
-0.4241 ± 0.7657j	0.485	-0.7360	-	74%

The purpose of the SC (which is derived in section 4.1.3) is to add damping to the system, i.e. it causes the electromagnetic torque ΔT_e to be in phase with the speed

deviation $\Delta\omega$. The derivation of the SC is based on Model 1, which excludes the equations for the field winding, damper windings, saturation and the excitation system. The author checked whether the field winding, saturation and excitation system have any significant affect the performance of the SC.

Figure 4-7 shows the Bode diagram of the following transfer function, as defined by Model 2:

$$TF1 = \frac{\Delta T_e}{\Delta\omega} \tag{4.11}$$

At very low frequencies, e.g. 10^{-4} Hz, the phase of $TF1$ is approximately 180^{o}. This is due to the high-pass filter of the SC. At frequencies beyond 10^{-2} Hz the phase is close to 0^{o}. At a frequencies in the range 3 - 5 Hz the phase is approximately -45^{o}. Therefore, the performance of the SC at such frequencies is not optimal. At A phase-lead compensator could be added to the SC to improve its performance in the frequency range 3 – 5 Hz. This is not investigated further in this thesis.

The author checked whether the SC and governor act in unison, or whether the counteract each other. Figure 4-7 shows the Bode diagrams of the transfer function:

$$TF2 = -\frac{\Delta T_m}{\Delta\omega} = \left.\frac{\Delta T_m}{\Delta\omega_e}\right|_{\Delta\omega_{ref}=0} \tag{4.12}$$

At frequencies lower than 10^{-2} Hz, there is a phase difference of more than 90° between $TF1$ and $TF2$. Therefore, at low frequencies the SC counteracts the governor. The counteraction is insignificant, since at such low frequencies the gain of $TF1$ is negligible compared to the gain of $TF2$.

At frequencies in the range 10^{-2} Hz – 1.0 Hz, $TF1$ and $TF2$ differ in phase by less than 90°, i.e. the SC and governor act in unison.

At frequencies larger than approximately 1 Hz the difference in the phase of $TF1$ and $TF2$ exceeds 90°, i.e. the SC and governor counteract each other. At higher frequencies the phase difference exceeds 90°, but the gain of $TF2$ is much lower than

that of $TF1$. At 4 Hz the gain of $TF2$ is 10 times lower than the gain of $TF1$. Therefore, the author considers the counteraction between the SC and the governor, at frequencies beyond 1 Hz, to be insignificant.

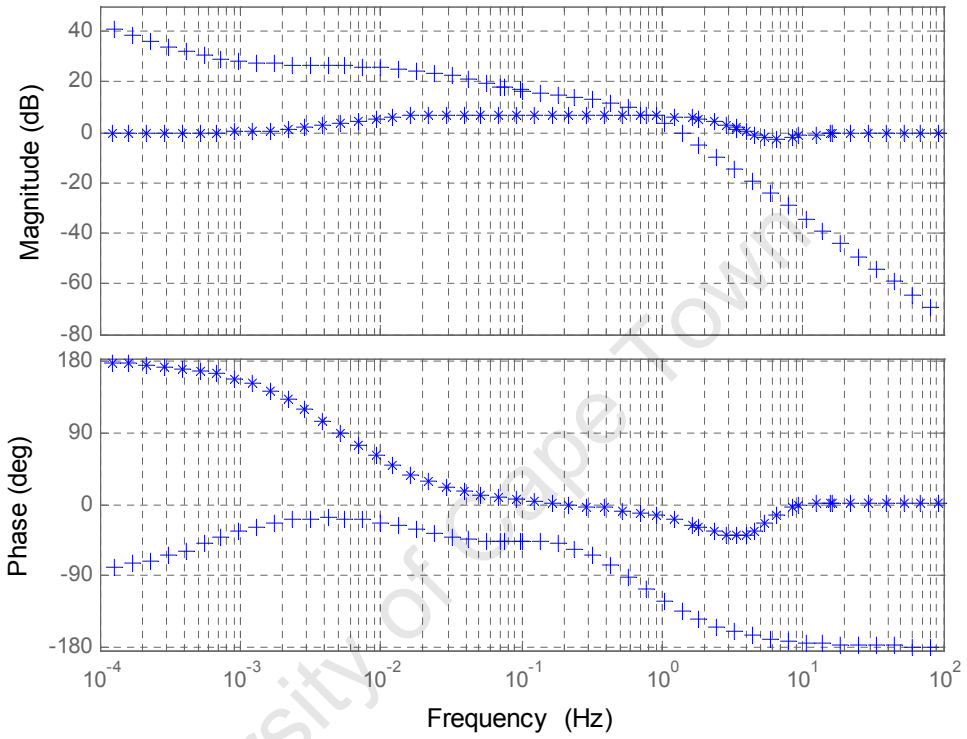

Figure 4-7: Bode diagrams of TF1 and TF2

4.3 Time-domain analysis neglecting the governor

In section 4.3.1 of the thesis the author confirms, by means of time-domain simulation, that the plant without governor is unstable. He compares the (negative) damping that he estimated from the time-domain analysis with the result from the frequency-domain analysis. In section 4.4.2 he confirms that the SC stabilises the plant.

4.3.1 Excluding the stabilising controller

Figure 4-8 shows the speed response of the generator connected to a 175 MW SR (0.826 p.u.), subjected to a step torque disturbance of 0.05 p.u. for 0.1 s. The acceleration increases as the speed increases. This confirms that the power plant without governor is unstable, and that the instability is aperiodic.

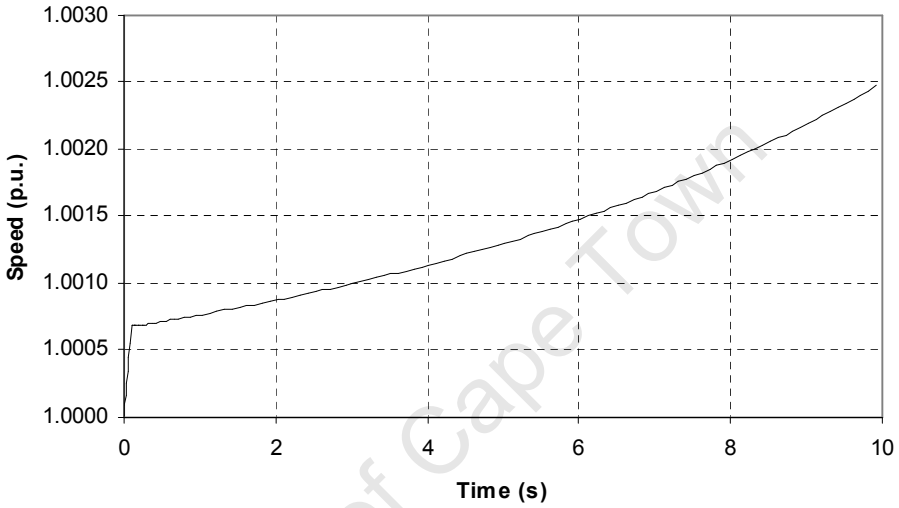

Figure 4-8: Response of plant to a small, temporary torque disturbance (excluding governor and SC)

Figure 4-9 shows the speed response of the generator connected to a 175 MW SR (0.826 p.u.), subjected to a constant torque disturbance of 0.01 p.u. In Appendix E the author calculates the negative damping from this figure. He obtains a result of 0.1339 s^{-1}, which is in close agreement with the figure of 0.1311s^{-1} obtained in section 4.1 (Table 4-3, DIgSILENT PowerFactory, $P_E = 0.826$ p.u.).

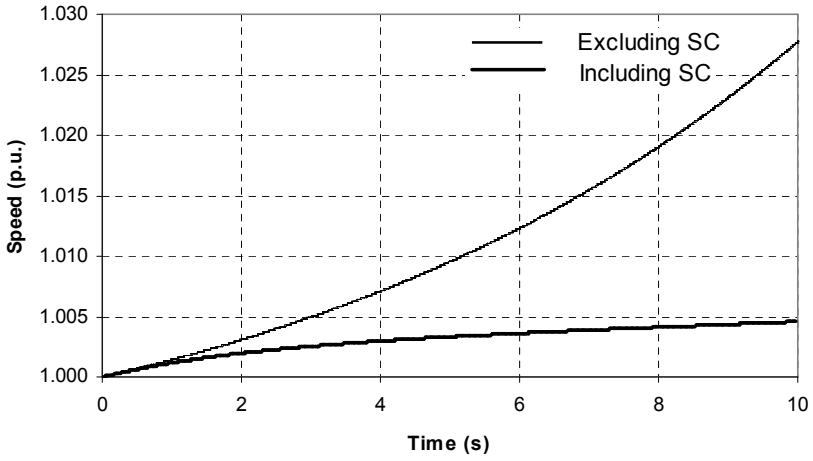

Figure 4-9: Response of plant to a small, permanent torque disturbance (excluding governor)

4.3.2 Including the stabilising controller

In section 4.1 the author calculated the damping of the plant without governor, but with SC. The result was 0.0144 s^{-1} (see Table 4-5). The author verified the magnitude of the positive damping using a time-domain simulation in DIgSILENT *PowerFactory*.

The response of the plant to a 0.01 p.u. disturbance torque, is shown in Figure 4-9. The plant is on the verge of instability, which corresponds to a damping of 0 s^{-1}.

4.4 Time-domain analysis considering the governor

The author investigates, by means of time-domain simulations, the stability of the plant (including governor) under small disturbances. He investigates the response of the plant to a temporary change in speed reference. In section 4.4.1 he excludes the SC from the models, whereas in section 4.4.2 he includes the SC.

In Appendix E the author simulates the response of the plant to a 5 MW change in power – he simulates the disconnection of the generator from the power system (initially operating at 180 MW, 0 MVAr), and the connection, without delay, of a

175 MW SR. In practice there would be a delay between the disconnection from the power system and the connection of the SR. This is considered in Chapter 5.

4.4.1 Excluding the stabilising controller

Figure 4-10 shows the response of the islanded plant (with an 175 MW SR), when its speed reference is decreased by 0.2 %. The disturbance was limited in magnitude and duration to ensure that the control valve would not reach its maximum output. The governor counteracts the decrease in electromagnetic torque, which results from the increase in speed. The response is well-damped.

Figure 4-11 shows the response of the islanded plant (with an 85 MW SR), when its speed reference is increased by 0.2 %. Again, the plant is well-damped.

In Figure 4-10 and Figure 4-11 there is a good agreement between the results from DIgSILENT *PowerFactory* and MATLAB SimPowerSystems. Minor differences in the results are attributed to different methods used to initialise the models: DIgSILENT *PowerFactory* calculates the initial conditions prior to the start of the simulation using equations. MATLAB SimPowerSystems uses a state-vector to initialise the model. The vector is obtained by running a simulation without any disturbance until a steady-state is achieved.

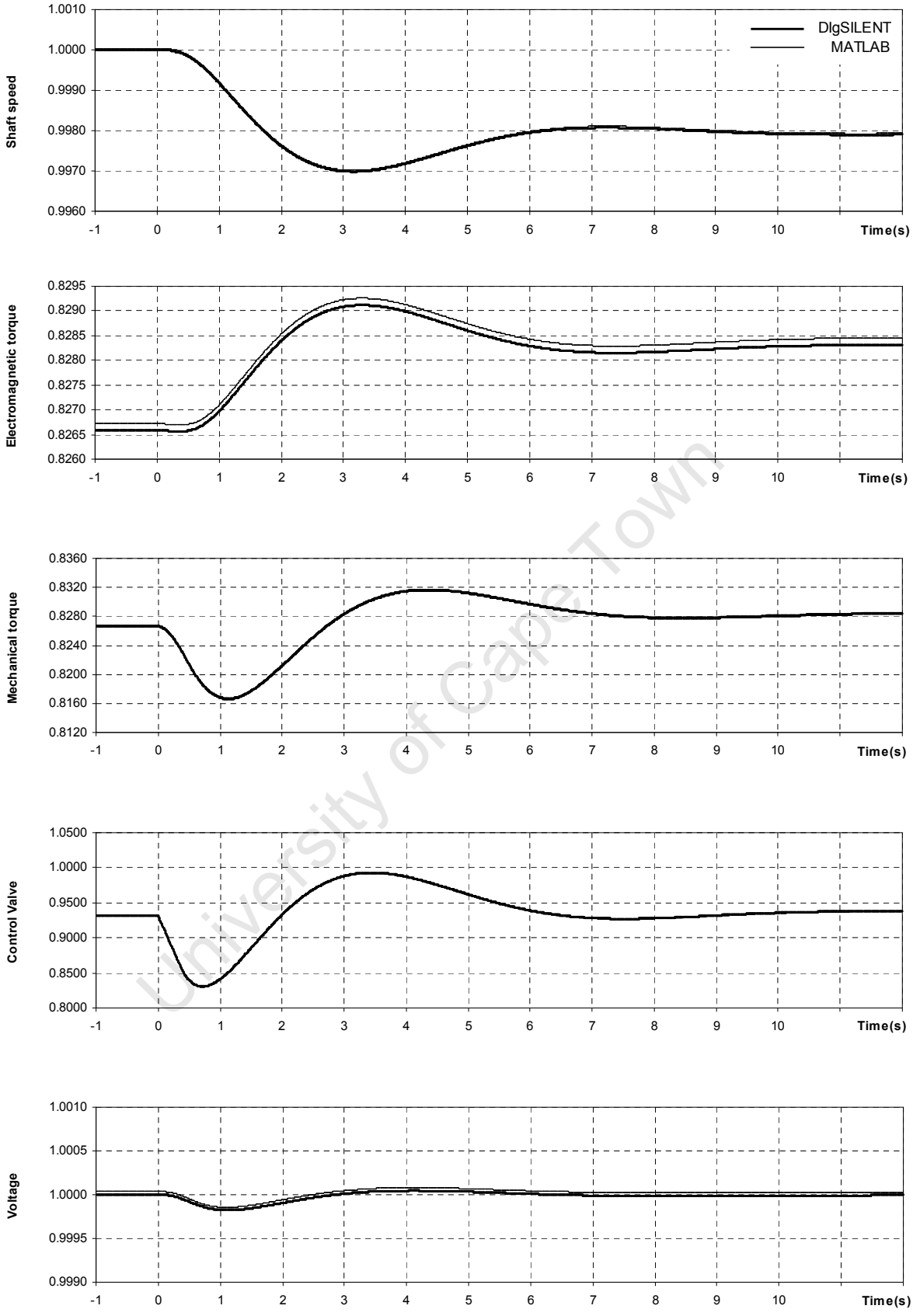

Figure 4-10: Response of the plant to a small disturbance (175 MW, excluding SC)

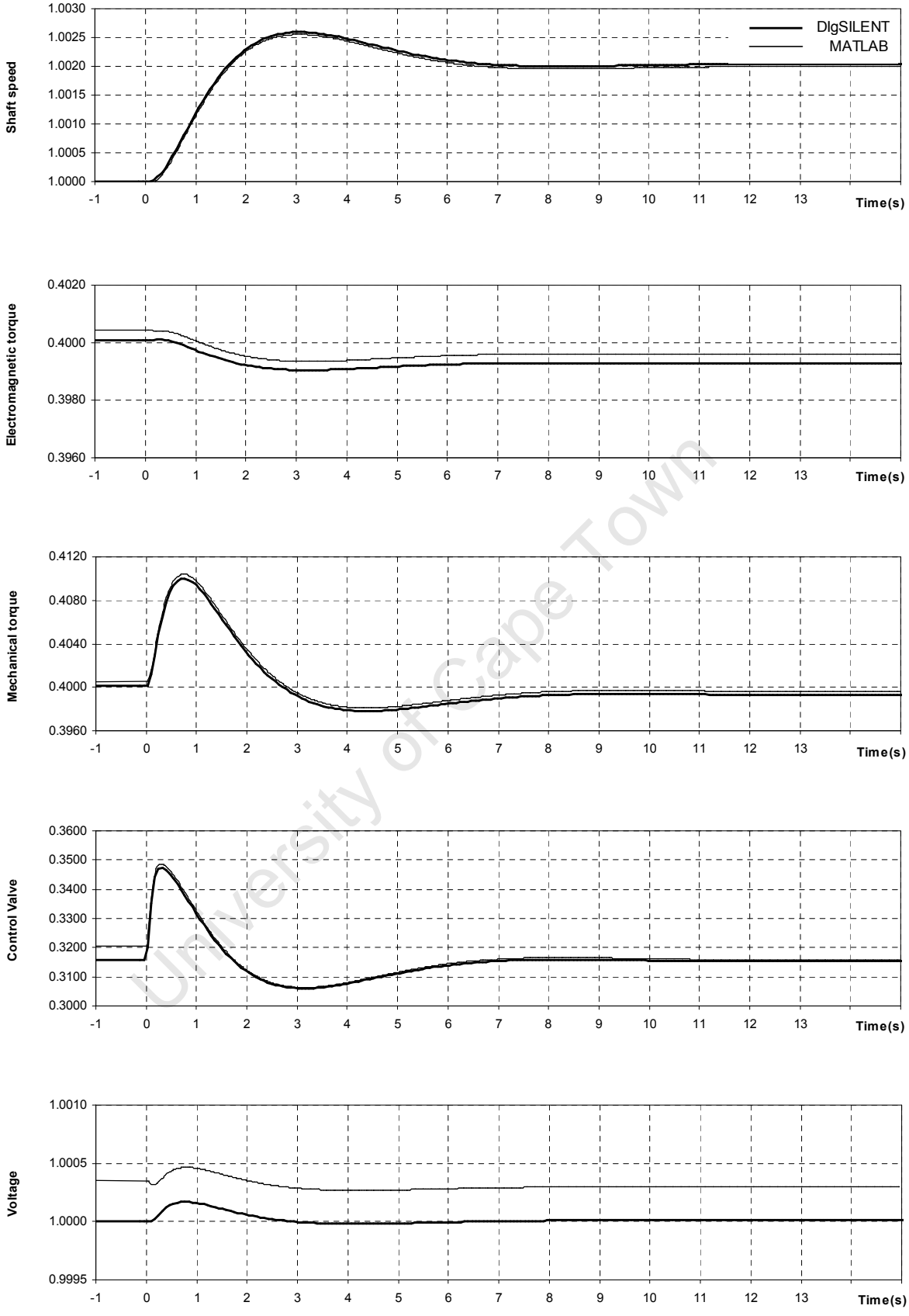

Figure 4-11: Response of the plant to a small disturbance (85 MW, excluding SC)

4.4.2 Including the stabilising controller

Figure 4-12 and Figure 4-13 show the response of the plant (including SC) when it is subjected to a change in speed reference. The disturbances are in section 4.4.1. The SC has the effect of increasing the damping.

There is a good agreement between the results from DIgSILENT *PowerFactory* and MATLAB SimPowerSystems.

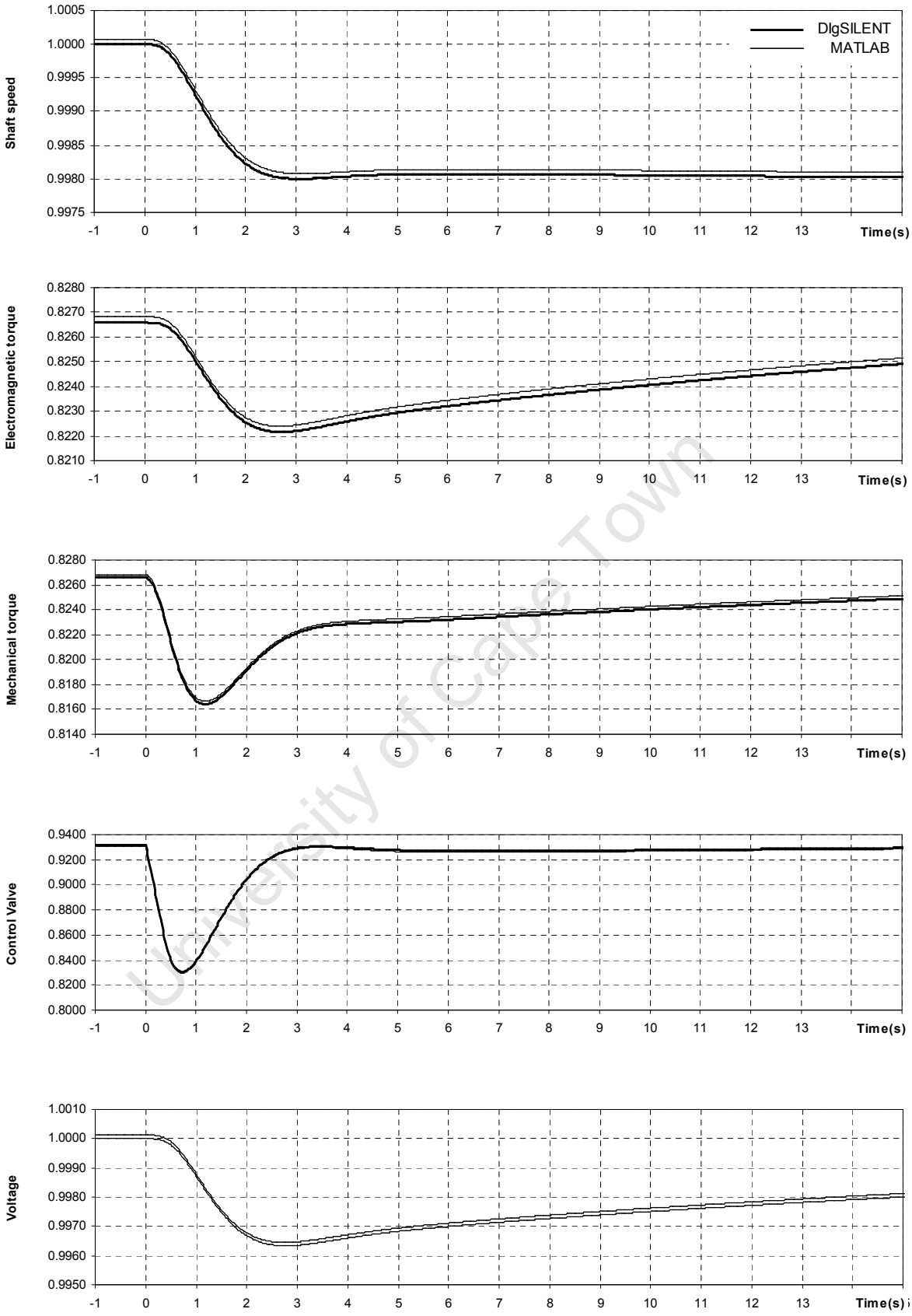

Figure 4-12: Response of the plant to a small disturbance (175 MW, including SC)

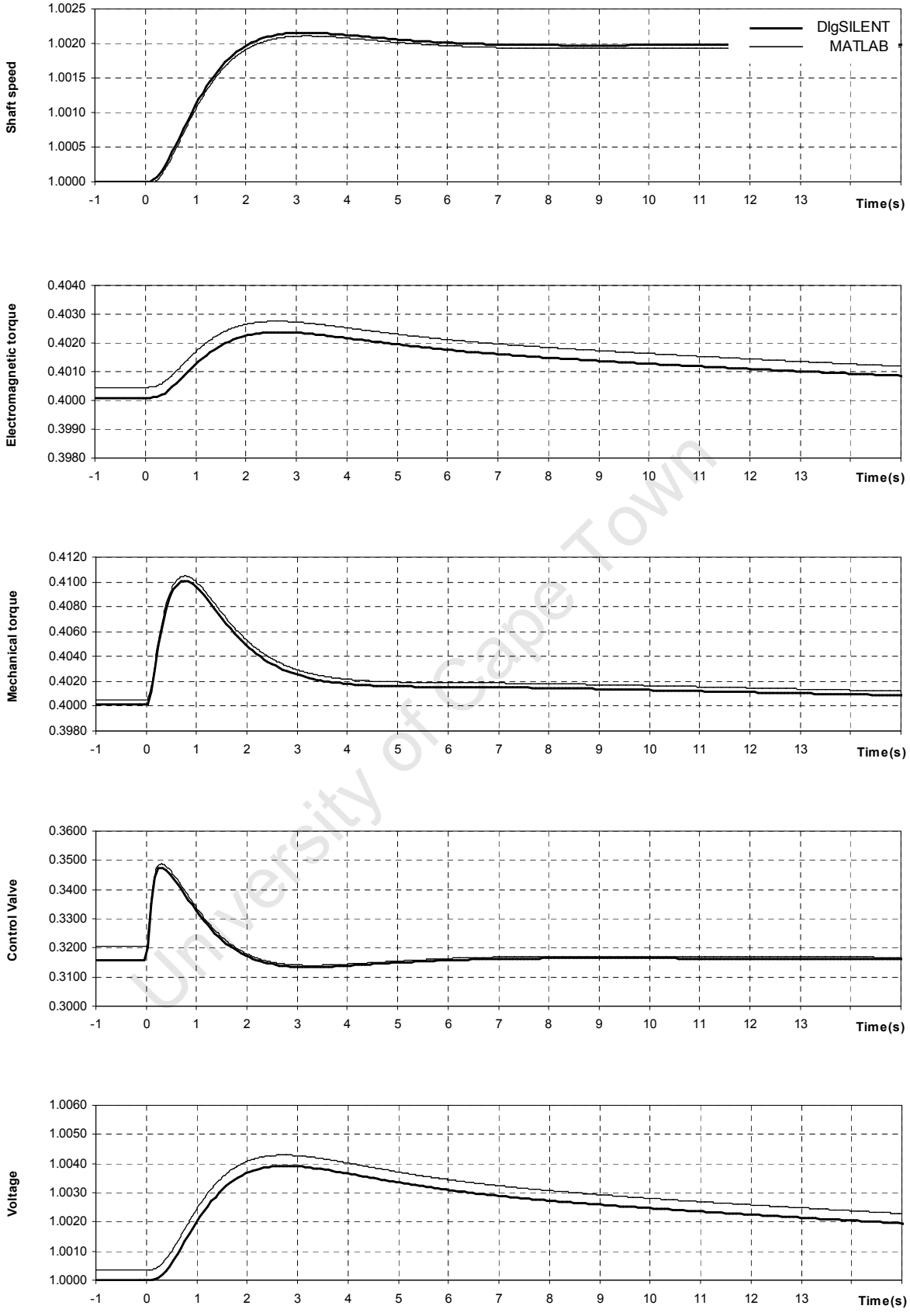

Figure 4-13: Response of the plant to a small disturbance (85 MW, including SC)

4.5 Additional investigations

In the following paragraphs the author investigates the importance of the turbine type and the damper windings on the stability of the islanded plant under small disturbances. He also investigates the response of the plant to a 2 MW increase in power.

4.5.1 Turbine type

In section 4.2, the author presented the eigenvalues of the plant, including the governor and excluding the SC. The analysis was based on the assumption that the turbine is a 'torque machine' (as defined in section 2.4.3). The author now calculates the eigenvalues of Model 2's assuming a power machine instead of a torque machine. For this purpose, he modified Model 2 as explained below.

Equation (4.11) shows a linear form of the relationship $P_m = T_m \cdot \omega$ (at the initial speed of $\omega_o = 1.0$ p.u., and the initial torque of T_{mo}):

$$\frac{\Delta T_m}{\Delta \omega} = \frac{\Delta P_m}{\Delta \omega} + T_{mo} \tag{4.13}$$

Therefore, the initial mechanical torque T_{mo} needs to be added to the transfer function of the turbine model to yield the transfer function $\Delta T_m / \Delta \omega$ of the power machine.

Table 4-9 lists the eigenvalues of Model 2 (based on incremental inductances). The difference in the two different turbine models is observed predominantly in the damping of the two slowest eigenvalues. The author considers the two different methods of modelling the turbine to be important in assessing the stability of the power plant.

Table 4-9: Effect of turbine type on damping

	Torque machine		Power machine		Difference
No.	Eigenvalues (s^{-1})	Damping ratio	Eigenvalues (s^{-1})	Damping ratio	Damping ratio
1,2	-0.4241 ± j0.7657	0.485	-0.5573 ± j0.7339	0.656	35%
3,4	-1.600 ± j0.6916	0.918	-1.524 ± j0.7195	0.904	1.5%
5	-5.262	5.26	-5.278	5.28	0.38%

The author compared the response of the two alternative plants (having either a torque machine or a power machine) by simulating a small disturbance in the time-domain.

Figure 4-14 shows the response of the two plants, to a 0.2 % decrease in speed reference. The plant with the power machine exhibits significantly better damping than the plant with the torque machine. This is in agreement with the eigenvalue analysis.

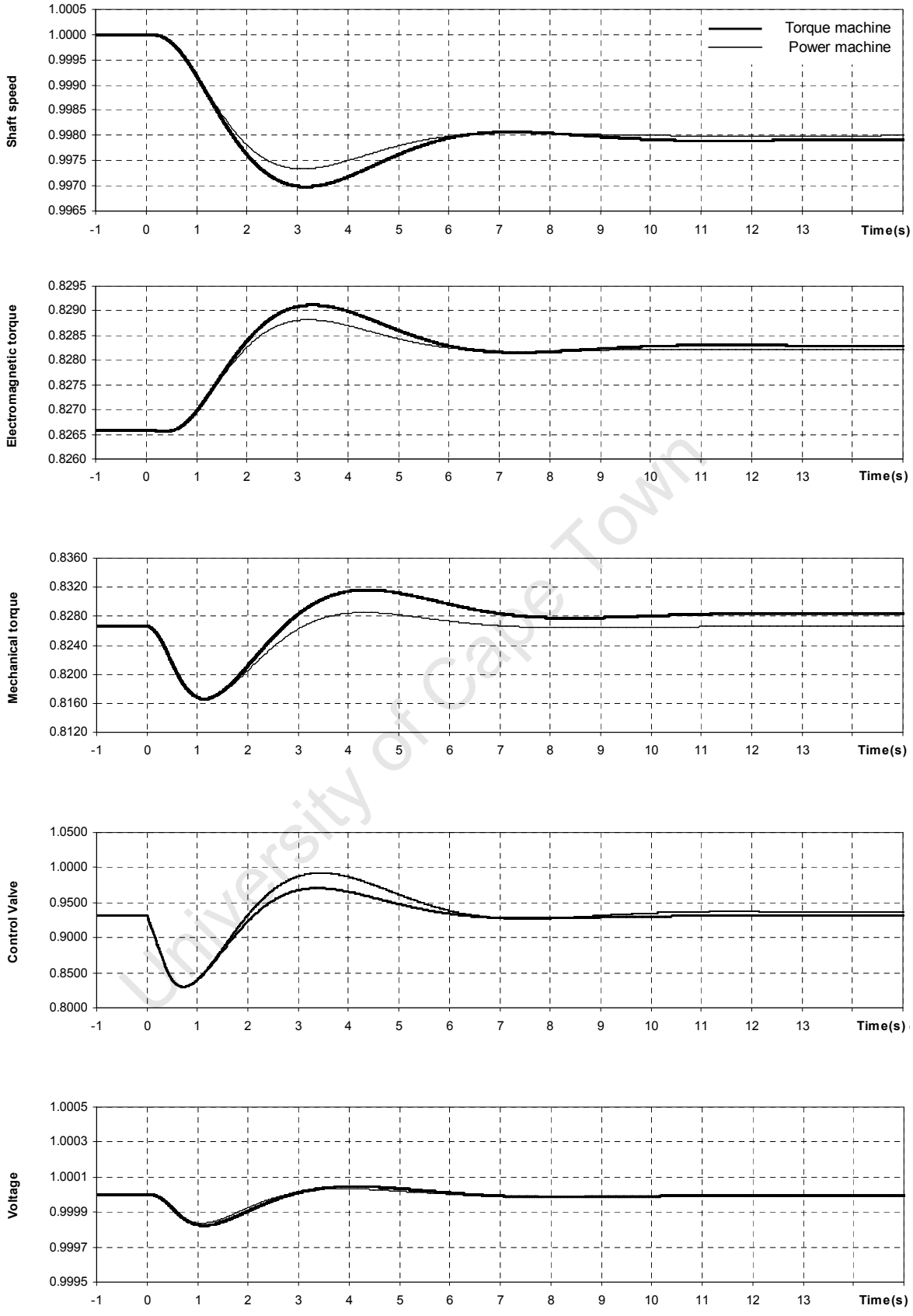

Figure 4-14: Response of the plant to a small disturbance (for different turbine types)

4.5.2 Damper windings

From the analyses in the frequency-domain (section 4.2.1) the author deduced that the damper windings had no significant effect on the stability of the plant under small disturbances. This is now verified using time-domain analyses.

The author temporarily modified the generator model to remove the effects of the damper windings, and simulated the response of the plant to a small disturbance (a change in power of 5 MW). He modified the generator model by setting $X''_d = X'_d$, and $X''_q = X'_q = X_q$.

Figure 4-15 compares the response of a plant without damper windings to the response of the plant with damper windings. The effect of the damper windings on the plant's stability (under small disturbances) is significant - the maximum difference between the speeds is less than 0.1 %. The plant with damper windings has a slightly higher speed overshoot than the plant without damper windings.

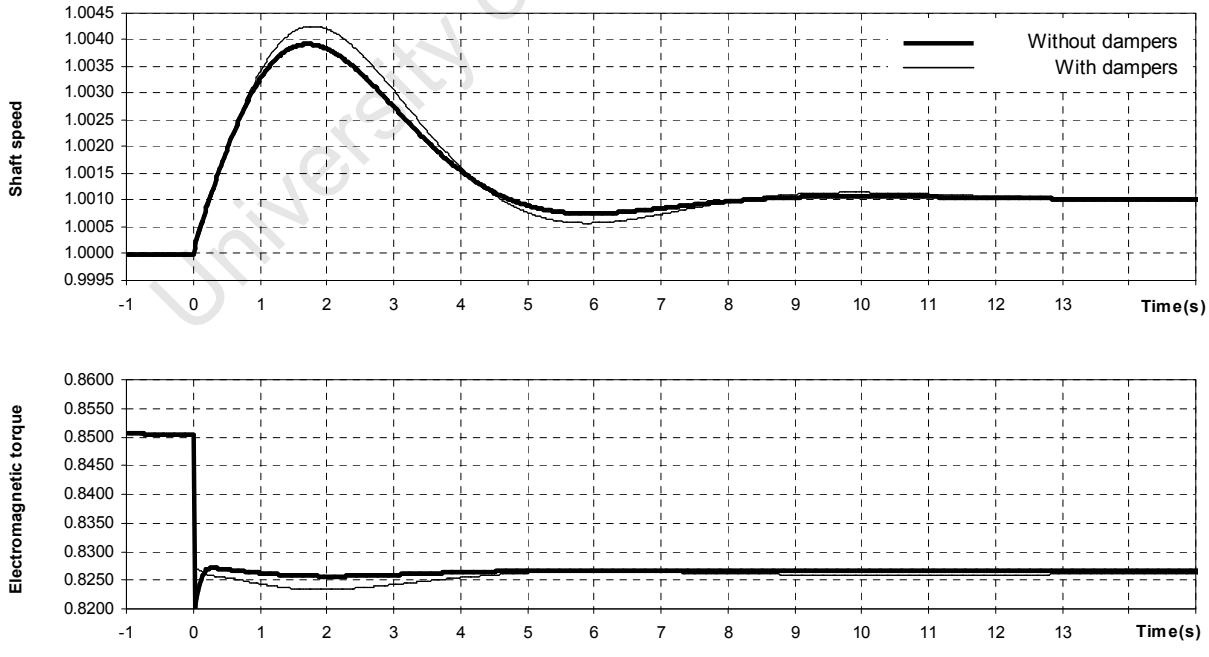

Figure 4-15: Response of the plant to a small disturbance (without and with damper windings)

4.5.3 Step change in power

Figure 4-16 shows the response of the plant (with a 175 MW SR), to a 2 MW increase in active power. If the plant has no SC there is a 6 s period during which the control valve is at its maximum. During this period the governor does not counteract the increasing electromagnetic torque effectively. The inclusion of the SC increases the damping significantly. The responses of additional variables are shown in Figure E-1.

In the case of the 85 MW SR there is no saturation of the control valve position. The response to a 2 MW increase in active power is shown in Figure E-2. As in the case of 175 MW SR, the SC increases the damping.

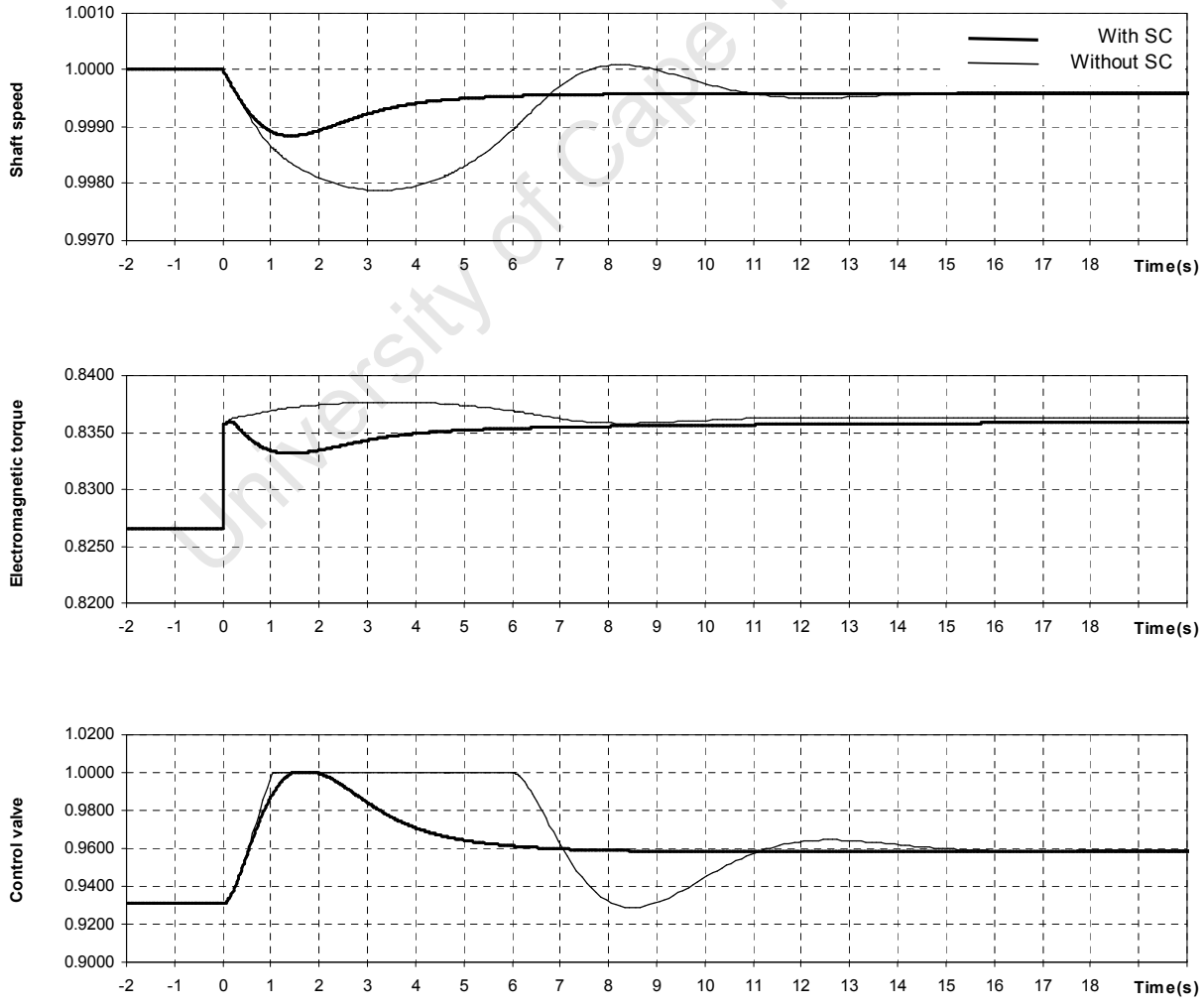

Figure 4-16: Response of plant to 2 MW increase in power (175 MW SR)

4.6 Main findings

The author investigates the stability of the islanded PBMR plant with respect to small disturbances. The SR introduces a destabilising effect, i.e. "negative damping". The generator terminal voltage is approximately constant due to the action of the excitation system, hence the load power is approximately constant. The generator's electromagnetic torque increases (decreases) in response to a frequency decrease (increase). The governor overcomes the destabilising effect, i.e. the plant (with governor) is stable under small disturbances. However, the destabilising effect is undesirable, since it opposes the action of the governor. The author introduces a SC to modify the relationship between electromagnetic torque and speed. The SC causes the generator terminal voltage to increase (decrease) in response to a speed increase (decrease). The inclusion of the SC improves the damping of the plant under small disturbances.

The stability of the plant is affected by turbine type. In the case of the power machine the damping is significantly greater than in the case of the torque machine. The power machine has a self-regulating characteristic, which is lacking in the torque machine.

The author uses models derived by hand, as well as models implemented in two software programmes. He finds that the software packages use saturated mutual inductances and not incremental mutual inductances. However, the results of eigenvalue analyses are not affected significantly by the method of modelling the mutual inductances.

The generator's damper windings do not affect the plant's stability under small disturbances significantly.

Chapter 5 Stability of the power plant under large disturbances

In this chapter the author investigates the stability of the PBMR plant (also referred to as the "system") under large disturbances. The investigation is about the transition to the islanded state. His analyses are done in the time-domain, using the software programmes DIgSILENT *PowerFactory* and MATLAB SimPowerSystems.

The author first investigates the islanding of the plant without connecting the SR. He shows that the shaft speed exceeds the maximum allowable level, leading to a plant shutdown.

Subsequent analyses consider the connection of the SR. The author shows that the SR prevents the speed from exceeding the tripping level. However, depending on the SR power and the turbine type, the plant may be unstable despite the connection of the SR (and despite the action of the governor). The author investigates the cause of the instability and proposes to use the SC, as discussed in Chapter 4. He shows that the combination of the SR and the SC ensures that the plant remains stable following its disconnection from the power system.

The author also investigates whether the plant's stability is affected significantly by the turbine type, by the damper windings, the reactive power prior to the disconnection from the power system, the rate at which the turbine valves can be re-opened and the valve critical flow rate.

5.1 Excluding the SR

If the PBMR plant excludes a SR, it needs to be tripped after being disconnected from the power system. If it is not tripped, the shaft speed may (depending on the initial power) increase beyond the design limit of 130 % - 140 %. This may lead to mechanical failure - the disintegration of rotating components.

The author simulated the response of the plant, initially delivering 180 MW, after being disconnected from the power system. The results, which are shown in Figure 5-1, show that the shaft speed increases beyond 140 % if the plant is not tripped.

If it were possible to increase the valve closing rate, then the shaft speed could be limited below the design limit. Figure 5-2 shows the relationship between the valve closing rate and the maximum shaft speed. For the shaft speed to be limited to 120% the valve closing rate would have to be increased from 0.2 p.u./s to approximately 0.7 p.u./s.

In the case of the PBMR, increasing the valve closing rate could not be achieved. Instead, a SR is connected to the generator terminals. The author investigates the effect of the SR on the plant's stability in section 5.2.

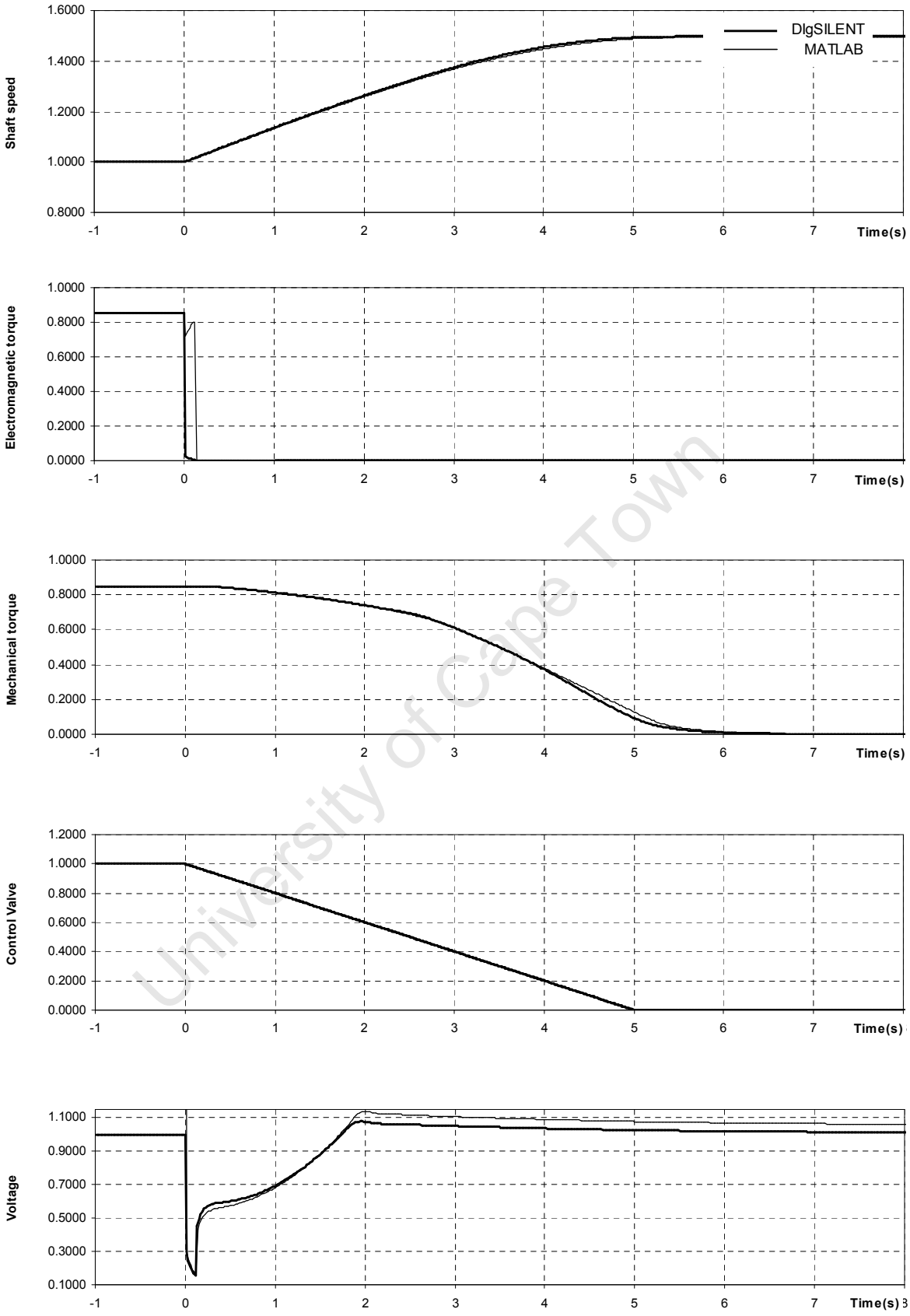

Figure 5-1: Plant response after islanding (excluding SR)

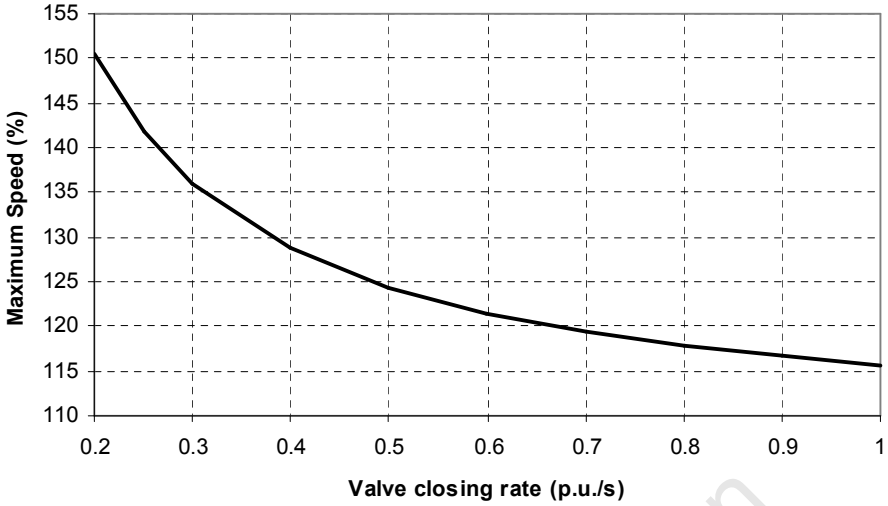

Figure 5-2: Relationship between valve closing rate and maximum shaft speed

5.2 Including the SR

The author investigates the stability of the PBMR plant (including a SR), when it is disconnected from the power system. Prior to the disconnection of the generator from the power system, its power is 180 MW, 0.9 power factor leading, i.e. under-excited. The author chose under-excited operation because it leads to more pessimistic results than over-excited operation – this is investigated further in section 5.3. The author initially assumes a SR rating of 175 MW, and subsequently investigates the effect of lower SR ratings. A 175 MW SR leaves 5 MW available for speed regulation.

The author assumes a three-phase fault, at the high-voltage windings of the transformer. The main breaker is tripped 120 ms after fault inception. After a further 80 ms, i.e. 200 ms after fault inception, the SR is connected. The delay of 80 ms allows for the processing time (i.e. the generation of the closing signal) and the switching time of the SR breakers.

5.2.1 Excluding the SC

Figure 5-3 shows the response of the plant (excluding SC) after being disconnected from the power system. The sudden reduction in electromagnetic torque causes an acceleration of the shaft. The governor responds to the speed increase by closing the valves, causing a reduction in mechanical torque. The connection of a 175 MW (0.826 p.u.) SR causes a sudden increase in electromagnetic torque, which prevents a further speed increase. The speed reaches a maximum of 112 %. The speed declines below the reference of 1.0 p.u. The generator voltage quickly settles at an approximately constant value due to the action of the excitation system. Therefore, the power dissipated by the SR is approximately constant. A decrease in speed causes an increase in electromagnetic torque, which causes a further shaft deceleration. The governor responds to the low speed by opening the valves. The mechanical torque increases to its maximum, but this is insufficient to accelerate the shaft. In summary, the SR has a stabilising effect, since it prevents the shaft speed from exceeding the design limit. However, the SR also has a destabilising effect – the plant becomes unstable after the speed has reached its maximum value.

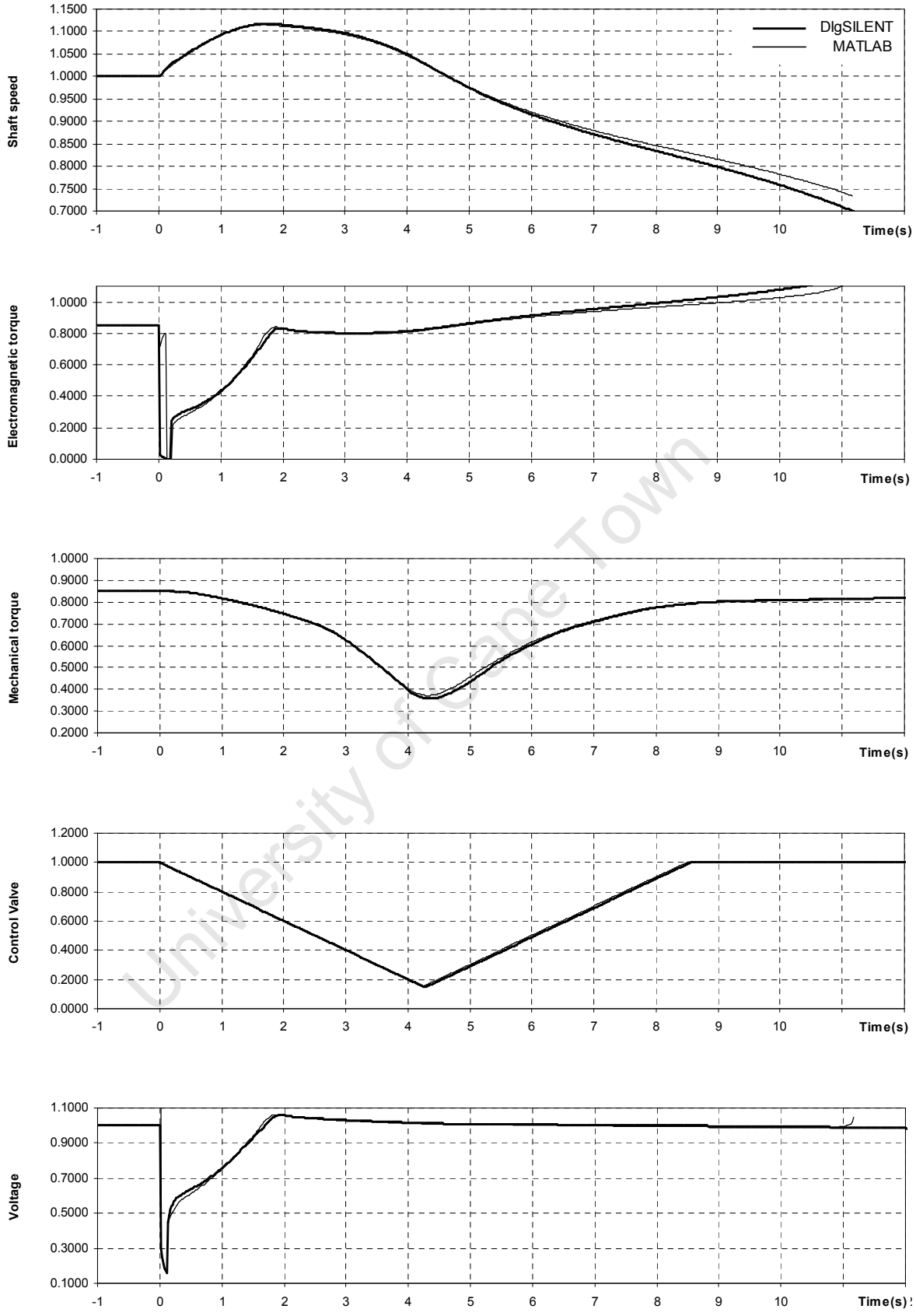

Figure 5-3: Plant response after islanding (including 175 MW SR, excluding SC)

An SR rating lower than 175 MW is advantageous, since it results in a reduction in physical space and cost. However, a reduction in SR rating leads to higher maximum speeds. Figure 5-4 shows the relationship between the SR rating and the maximum speed. To limit the speed below 130 % the SR rating needs to be about 80 MW.

A reduction in SR rating also increases the burden on the mechanical plant - the power that is not dissipated by the SR leads to an increase in the gas temperature. The study of this effect is beyond the scope of the thesis.

Figure 5-4: Relationship between SR rating and maximum speed

The author also considers the stability of the plant equipped with an 85 MW (0.40 p.u.) SR. He simulates the islanding of the plant, assuming an initial generator power of 180 MW, 0.9 power factor leading. The speed response is shown in Figure 5-5. The plant is on the verge of instability, i.e. it is very poorly damped. The mechanical torque exhibits cycles, having amplitude of approximately 70 % and duration of 10 s. Oscillations in the electromagnetic torque approximately coincide with those in mechanical torque, i.e. the electromagnetic torque counteracts the effect of the governor.

It is noted that the analyses in Chapter 4 showed the islanded plant (with an 85 MW SR) to be stable and well damped under small disturbances. Therefore, the poor damping only applies to large disturbances. In section 5.3.1 the author shows that poor stability occurs also if the turbine is a power machine. The destabilising effect between electromagnetic torque and speed is not the primary cause of the poor damping, but it contributes to the poor damping.

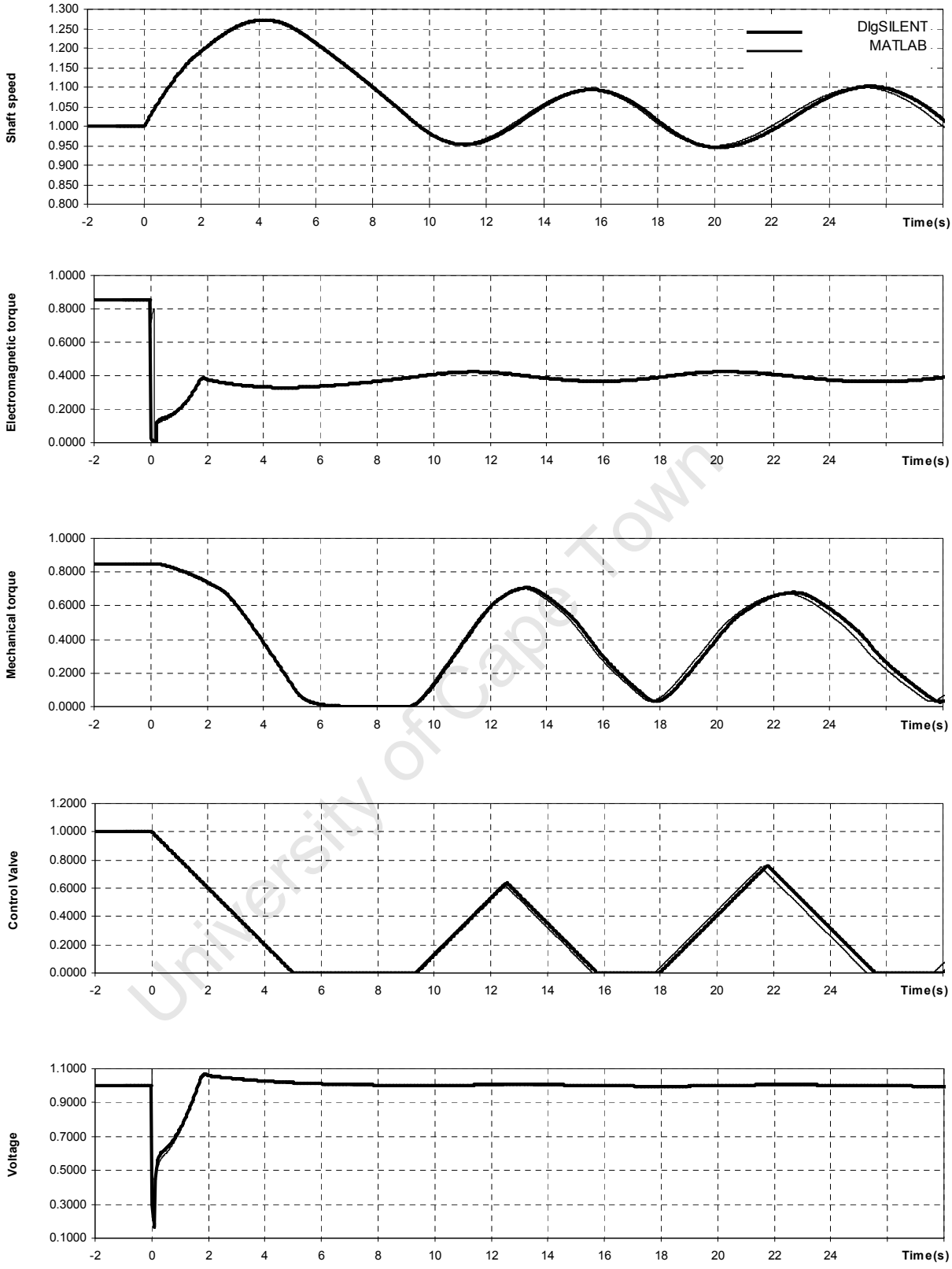

Figure 5-5: Plant response after islanding (including 85 MW SR, excluding SC)

5.2.2 Including the SC

As explained in the previous section, the SR limits the maximum speed to a safe value, but it also introduces a destabilising effect. The stabilising effect of the governor is limited by the rate at which mechanical power can be increased, the turbine type (power machine or torque machine) and by the maximum turbine torque. The author proposes a SC, which "removes" the destabilising relationship between electromagnetic torque and speed, and improves the plant's stability.

Figure 5-6 shows the response of the plant (including a 175 MW SR and a SC) after islanding from the power system. As in the analyses of section 5.2.1, the author assumes a fault at the high-voltage side of the transformer, the opening of the main breaker after 120 ms, and the connection of the SR after a further 80 ms. The plant is stable due to the combined action of the governor and the SC. The maximum speed is 112 %, and the speed response is well damped. The SR limits the maximum speed, whereas the SC ensures the plant remains stable after being disconnected from the power system.

Figure 5-7 shows the response of a similar analysis, but based on an 85 MW SR. The plant with the SC no longer exhibits the limit cycles observed in Figure 5-5. It may be possible to improve the plant's response further using phase-lead compensation in the governor. This could be considered in the final design.

There is a good correlation between the results from DIgSILENT *PowerFactory* and MATLAB SimPowerSystems.

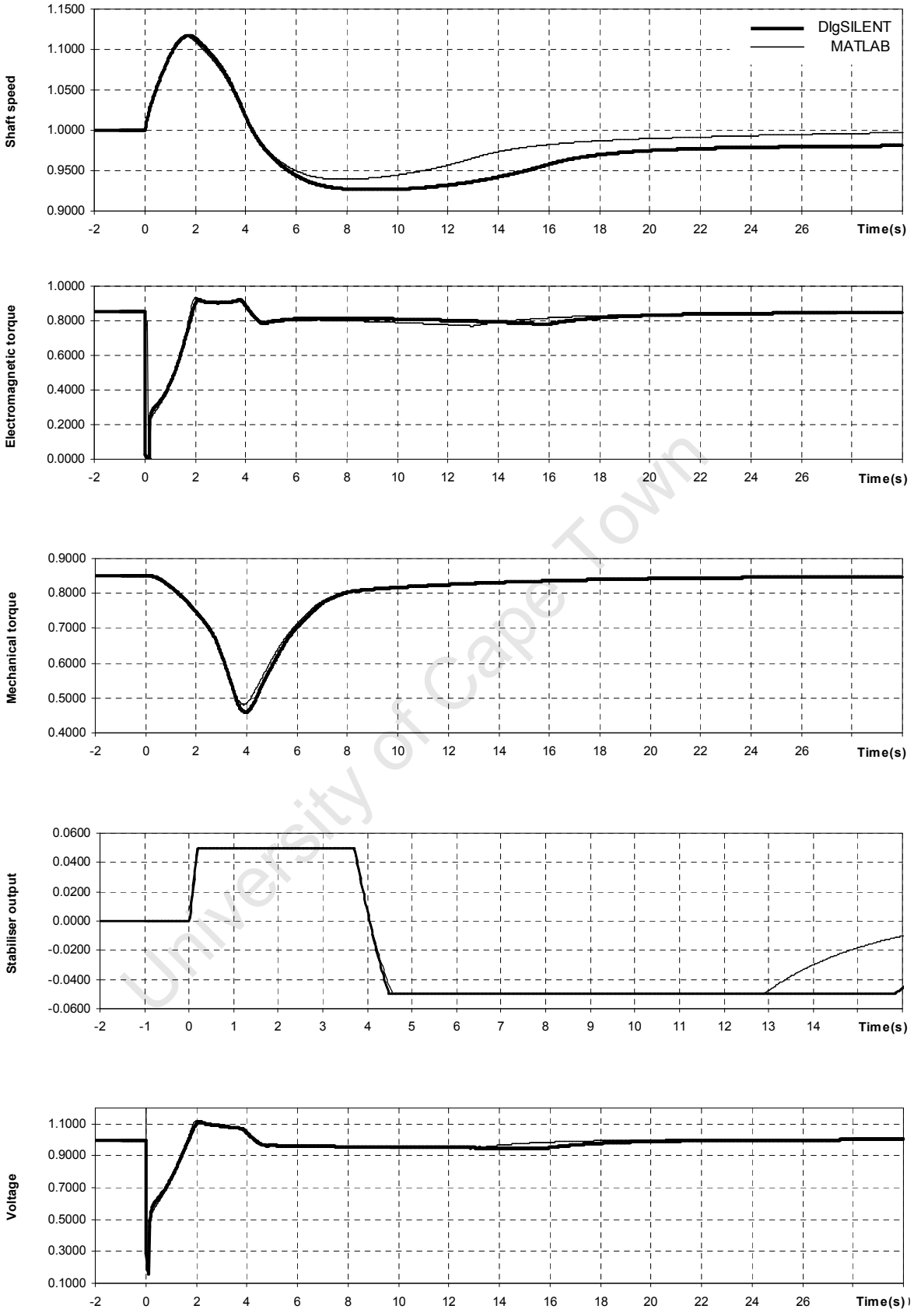

Figure 5-6: Plant response after islanding (including 175 MW SR and SC)

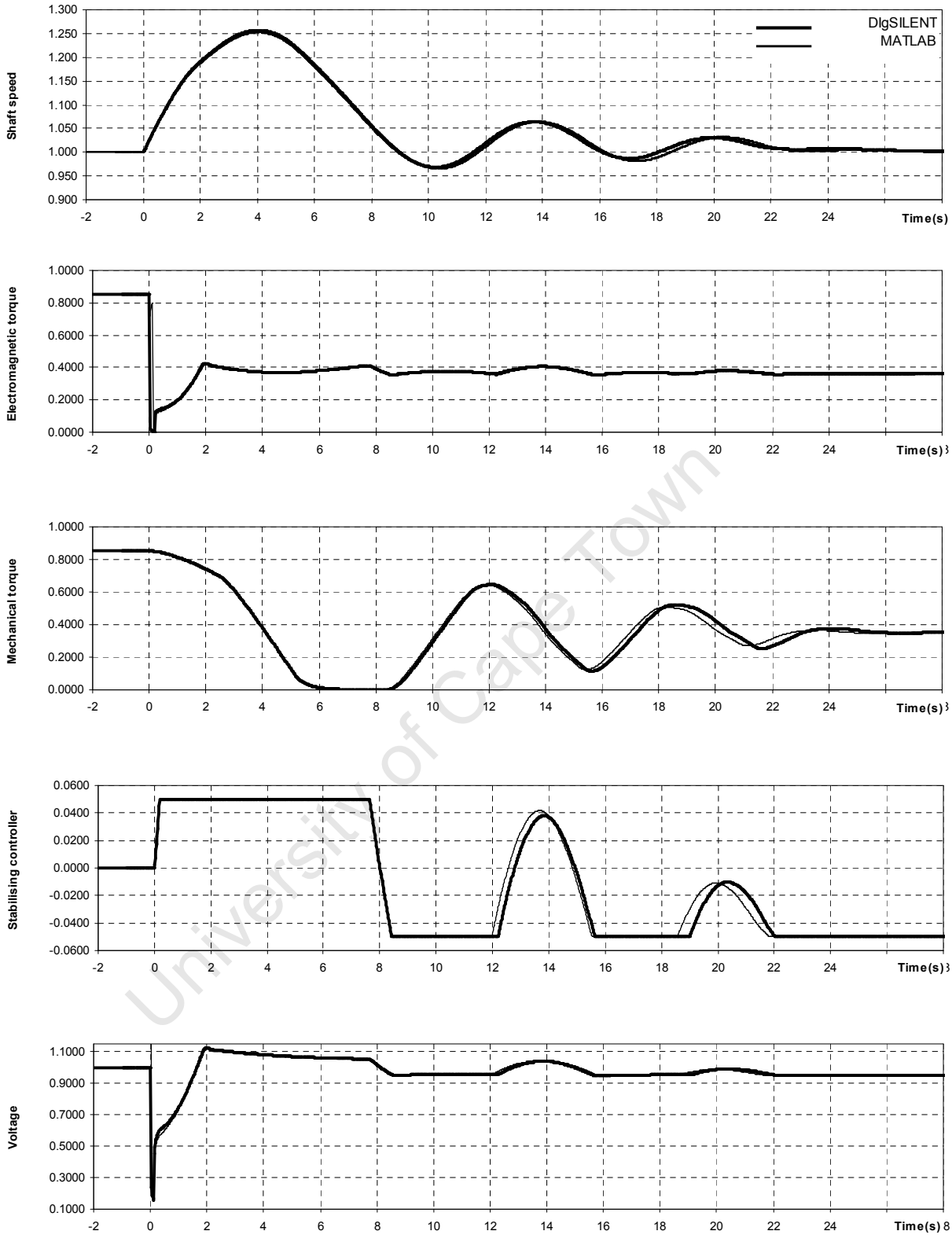

Figure 5-7: Plant response after islanding (including 85 MW SR and SC)

5.3 Additional investigations

In this section the author continues the investigation into the stability of the PBMR plant, when it islands from the power system. He investigates the following:

- The effect of the turbine type (power machine versus torque machine).
- The impact that the damper windings have on the plant's response.
- The effect of the reactive power prior to disconnecting the plant from the power system.
- The effect of increasing the valve opening rate.
- The effect of valve critical flow rate (i.e. valve choking).

The author performed all analyses using the software DIgSILENT *PowerFactory*. The following sections summarise the analyses corresponding to the above.

5.3.1 Turbine type

In section 5.2 the author assumes that the turbine is a torque machine. In Chapter 4 the author showed the plant would be better damped if the turbine was a power machine rather than a torque machine. In a power machine, mechanical torque increases (decreases) in response to a speed decrease (increase), even without governor action. This effect counteracts speed deviations, and it counteracts the destabilising response of the electromagnetic torque.

Figure 5-8 and Figure 5-9 show the effect that the turbine type has on the plant's stability (the responses of additional variables are shown in Figure F-1 and Figure F-2). As in the case of the analyses in sections 5.1and 5.2, the initial operating power is 180 MW, 0.9 power factor leading. In the case of the 175 MW SR the turbine type is very important - the plant having a power machine is stable; whereas the plant with the torque machine is unstable. In the case of the 85 MW

SR the turbine type is less important – the plant exhibits significant oscillations regardless of the turbine type.

It is interesting to note that the response of the plant with the power machine and no SC is worse than the response of the plant with a torque machine and SC.

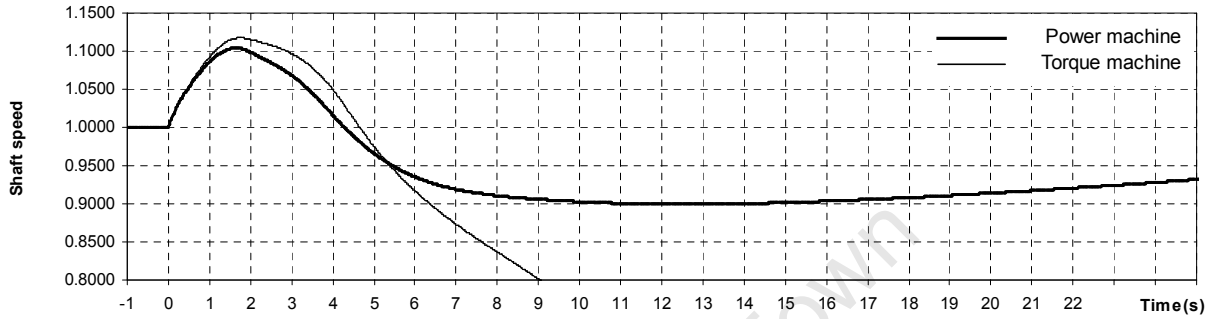

Figure 5-8: Plant response after islanding, and effect of turbine type (175 MW SR, excluding SC)

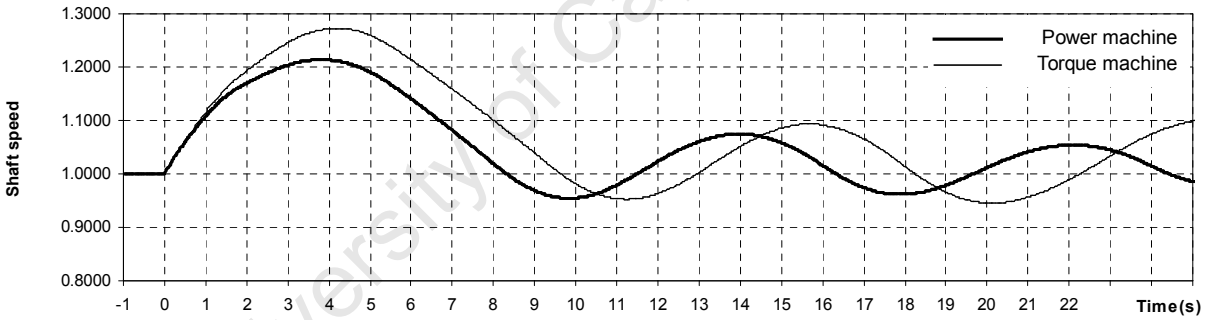

Figure 5-9: Plant response after islanding, and effect of turbine type (85 MW SR, excluding SC)

5.3.2 Damper windings

The author investigated the effect of the damper windings by comparing the response of the plant without damper windings to a plant with damper windings. The model of the plan without damper windings is obtained by setting $X''_d = X'_d$, and $X''_q = X'_q = X_q$.

Figure 5-10 shows the response of speed and electromagnetic torque (the responses of additional variables are shown in Figure F-3). As before, the disturbance is

defined by a short circuit at the high-voltage terminals of the unit transformer at time 0 s, the tripping of the main breaker after 120 ms, and the closure of the SR breaker at time 200 ms. The generator initially delivers 180 MW, 0.9 power factor leading.

The damper windings do not affect the magnitude of the maximum speed significantly. The effect of the damper windings is to lower the minimum speed. The damper windings retard changes in the electromagnetic torque, and reduce the stability of the islanded plant under large disturbances.

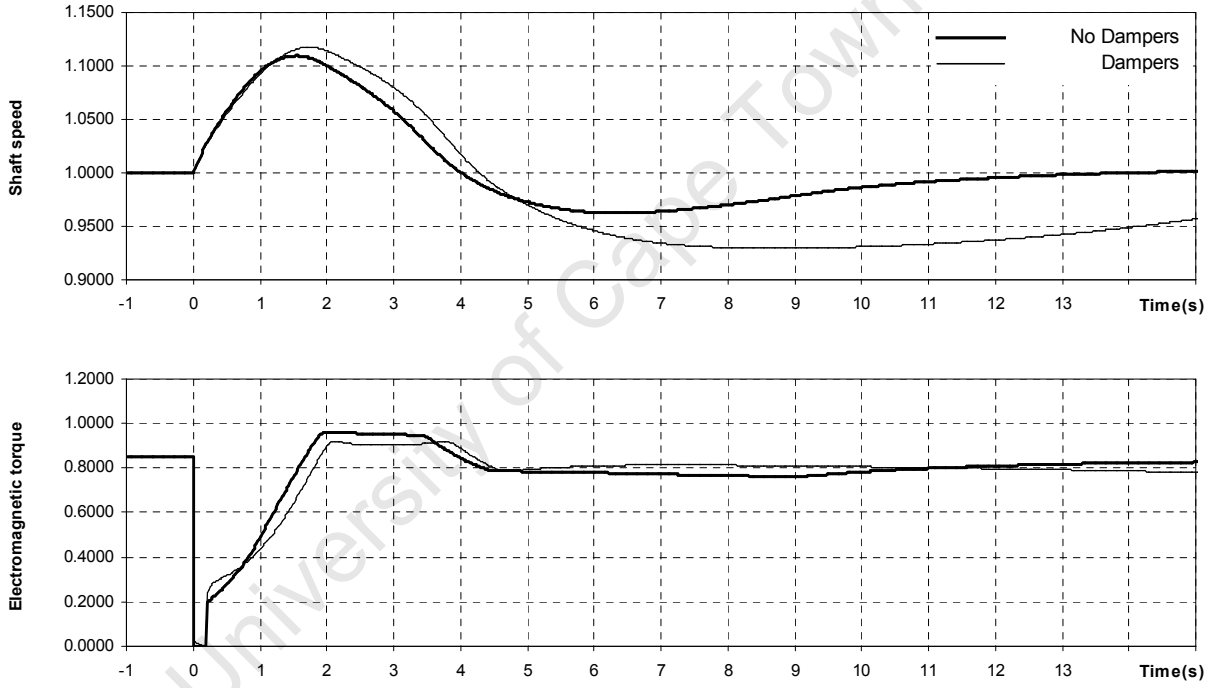

Figure 5-10: Plant response after islanding, and effect of damper windings (including 175 MW SR and SC)

5.3.3 Reactive power prior to islanding

The level of reactive power prior to islanding affects the speed response after islanding. This is because the excitation current affects the electromagnetic torque, and the excitation current cannot change instantly when the plan is disconnected from the power system.

Figure 5-11 shows the plant's response assuming three different initial levels of reactive power (corresponding to power factors of 0.90 under-excited, 1.00, and 0.90 over-excited). The disturbance is as in section 0. The responses of additional variables are shown in Figure F-4.

The reactive power prior to islanding has a significant effect on the plant's stability under large disturbances. The low level of excitation current corresponding in the case of under-excited operation leads to a significant drop in voltage when the SR is connected, and hence a relatively low level of electromagnetic torque.

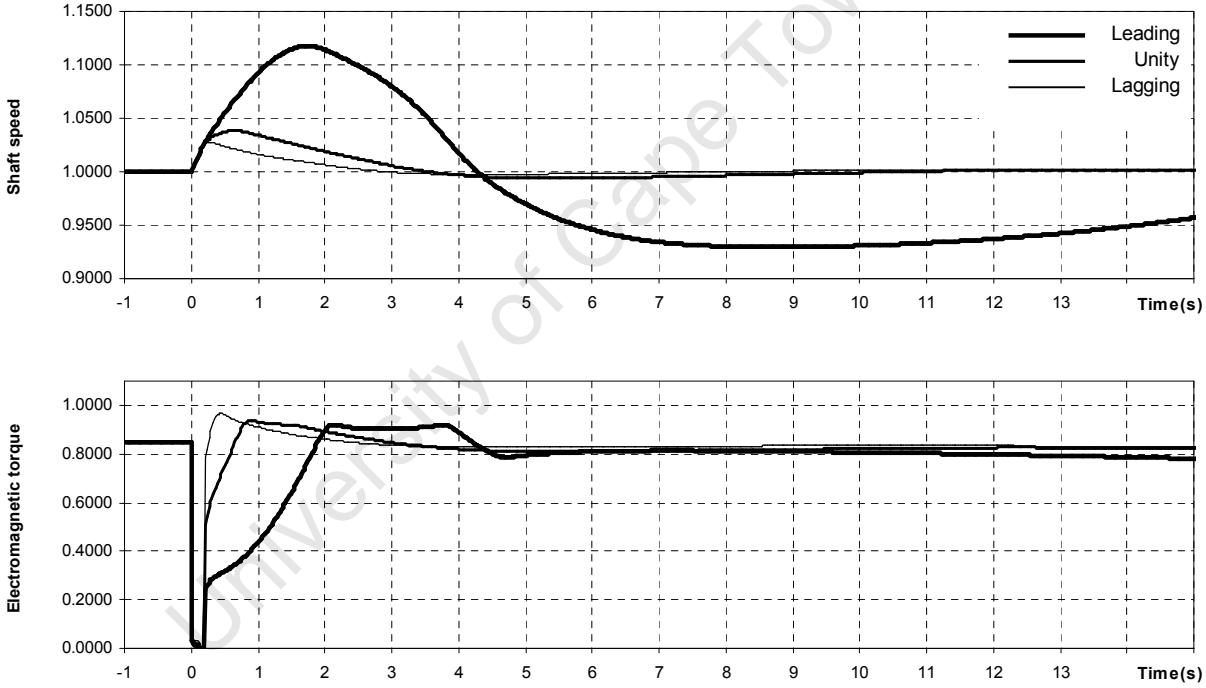

Figure 5-11: Plant response after islanding, and effect of reactive power (including 175 MW SR and SC)

5.3.4 Valve opening rate

The author investigates the effect of the rate of increase in mechanical torque. More specifically, he investigates the effect of an increase in the maximum valve opening rate (from 0.2 p.u./s to 1.2 p.u./s). He considers two SR ratings – 175 MW (0.826 p.u.) and 85 MW (0.40 p.u.).

The speed responses are shown in Figure 5-12 (175 MW SR) and Figure 5-13 (85 MW SR). The responses of additional variables are shown in Figure F-5 and Figure F-6. In the case of the 175 MW SR, the author found that no rate of increase in the valve opening rate would stabilise the plant, i.e. the SC is essential in ensuring the plant's stability. In the case of the 85 MW SR, an increase in the valve opening significantly improves the plant's stability.

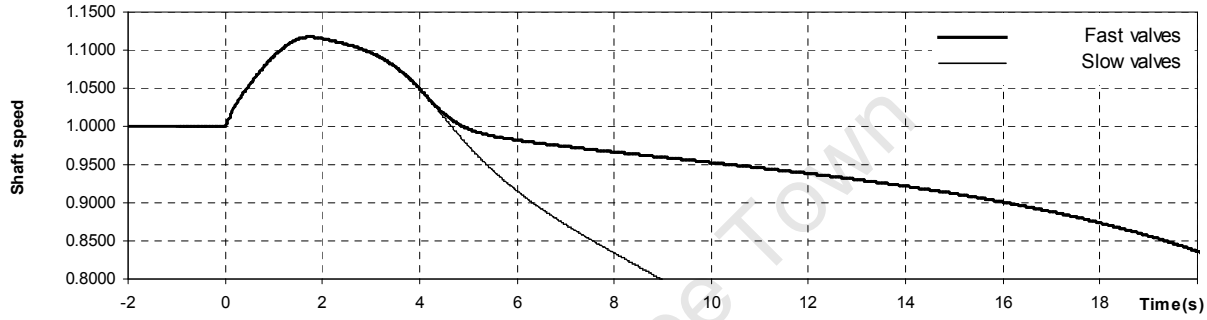

Figure 5-12: Plant response after islanding (175 MW SR, no SC, fast valves)

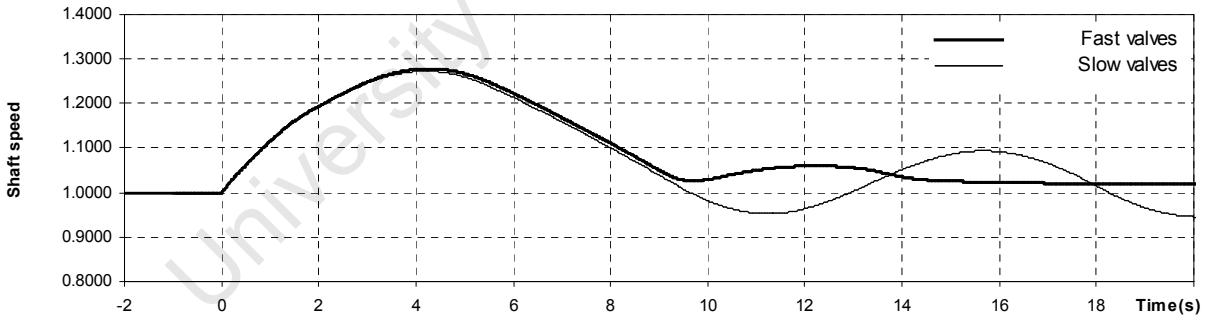

Figure 5-13: Plant response after islanding (85 MW SR, no SC, fast valves)

5.3.5 Valve critical flow rate

The author repeated the analyses of section 5.2.2, i.e. including SR and SC, also considering the critical flow rate. He found that, in the case of the 175 MW SR there was no significant valve choking – the variable A remained above 0.999 throughout the simulation. In the case of the 85 MW SR valve choking has a significant impact

on the plant's response – see Figure 5-14 (the responses of additional variables are shown in Figure F-7). However, considering valve choking in the simulation does not change the conclusions of section 5.2.2.

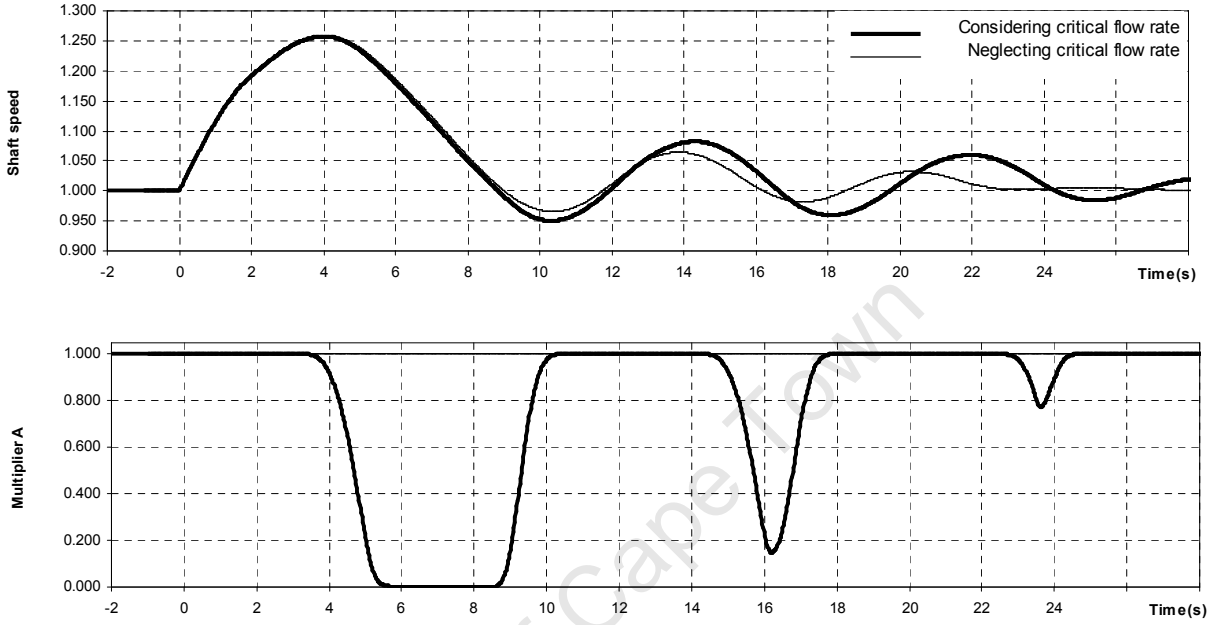

Figure 5-14: Plant response after islanding (85 MW SR, SC, considering valve critical flow rate)

5.4 Main findings

The author studies the stability of the plant under large disturbances. He simulates the disconnection of the plant, initially operating at 180 MW, from the power system, followed by the connection of the SR. The connection of a SR limits the maximum speed below 130 %. For example, a 175 MW SR limits the speed below 115 %, and an 85 MW SR limits the speed below 130 %.

In the case of the 175 MW the plant is unstable despite the connection of the SR. This is because of the destabilising effect of the electromagnetic torque in response to speed changes. The governor counteracts the destabilising effect, but it fails to stabilise the plant due to saturation of its output. The author shows that the plant

remains stable if the plant has a SC, i.e. the plant remains stable under the combined action of the SR, governor and SC.

In the case of an 85 MW SR the plant is on the verge of instability – the counteraction of electromagnetic torque and mechanical torque contributes to the poor stability. The inclusion of the SC stabilises the plant.

The stability is affected significantly by the turbine type – a plant with a power machine, a 175 MW SR and no SC is stable, whereas the plant with a torque machine is unstable.

The level of reactive power prior to islanding has a significant effect on the speed response. The highest speed overshoot occurs if the plant initially operates at its maximum leading power factor (under-excited).

The author showed that the generator damper windings have a moderate effect on the speed response.

Chapter 6 Conclusions and recommendations

The development of the Pebble Bed Modular Reactor (PBMR) – a new generation nuclear power plant – brought about many new challenges. The designers selected a particularly high gas temperature (in excess of 900°C) in order to achieve high plant efficiency. This places severe constraints on the design of the turbine valves, and hence on the control of mechanical power. A sudden loss of electrical load required the plant to be tripped through the operation of shutdown valves. If the plant is not tripped the shaft speed increases above the design limit of 140 %, which can lead to mechanical failure.

The PBMR plant's investors require the plant to be capable of islanding, i.e. continuing operation following its disconnection from the power system. To achieve this requirement, the designers proposed that a high-energy resistor – the stabilising resistor (SR) – should be connected to the generator terminals during islanded operation. The SR should limit the shaft speed below the design limit, even without shutting down the plant.

The author investigates whether the SR does indeed stabilise the generator. He prepares models of the PBMR plant and implements these in two software programmes. He investigates the plant's stability under large disturbances, namely transitions from normal operation to islanded operation. He also investigates the stability of the islanded plant under small disturbances.

The author finds that the SR limits the shaft speed below the design limit, as expected. The SR rating should be between 85 MW and 175 MW. If the initial generator power is 180 MW then an 85 MW SR limits the speed to 127 %, leaving 95 MW reserve power. A 175 MW SR limits the speed to 112 %, leaving 5 MW of reserve power. A designer would prefer a relatively low SR rating to limit the cost

and physical size. On the other hand, the margin between the maximum speed and the allowable speed decreases as the SR rating is decreased.

The SR stabilises the plant in that it prevents the shaft speed from exceeding the design limit. However, the SR also introduces a destabilising effect: This is due to the fact that the SR acts (approximately) as a constant power load, since the excitation system maintains (approximately) a constant voltage at the generator terminals, and the resistance does not vary with frequency. Therefore, the SR power is independent of speed. A decrease (increase) in speed leads to an increase (decrease) in electromagnetic torque, which tends to cause a further decrease (increase) in speed. The SR could be said to introduce "negative damping". This is in contrast to the load of a typical power system, in which electrical power decreases (increases) with a decrease (increase) in frequency.

In the case of small disturbances the governor counteracts the destabilising effect described above. However, this is not necessarily the case in large disturbances. The author found that the plant may become unstable within a few seconds after the SR is connected. The governor initially closes the valves, causing a reduction in mechanical torque. When the speed drops below 100 % the governor opens the valves. The mechanical torque does not increase fast enough to counteract the electromagnetic torque, i.e. the deceleration is not stopped.

Some basic design parameters, such as the inertia, will have a profound effect on the plant's stability. The author investigated the effect of the following characteristics on the plant's stability in detail: (1) the turbine's 'natural' torque-speed characteristic; (2) the rate at which mechanical power can be increased, and (3) the SR rating. The effects of these characteristics on the plant's stability are explained below.

1. The turbine's natural torque-speed characteristic refers to the variation in mechanical torque due to variations in speed, at constant inlet gas conditions and constant valve positions, i.e. excluding the effects of the governor. The author deduced from the literature that power system analysts are uncertain

about the torque-speed characteristics of turbines. The author introduces the terms 'torque machine' and 'power machine' to distinguish between turbines having very different torque-speed characteristics. The torque of a 'torque machine' is independent of speed, whereas the torque of a 'power machine' varies with speed such that power is independent of speed. The power machine has a self-regulating characteristic not present in the torque machine – a decrease (increase) in speed leads to an increase (decrease) in torque. He author considers both types of turbines in his analyses. The turbine's torque-speed characteristic is important to the stability of the islanded plant due to the negative damping described above.

2. The importance of the rate at which mechanical torque can be decreased is easily understood – it determines the maximum speed of the plant after being disconnected from the power system. The rate at which mechanical power can be increased is also important: The shaft can only accelerate if the mechanical torque exceeds the electromagnetic torque. To prevent instability at speeds below 100 %, the mechanical torque needs to increase fast enough to counteract the electromagnetic torque; and the electromagnetic torque varies with speed. The author considers the rate of change of mechanical torque by studying the effect of different valve opening rates.

3. The higher the SR rating the larger the change in electromagnetic torque for any given change in speed. Therefore, the destabilising effect (or negative damping) described above is more prominent at high SR ratings.

In the case of the 175 MW SR, the characteristics (1) and (3) are particularly important. The plant with the torque machine is unstable. The negative damping due to SR is so high that the electromagnetic torque increases above the maximum mechanical torque, i.e. the turbine (and governor) cannot stabilise the plant. Regarding characteristic (2), the author found that a six-fold increase in the valve opening rate did not circumvent the instability. The plant with the power machine is stable.

In the case of the 85 MW SR, the characteristic (2) are particularly important. At relatively slow valve opening rates the plant is on the verge of instability. If the valve opening rate is increased the plant is stable. Characteristics (1) and (3) do affect the stability, but not as severely as in the case of the 175 MW SR.

The author concluded that the turbine's torque-speed characteristic is important to the stability of the plant.

The author finds a simple way of circumventing the destabilising effect described in (1) above. He designs a stabilising controller (SC), which responds to speed changes and acts on the excitation system. As the speed decreases (increases) the SC causes a reduction (increase) in generator terminal voltage, which leads to a decrease (increase) in electromagnetic torque. The change in generator voltage due to the SC is limited to ±5 %. Therefore, the SC can cause changes in the electrical power by up to ±10 % of the SR rating. The SC has a structure similar to a conventional power system stabiliser (PSS). The main difference between the SC and PSS is that SC improves frequency stability whereas the PSS improves rotor angle stability. The author shows that the SC prevents the stability problems described above. The plant with the 175 MW SR and a SC is stable, regardless of the turbine type. The plant with the 85 MW SR and SC is stable even at the lowest valve opening rate.

The author investigates the stability of the plant under small disturbances. He finds that the plant is stable, regardless of the turbine type, the rate at which power can be increased and the SR rating. The investigations include analyses in both the frequency-domain and the time-domain. For most analyses he uses the software package DIgSILENT *PowerFactory*. He verifies many of the results using MATLAB SimPowerSystems. He uses the software packages' numerical linearisation functions for the eigenvalue calculations. He develops a linear model of the plant analytically. The analytical model allows the author the construct Bode diagrams of mechanical torque and electromagnetic torque against speed. The author uses these diagrams to verify that the SC and governor act in unison over a wide frequency range.

The level of reactive power, prior to the disconnection of the plant from the power system, is important. If the plant is initially under-excited, then the voltage recovers slowly after the SR is connected (compared to the case where the generator is initially over-excited). Therefore, it takes relatively long before full breaking torque is achieved.

In conclusion, the SR stabilises the PBMR plant when it islands from the power system – it limits the maximum shaft speed to a safe value. After the speed reaches a maximum the plant may become unstable, depending on the turbine type, the rate at which mechanical torque can be increased and the SR rating. The instability is prevented by the SC. After the islanded plant reaches steady-state operation it is stable with respect to small disturbances, regardless of the turbine type and the SR rating. The plant may be reconnected to the power system as soon as the fault has been cleared.

6.1 Recommendations for further work

Additional research should be done on the modelling of turbines. Specifically, the relationship between mechanical torque and shaft speed should be investigated. The research should consider both small and large speed deviations. This research could be complemented by practical tests, in which the generator supplies a purely resistive load. The detailed research into turbines' torque-speed characteristics is outside the scope of the thesis.

References

1 Anderson P. M., Fouad A. A., Power System Control and Stability, Volume I, The Iowa State University Press, AMES, Iowa, U.S.A., 1980

2 Bagnasco A., Delfino B., Denegri G. B., Massucco S., Management and Dynamic Performance of Combined Cycle Power Plants During Parallel and Islanding Operation, IEEE Transactions on Energy Conversion, Vol. 13, No. 2, pp. 194-201, June 1998

3 Carvalho V. F., Use of Generator and Customer Load Rejection in Ontario Hydro to Increase Power Transfer Limits, CIGRE Paper 32-79-00-56, presented at the Study Committee 32 Meeting, Minneapolis, 1979

4 Church E. F., Steam Turbines, McGraw-Hill Book Company Inc., 2nd edition

5 Cigré SC38-WG02 Report, State of the Art in Non-Classical Means to Improve Power System Stability, Electra, No. 118, pp. 88-113, May 1988

6 Czech Grid Code, Rules for Transmission System Operation, Part I. Basic conditions for the use of the Czech Transmission System, Revision 06, January 2006

7 de Mello F. P., Concordia C., Concepts of Synchronous Machine Stability as Affected by Excitation Control, IEEE Transactions PWRS, Vol. 88, No. 4, April 1969, pp. 316-329

8 de Mello F. P., Laskowski T. F., Concepts of Power System Dynamic Stability, IEEE Transactions PWRS, Vol. 94, No. 3, May/ June 1975

9 DIgSILENT *PowerFactory* manual, version 13.2, build 339

10 Ellis H. M., Hardy J. E., Blythe A. L., Skooglund J. W., Dynamic Stability of the Peace River Transmission System, IEEE Transactions PWRS, Vol.-85, pp. 586-600, June 1966

11 EPRI Report TR-103902, Dynamic Brake Control to Reduce Turbine Shaft Transient Torque, Final Report of Project 2473-39, prepared by The Department of Electrical Engineering, Montana State University, September 1994

12 IEEE/ CIGRÉ Joint Task Force on Stability Terms and Definitions, Definition and Classification of Power System Stability, IEEE Transactions PWRS, Vol. 19, No. 2, May 2004

13 IEEE Guide for Synchronous Generator Modelling, IEEE Standard 1110, 1991

14 IEEE Power System Damping Ad Hoc Task Force of the Power System Damping Performance Committee, Damping Representation for Power System Stability Studies, IEEE Transactions PWRS, Vol. 14, No. 1, February 1999

15 IEEE Standards Board, Recommended Practice for Excitation Systems Models for Power System Stability Studies, IEEE Std.421.5-1992

16 IEEE Standards Board, IEEE Standard definitions for Excitation Systems for Synchronous Machines, Std. 421.1-1986

17 IEEE Standards Board, IEEE Recommended Practice for Functional and Performance Characteristics of Control Systems for Steam-Generator Units, IEEE Std. 122-1991

18 IEEE Task Force Report, A Description of Discrete Supplementary Controls for Stability, IEEE Transactions PWRS, Vol. 97, pp. 149-165, January/ February 1978

19 IEEE Working Group Report, "Guidelines for Enhancing Power Plant Response to Partial Load Rejections", IEEE Transactions PWRS, Vol. 102, No. 6, pp. 1501-

1504, June 1983

20 IEEE Working Group Report of panel discussion, Turbine Fast Valving to Aid System Stability: Benefits and other Considerations, IEEE Transactions PWRS, Vol. 1, pp. 143-153, February 1986

21 IEEE Working Group on Prime Mover and Energy Supply Models for System Dynamic Performance Studies, Dynamic Models for Fossil Fuelled Steam Units in Power System Studies, IEEE Transactions PWRS, Vol. 6, No. 2, pp. 753-761, May 1991

22 Kaberere K., Petroianu A., Folly K., Analytical Investigation of the Effect of Generator Modelling on Electromechanical Mode Damping, IFAC 2005

23 Krause P. C., Analysis of Electric Machinery, McGraw-Hill, 1986, Section 12.5

24 Kundur P., Power System Stability and Control, McGraw-Hill, Inc., 1993

25 Kundur P., Beaulieu R.E., Munro C., Starbuck P. A., Steam Turbine Fast Valving: Benefits and Technical Considerations, ST267 position paper, presented at the Canadian Electrical Association, Spring Meeting, March 1986

26 Kundur P., Bayne J. P., A Study of Early Valve Actuation using Detailed Prime Mover and Power System Simulation, IEEE Transactions PWRS, Vol. 94, No. 4, pp. 1275-1287, July 1975

27 Kundur P., Hogg W. G. T., Use of Generation Rejection in Ontario Hydro to Increase Power Transfer Capability, Paper presented at panel session on generator tripping, IEEE PES winter meeting, New York, January/ February 1982

28 MATLAB® manual, version 6.5, release 13

29 National Electricity Regulator, The South Africa Grid Code, 2003

30 Ogata K., Modern Control Engineering, Prentice-Hall, 1988, ISBN-0- 87692-147-0

31 Soon K.Y., Hughes F.M., Milanovic' J.V., Comparative Analysis and Reconciliation of Gas Turbine Models for stability Studies, IEEE PWRS, 2007

32 Shelton M. L., Mittelstadt W. A., Winkelman P. F., Bellerby W. J., Bonneville Power Administration 1400-MW Braking Resistor, IEEE Power Engineering Society Summer Meeting & Energy Conference, May 1974

33 Transmission Code 2007, Netz- und Systemregeln der deutschen Übertragungsnetzbetreiber, Version 1.1, August 2007, Verband der Netzbetreiber

34 Weber G. A., Winter M. C., and S. M. Follen, "Nuclear Plant Response to Grid Electrical Disturbances", EPRI Report NP-2849, February 1983

Bibliography

35 Adibi M. M., Fink L. H., "Power System Restoration Planning", IEEE Transactions PWRS, Vol. 9, No. 1, pp. 22-28, February 1994

36 Balu N. J., Fast Turbine Valving and Independent Pole Tripping Breaker Applications for Plant Stability, IEEE Transactions PWRS, Vol. 99, pp. 1330-1342, July/ August 1980

37 Berglund R. O., Mittelstadt W. A., Shelton M. L., Barkan P., Dewey C. G., Skreiner K. M., One-Cycle Fault Interruption at 500kV : System Benefits and Breaker Design, IEEE Transactions PWRS, Vol. 93, pp. 1240-1251, September/ October 1974

38 Carvalho V. F., Power Plant Control, CIGRE SC39/WG04 Survey Paper D, CIGRE SC39/ IFAC Meeting, Florence, September 1983

39 Chou Q. B., Kundur P., Acchione P. N., Lautsch B., Improving Nuclear Generating Station Response for Electrical Grid Islanding, IEEE Transactions on Energy Conversion, Vol. 4, No. 3, pp. 406-411, September 1989

40 Cigré SC38, Analysis and Control of Power System Oscillations, Final Report, Task Force 07, December 1996

41 Cushing E. W., Drechsler G. E., Killgoar W. P., Marshall H. G., Stewart H. R., Fast Valving as an Aid to Power System Transient Stability and Prompt Resynchronization and Rapid Reload after Full Load Rejection, IEEE Transactions PWRS, Vol. 91, pp. 1624-1636, July/ August 1972

42 de Mello F. P., Ewart D. N., Temoshok M., Eggenberger M. A., Turbine Energy Controls Aid in Power System Performance, Proceedings of the American Power Conference, Vol. 28, pp. 438-445, 1966

43 de Mello F. P., Westcott J. C., Steam Plant Startup and Control in System Restoration, IEEE Transactions on Power Systems, Vol. 9, No.1, pp. 93-101, February 1994

44 Dunlop R.D., Ewart D.N., System Requirements for Dynamic Performance and Response of Generating Units, IEEE Transactions PWRS, Vol. 94, No. 3, pp. 838-849, May/ June 1975

45 Durrant O. W., Boiler Response to Partial Load Rejections Resulting From System Upsets, IEEE Transactions PWRS, Vol. 101, No. 8, pp. 2630-2638, August 1982

46 Edwards L., Thomas R. J., Hogue D. C., Hughes P., Novak W., Weiss G., Welsh J. E., Sustained Fast Valving at TVA's Cumberland Steam Plant: Background and Test Results, Proceedings of the American Power Conference, Vol. 43, pp. 142-152, April 1981

47 El-Abiad A., Nagappan K., Transient Stability Regions of Multimachine Power Systems, IEEE Transactions PWRS, Vol. 85, No. 2, February 1966, pp. 169-179

48 EPRI Report EL-5859, Technical Limits to Transmission System Operation, Final Report of Project 5005-2, prepared by Power Technologies Inc., June 1988

49 Fusco G., Venturini D., Mazzoldi F., Possenti A., Thermal Units Contribution to the Electric Power System Restoration after a Black-out, CIGRE Session Paper 32-21, 1982.

50 Gleiss G. E., Direct Method of Lyapunov Applied to Transient Power System Stability, IEEE Transactions PWRS, Vol. 85, No. 2, February 1966, pp. 159-168

51 Hillery R. H., Holdup E. D., Load Rejection Testing of Large Thermal Electric Generating Units, IEEE Transactions PWRS, Vol. 87, pp. 1440-1453, June 1968

52 Horne J., Flynn D., Littler T., Frequency Stability Issues for Islanded Power Systems, IEEE PES Power System Conference and Exposition, Vol. 1, pp. 299-

306, 10-14 October 2004

53 IEC60034, Standard for Rotating Electrical Machines

54 IEEE Committee Report, HVDC Controls for System Dynamic Performance, IEEE Transactions PWRS, Vol. 6, No. 2, pp. 743-752, May 1991

55 Jones G. A., Transient Stability of a Synchronous Generator Under Conditions of Bang-bang excitation scheduling, IEEE Transactions PWRS, Vol. 84, February 1965, pp. 114-121

56 Jyrinsalo J., Lakervi E., Islanding Strategies for Regional Power Producers, PSCC 11th Power Systems Computation Conference, Avignon, France, 30 August - 3 September 1993, pp. 1227-1233

57 Kundur P., A Survey of Utility Experiences with Power Plant Response during Partial Load Rejection and System Disturbances, IEEE Transactions PWRS, Vol. 100, No. 5, pp. 2471-2475, May 1981

58 Kundur P., Dandeno P. L., Implementation of Advanced Generator Models into Power System Stability Programs, IEEE Transactions PWRS, Vol. 102, pp. 2047-2052, July 1983

59 Kundur P., Lee D. C., Bayne J. P., Dandeno P. L., Impact of Turbine Generator Overspeed Controls on Unit Performance under System Disturbance Conditions, IEEE Transactions PWRS, Vol. 104, No. 6, pp. 1262-1269, June 1985

60 Larsen E. V., Chow J. H., SVC Control Design for System Dynamic Performance, IEEE Special Symposium on Application of SVC for System Dynamic Performance, Publication 87TH0187-5-PWR, 1987

61 Lee D. C., Kundur P., Advanced Excitation Controls for Power System Stability Enhancement, Cigré 38-01, 1986

62 Limebeer D. J. N, Harley R. G., Synchronous Machine Stability using Composite Governor and Voltage Regulator Models, Electric Power Systems Research, 1977/78, pp. 97 - 111

63 Maliszewski R. M., Pasternack B. M., Rana R. D., Temporary Fast Turbine Valving on the AEP System, Proceedings of the American Power Conference, Vol. 44, pp. 118-125, 1982

64 Mansour M., Stability Analysis and Control of Power Systems, published in "Real-Time Control of Electric Power Systems", edited by E. Handschin, Elsevier, 1972, ISBN 0-444-41045-7

65 Martin H. F., Tapper D. N., Alston T. M., Sustained Fast Valving Applied to TVA's Watts Bar Nuclear Units, Paper 76-JPGC-PWR-5, presented at the 1976 Joint Power Generation Conference, Buffalo, N. Y., September 1976, ASME Transactions, Series A, Vol. 99, No. 1, 1977

66 McGaha P. L., Dresner T. L., A Nuclear Steam Turbine Intercept Valve and Control System for Fast Valving, Paper presented at the 1977 Joint Power Generation Conference, Long Beach, Calif., September 1977

67 Morgan W. A., Peck H. B., Holland D. R., Cullen F. A., Ruzek J. B., Modern Stability Aids for Calvert Cliffs Units, IEEE Transactions PWRS, Vol. 90, pp. 1-10, January/ February 1971

68 Padiyar K. R., Power System Dynamics – Stability and Control, John Wiley & Sons (Asia) Pte Ltd, 1996

69 Park R. H., Fast Turbine Valving, IEEE Power Engineering Society, 1972 Joint IEEE/ ASME Power Generation Conference, Boston, September 1972

70 Park R. H., Improved Reliability of Bulk Power Supply by Fast Load Control, Proceedings of the American Power Conference, Vol. 30, pp. 1128-1141, 1968

71 Park R. H., Fast Turbine Valving, IEEE Transactions PWRS, Vol. 92, pp. 1065-1073, May/ June 1973

72 Ramey R. G., Sismour A. C., Kung G. C., Important Parameters in Considering Transient Torques on Turbine-Generator Shaft Systems, IEEE Transactions PWRS, Vol. 99, No.1, pp. 311-317, January/ February 1980

73 Rawdon A. H., Palacios F. A., Effects of Partial Load Rejection on Fossil Fuel Utility Steam Generators, IEEE Transactions PWRS, Vol. 101, No. 8, pp. 2533-2536, August 1982

74 Rowen W.I., Simplified Mathematical Representations of Heavy-Duty Gas Turbines, American Society of Mechanical Engineers – Fournal of Engineering for Power, Vol. 105, pp.865-869, 1983

75 Rumpel D. et al., Tripping to Houseload – Methods, Application, Experience, CIGRE SC39/ IFAC Meeting, Florence, September 1983

76 Taylor C. W., Mechenbier J. R., Matthews C. E., Transient Excitation Boosting at Grand Coulee Third Power Plant: Power System Application and Field Tests, IEEE Transactions PWRS, Vol. 8, No. 3, pp. 1291-1297, August 1993

77 Taylor C. W., Nassief F. R., Cresap R. L., Northwest Power Pool Transient Stability and Load Shedding Controls for Generation-Load Imbalances, IEEE Transactions PWRS, Vol. 100, pp. 3486-3495, July 1981

78 Wang Y., Hill D. J., Middleton R. H., Gao L., Transient Stability Enhancement and Voltage Regulation of Power Systems, IEEE Transactions PWRS, Vol. 8, No. 2, pp. 620-627, May 1993

79 Weiss J. R., Transient Asymptotic Stability of Power Systems as Established with Lyapunov Functions, IEEE Transactions PWRS, Vol. 95, No. 4, pp. 1480-1485, July 1976

80 Willems J. L., Improved Lyapunov function for transient power-system stability, Proc. IEEE, Vol. 115, No. 9, September 1968, pp. 1315-1317

81 Younkins T. D., Chow J. H., Brower A. S., Kure-Jensen J., Wagner J. B., Fast Valving with Reheat and Straight Condensing Steam Turbines, IEEE Transactions PWRS, Vol. 2, pp. 397-405, May 1987

82 Younkins T. D., Johnson L. H., Steam Turbine Overspeed Control and Behaviour during System Disturbances, IEEE Transactions PWRS, Vol. 100, No. 5, pp. 2504-2511, May 1981

Appendix A Power Plant Parameters

A1: Synchronous generator parameters

Table A-1: Parameters of the generator model

Symbol	Value*	Description
S_r	211.76 MVA	Rated apparent power
P_r	180 MW	Rated active power
pf_r	0.85	Rated power factor (lagging)
H	** 3.07 s	Inertia constant
X_d	2.01	Unsaturated direct-axis synchronous reactance
X_q	1.96	Unsaturated quadrature-axis synchronous reactance
X'_d	0.24	Unsaturated direct-axis transient reactance
X'_q	0.41	Unsaturated quadrature-axis transient reactance
X''_d	0.17	Direct-axis subsynchronous reactance
X''_q	0.17	Quadrature-axis subsynchronous reactance
X_l	0.14	Leakage reactance
T'_{do}	11 s	Direct axis open-circuit transient time constant
T''_{do}	0.044 s	Direct axis open-circuit subtransient time constant
T'_{qo}	1.2 s	Quadrature axis open-circuit transient time constant
T''_{qo}	0.076 s	Quadrature axis open-circuit subtransient time constant

* In per unit, based on generator rating, unless otherwise indicated

** Applies to total inertia, i.e. generator and turbine

A2: Excitation system parameters

Table A-2: Parameters of the excitation system

Symbol	Value	Description
T_r	0.01 s	Voltage measurement transducer time constant
T_B, T_C	5 s, 3s	Time constants of lag-lead compensator
K_a	200	Excitation system gain
T_a	0.02 s	Excitation system time constant
K_C	0.0	Commutation loss constant
$V_{r\max}$	5.5	Maximum output of excitation system, at rated generator terminal voltage
$V_{r\min}$	-3.0	Minimum output of excitation system

The author tested the excitation system model by simulating the response of the generator to a step change in the reference voltage *usetp*. The simulation was done in DIgSILENT *PowerFactory*. The results are shown in Figure A- 1. The excitation system responded to the step increase in reference voltage by increasing the excitation voltage. The excitation current increased, causing the generator voltage to increase. The generator voltage settled at a steady-state value equal to the reference voltage (1.02 p.u.).

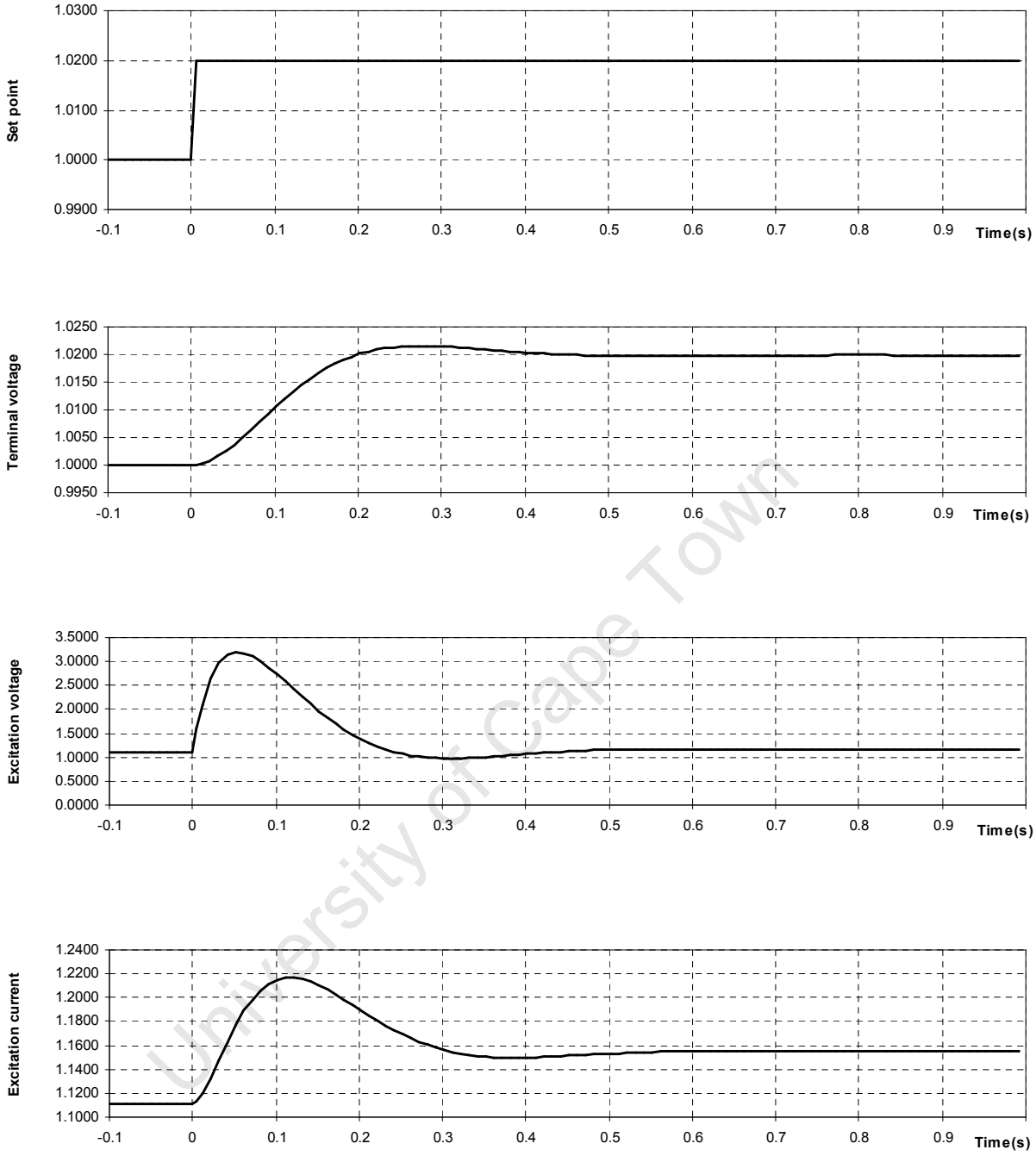

Figure A- 1: Excitation step response test

A3: Turbine parameters

Table A- 3: Parameters of the turbine model

Symbol	Value	Description
T_{ch}	0.3 s	Inlet chest time constant
T_{co}	0.5 s	Crossover time constant
T_{ip}	0.01 s	Intermediate pressure stage time constant
T_{rh}	7.0 s	Reheater time constant
r_c	0.547	Valve choking parameter*
k	1.3	Valve choking parameter
P_{drop}	0.02	Pressure drop across valve
Con	1	Conversion factor for DIgSILENT *PowerFactory* and Matlab SimPowerSystems models
F_{hp}	0.3	High-pressure turbine torque factor
F_{ip}	0.3	Intermediate-pressure turbine torque factor
F_{lp}	0.4	Low-pressure turbine torque factor
$P_{r\min}$	0	Minimum reheater pressure
$P_{r\max}$	1.05	Maximum reheater pressure (limited by safety valves)

* r_c is set to 0.0 in all analyses except those presented in section 5.3.5.

The non-linear relationship between valve position and valve opening was estimated using a diagram in [26]. It is represented with the following equations:

$$Area = \begin{cases} 1.490 \cdot Pos + 0.000 \ \ if \ Pos = 0.35 \\ 1.440 \cdot Pos + 0.017 \ \ if \ Pos = 0.35 \\ 0.545 \cdot Pos + 0.491 \ \ if \ Pos = 0.35 \\ 0.400 \cdot Pos + 0.600 \ \ if \ Pos = 0.35 \end{cases} \tag{A.1}$$

where $Area$ is the valve opening area, and Pos is the valve position.

The same characteristic was used for the control valve and the intercept valve.

A4: Governor parameters

Table A- 4: Parameters of the governor model

Symbol	Value	Description
K_G	25	Gain (with load reference offset and without load reference offset respectively)
$K1$	2.5	Intercept valve control gain
T_{pc}, T_{zc}	0 s, 0 s	Control valve compensator
T_{sm}	0.1 s	Control valve servomotor time constant
L_{c1}, L_{c2}	1.2, -0.2	Control valve maximum opening rate, closing rate
CVP_1, CVP_2	1, 0	Control valve maximum opening, closing position
T_{pi}, T_{zi}	0 s, 0 s	Intercept valve compensator
T_{si}	0.1 s	Intercept valve servomotor time constant
L_{i1}, L_{i2}	0.2, -0.2	Intercept valve maximum opening rate, closing rate
IVP_1, IVP_2	1, 0	Intercept valve maximum opening, closing position

Appendix B Derivation of Model 2

B1 : Derivation of Model 2

Equations (B.1) to (B.9) represent the model of a synchronous generator, neglecting the damper windings:

$$\psi_d = -L_l i_d + \psi_{ad}$$
$$\psi_{ad} = L_{ads}(-i_d + i_{fd}) \quad \text{(B.1)}$$

$$\psi_q = -L_l i_q + \psi_{aq}$$
$$\psi_{aq} = -L_{aqs} i_q \quad \text{(B.2)}$$

$$\psi_{fd} = \psi_{ad} + L_{fd} i_{fd} \quad \text{(B.3)}$$

$$L'_{ads} = \frac{L_{ads} L_{fd}}{L_{ads} + L_{fd}} \quad \text{(B.4)}$$

$$T_e = \psi_d i_q - \psi_q i_d \quad \text{(B.5)}$$

$$e_d = -R_a i_d - \omega \psi_q \quad \text{(B.6)}$$

$$e_q = -R_a i_q + \omega \psi_d \quad \text{(B.7)}$$

$$e = \sqrt{e_d^2 + e_q^2} \quad \text{(B.8)}$$

$$p\psi_{fd} = \frac{\omega R_{fd}}{L_{adu}} E_{fd} - \omega R_{fd} i_{fd} \quad \text{(B.9)}$$

The following equations apply to the electrical circuit connected to the generator:

$$e_d = R_E i_d \quad \text{(B.10)}$$

$$e_q = R_E i_q \tag{B.11}$$

The total resistance R_T and the initial speed ω_o are used in the derivation of Model 2. These terms are defined as follows:

$$R_T = R_a + R_E \tag{B.12}$$

$$\omega_o = 1 \tag{B.13}$$

Equations are required for the currents i_d and i_q in terms of ω and ψ_{fd}. These equations will later be differentiated with respect to ω and ψ_{fd}.

From (B.6) and (B.10) an equation for i_d is obtained in terms of ω and ψ_q.

$$i_d = -\frac{\omega \psi_q}{R_T} \tag{B.14}$$

Using (B.2),

$$i_d = \frac{\omega}{R_T} i_q \left(L_l + L_{aqs} \right) \tag{B.15}$$

Equation (B.15) is required in the derivation of i_q (in terms of ω and ψ_{fd}) which follows:

From (B.7), (B.11) and (B.12):

$$i_q = \frac{\omega \psi_d}{R_T} \tag{B.16}$$

and from (B.3):

$$i_{fd} = \frac{\psi_{fd} - \psi_{ad}}{L_{fd}} \tag{B.17}$$

and from (B.1):

$$\psi_{ad} = \frac{L_{ads} L_{fd}}{L_{fd} + L_{ads}} \cdot \left(-i_d + \frac{\psi_{fd}}{L_{fd}} \right) \tag{B.18}$$

This equation is rewritten as follows:

$$i_q = \frac{\omega}{R_T} \left\{ -i_d \left(L_l + \frac{L_{ads} L_{fd}}{L_{ads} + L_{fd}} \right) + \frac{L_{ads}}{L_{ads} + L_{fd}} \psi_{fd} \right\} \tag{B.19}$$

Substituting (B.15) into (B.19) yields an equation for i_q in terms of ω and ψ_{fd}:

$$i_q = \frac{\omega R_T}{D} \cdot \left(\frac{L_{ads}}{L_{ads} + L_{fd}} \right) \cdot \psi_{fd} \tag{B.20}$$

where

$$D = R_T^2 + \omega^2 \cdot \left(L_l + L_{aqs} \right) \cdot \left(L_l + L_{ads}^{'} \right) \tag{B.21}$$

Substituting (B.20) into (B.15) yields an equation for i_d in terms of ω and ψ_{fd}:

$$i_d = \frac{\omega^2 \left(L_l + L_{aqs} \right) \left(\frac{L_{ads}}{L_{ads} + L_{fd}} \right) \psi_{fd}}{D} \tag{B.22}$$

Equations (B.20) and (B.22) are linearised as follows: expressions for the derivatives of i_d and i_q at the initial operating speed ω_o are found. In these expressions the derivative operator d is replaced with Δ. ω_o is replaced with 1.0, as defined in (B.13). The following linear equations result for Δi_d and Δi_q in terms of $\Delta\omega$ and $\Delta\psi_{fd}$:

$$\begin{aligned} \Delta i_d &= a\Delta\omega + b\Delta\psi_{fd} \\ \Delta i_q &= c\Delta\omega + d\Delta\psi_{fd} \end{aligned} \tag{B.23}$$

where:

$$a = 2X_{Tq} \cdot \frac{\psi_{fdo}}{D} \cdot \left(\frac{L_{adsi}}{L_{adsi} + L_{fd}} \right) \cdot \left\{ 1 - \frac{X_{Tq} X_{Td}}{D} \right\} \tag{B.24}$$

$$b = \frac{X_{Tq}}{D} \cdot \left(\frac{L_{adsi}}{L_{adsi} + L_{fd}} \right) \tag{B.25}$$

$$c = R_T \cdot \frac{\psi_{fdo}}{D} \cdot \left(\frac{L_{adsi}}{L_{adsi} + L_{fd}} \right) \cdot \left\{ 1 - \frac{2X_{Td} X_{Tq}}{D} \right\} \tag{B.26}$$

$$d = \frac{R_T}{D} \cdot \left(\frac{L_{adsi}}{L_{adsi} + L_{fd}} \right) \tag{B.27}$$

$$\begin{aligned} X_{Tq} &= \omega_o \cdot \left(L_l + L_{aqs} \right) \\ X_{Td} &= \omega_o \cdot \left(L_l + L_{ads}^{'} \right) \\ D &= R_T^2 + X_{Td} \cdot X_{Tq} \end{aligned} \tag{B.28}$$

An equation for ΔT_e is now obtained in terms of $\Delta\omega$ and $\Delta\psi_{fd}$.

Equations (B.18) and (B.2) provide expressions for ψ_{ad} and ψ_{aq} in terms of i_d and i_q. Substituting (B.20) and (B.22) yields expressions for ψ_{ad} and ψ_{aq} in terms of ω and ψ_{fd}. These expressions are linearised (by differentiation with respect to ω and ψ_{fd}) to yield the following:

$$\Delta\psi_{ad} = \left(-a \cdot L_{ads}^{'} \right) \Delta\omega + L_{ads}^{'} \left(\frac{1}{L_{fd}} - b \right) \Delta\psi_{fd} \tag{B.29}$$

$$\Delta\psi_{aq} = \left(-c \cdot L_{aqs} \right) \Delta\omega - \left(d \cdot L_{aqs} \right) \Delta\psi_{fd} \tag{B.30}$$

An equation for electromagnetic torque is developed from (B.1), (B.2) and (B.5):

$$T_e = \psi_{ad} i_q - \psi_{aq} i_d \tag{B.31}$$

Equation (B.31) is linearised (by differentiation with respect to ω and ψ_{fd}), and equations (B.23), (B.29) and (B.30) are used to write:

$$\Delta T_e = K_{t\omega}\Delta\omega + K_{t\psi}\Delta\psi_{fd} \tag{B.32}$$

where:

$$\begin{aligned} K_{t\omega} &= -a\left(L_{ads}^{'}\cdot i_{qo} + \psi_{aqo}\right)\cdot i_{qo} + c\left(\psi_{ado} + L_{aqs}\cdot i_{do}\right) \\ K_{t\psi} &= -b\left(L_{ads}^{'}\cdot i_{qo} + \psi_{aqo}\right) + d\left(\psi_{ado} + L_{aqs}\cdot i_{do}\right) + \frac{L_{ads}^{'}}{L_{fd}} i_{qo} \end{aligned} \tag{B.33}$$

Equation (B.33) is simplified using (B.1), (B.2) and (B.7):

$$\begin{aligned} K_{t\omega} &= a\cdot i_{qo}\left(X_q - X_d^{'}\right) + c\left(e_{qo} + R_a\cdot i_{qo} + X_q\cdot i_{do}\right) \\ K_{t\psi} &= b\cdot i_{qo}\left(X_q - X_d^{'}\right) + d\left(e_{qo} + R_a\cdot i_{qo} + X_q\cdot i_{do}\right) + \frac{L_{ads}^{'}}{L_{fd}} i_{qo} \end{aligned} \tag{B.34}$$

where:

$$\begin{aligned} X_d^{'} &= \omega_o L_{ads}^{'} \\ X_q &= \omega_o L_{aqs} \end{aligned} \tag{B.35}$$

An equation for $\Delta\psi_{fd}$ in terms of $\Delta\omega$ and ΔE_{fd} is required. Equation (B.17) is written in terms of perturbed variables:

$$\Delta i_{fd} = \frac{\Delta\psi_{fd} - \Delta\psi_{ad}}{L_{fd}} \tag{B.36}$$

Equation (B.36) is written in terms of $\Delta\omega$ and $\Delta\psi_{fd}$ using (B.29):

$$\Delta i_{fd} = \frac{1}{L_{fd}}\left(1 - \frac{L_{ads}^{'}}{L_{fd}} + b\cdot L_{ads}^{'}\right)\Delta\psi_{fd} + \frac{a\cdot L_{ads}^{'}}{L_{fd}}\Delta\omega \tag{B.37}$$

Equation (B.9) is written in terms of perturbed variables, and the operator p is replaced by the operator s:

$$\Delta\psi_{fd} = \frac{K_{fd}}{sT_{fd}+1}\left\{\Delta E_{fd} - K_{f\omega}\Delta\omega\right\} \tag{B.38}$$

where:

$$T_{fd} = \left\{\frac{-1}{L_{fd}}\left(1 - \frac{L'_{ads}}{L_{fd}} + b \cdot L'_{ads}\right)\right\}^{-1}$$
$$K_{fd} = \frac{R_{fd}}{L_{adu}} T_{fd} \tag{B.39}$$
$$K_{f\omega} = \frac{-1}{K_{fd}}\left\{\frac{E_{fdo}R_{fd}}{L_{adu}} - R_{fd} \cdot i_{fdo} - \frac{R_{fd}}{L_{fd}} \cdot a \cdot L'_{ads}\right\}$$

The variation in field voltage ΔE_{fd} is obtained from the excitation system model. The input to the excitation system model is the variation in terminal voltage. An equation is derived for the variation in generator voltage Δe in terms of $\Delta\omega$ and $\Delta\psi_{fd}$.

From (B.8):

$$e^2 = e_d^2 + e_q^2 \tag{B.40}$$

Equation (B.40) is expanded to include a perturbation voltage:

$$(e_o + \Delta e)^2 = (e_{do} + \Delta e_d)^2 + (e_{qo} + \Delta e_q)^2 \tag{B.41}$$

An approximate expression for Δe is found by expanding equation (B.41) and neglecting second-order terms:

$$2e_o\Delta e = 2e_{do}\Delta e_d + 2e_{qo}\Delta e_q$$
$$\Delta e = \frac{e_{do}}{e_o}\Delta e_d + \frac{e_{qo}}{e_o}\Delta e_q \tag{B.42}$$

$$\Delta e = \frac{e_{do}}{e_o}\Delta e_d + \frac{e_{qo}}{e_o}\Delta e_q \tag{B.43}$$

Δe_d and Δe_q are written as functions of $\Delta\omega$ and $\Delta\psi_{fd}$ using (B.6) and (B.7):

$$\Delta e_d = \Delta\omega\left(-aR_a - \psi_{qo} + cX_{Tq}\right) + \Delta\psi_{fd}\left(-bR_a + dX_{Tq}\right) \tag{B.44}$$

$$\Delta e_q = \Delta\omega\left(-cR_a + \psi_{do} - aX_{Td}\right) + \Delta\psi_{fd}\left(-dR_a - bX_{Td} + {L_{ads}^{'}}/{L_{fd}}\right) \tag{B.45}$$

Equations (B.44) and (B.45) are substituted into (B.43):

$$\Delta e = K_{e\omega}\Delta\omega + K_{e\psi}\Delta\psi_{fd} \tag{B.46}$$

where:

$$K_{e\psi} = \frac{e_{do}}{E_{to}}\left(-bR_a + dX_{Tq}\right) + \frac{e_{qo}}{E_{to}}\left(-dR_a - bX_{Td} + {L_{ads}^{'}}/{L_{fd}}\right) \tag{B.47}$$

$$K_{e\omega} = \frac{e_{do}}{E_{to}}\left(-aR_a - \psi_{qo} + cX_{Tq}\right) + \frac{e_{qo}}{E_{to}}\left(-cR_a + \psi_{do} - aX_{Td}\right) \tag{B.48}$$

B2 : Calculation of parameters for Model 2

The parameters for Model 2 in Chapter 3 are calculated using the following equations:

$$L_{ads} = K_{sd} \cdot L_{adu}$$
$$L_{aqs} = K_{sq} \cdot L_{aqu} \quad \text{(B.49)}$$

$$K_{sd} = \frac{\psi_{ato}}{\psi_{ato} + \psi_I} \quad \text{(B.50)}$$

$$\psi_I = 0 \quad if\ \psi_{ato} \le \psi_I$$
$$\psi_I = A \cdot e^{B(\psi_{ato} - \psi_{TI})} \quad if\ \psi_{ato} > \psi_I \quad \text{(B.51)}$$

$$\psi_{ato} = \left| e_o + i_o (R_a + jX_l) \right| \quad \text{(B.52)}$$

$$\delta_{io} = \tan^{-1} \frac{i_o X_{qs} \cos\phi_o - i_o R_a \sin\phi_o}{e_o + i_o R_a \cos\phi_o + i_o X_{qs} \sin\phi_o} \quad \text{(B.53)}$$

$$e_{do} = e_o \sin\delta_{io}$$
$$e_{qo} = e_o \cos\delta_{io} \quad \text{(B.54)}$$

$$i_{do} = i_o \sin(\delta_i + \phi)$$
$$i_{qo} = i_o \cos(\delta_i + \phi) \quad \text{(B.55)}$$

$$i_{fdo} = \frac{e_{qo} + R_a i_{qo} + L_{ds} i_{do}}{L_{ads}} \quad \text{(B.56)}$$

$$\psi_{ado} = L_{ads}(-i_{do} + i_{fdo})$$
$$\psi_{aqo} = -L_{ads} \cdot i_{qo} \quad \text{(B.57)}$$

$$L_{adsi} = K_{sdi} \cdot L_{adu}$$
$$L_{aqsi} = K_{sqi} \cdot L_{aqu} \quad \text{(B.58)}$$

$$K_{sdi} = \frac{1}{1 + B \cdot A \cdot e^{B(\psi_{ato} - \psi_{TI})}} \quad if\ \psi_{ato} \geq \psi_{TI}$$
$$K_{sdi} = 1 \quad if\ \psi_{ato} < \psi_{TI} \tag{B.59}$$

$$a = \frac{2X_{Tqi} \cdot \psi_{fdo}}{D}\left(\frac{L_{adsi}}{L_{adsi} + L_{fd}}\right) * \left\{1 - \frac{X_{Tdi}X_{Tqi}}{D}\right\} \tag{B.60}$$

$$b = \frac{X_{Tqi}}{D}\left(\frac{L_{adsi}}{L_{adsi} + L_{fd}}\right) \tag{B.61}$$

$$c = \frac{R_T}{D}\left(\frac{L_{adsi}}{L_{adsi} + L_{fd}}\right)\psi_{fdo} * \left\{1 - \frac{X_{Tdi}X_{Tqi}}{D}\right\} \tag{B.62}$$

$$d = \frac{R_T}{D}\left(\frac{L_{adsi}}{L_{adsi} + L_{fd}}\right) \tag{B.63}$$

$$L_{adsi}^{'} = \left[L_{adsi}^{-1} + L_{fd}^{-1}\right]^{-1} \tag{B.64}$$

$$X_{Tqi} = (L_{aqsi} + L_l)$$
$$X_{Tdi} = (L_{adsi}^{'} + L_l) \tag{B.65}$$

$$R_T = R_a + R_E$$
$$D = R_T^2 + X_{Tqi}X_{Tdi} \tag{B.66}$$

$$K_{t\psi} = b \cdot i_{qo}\left(L_{aqsi} + L_l - L_{adsi}^{'}\right) + d\left(e_{qo} + R_a \cdot i_{qo} + L_{qsi} \cdot i_{do}\right) + \frac{L_{adsi}^{'}}{L_{fd}} i_{qo} \tag{B.67}$$

$$K_{fd} = \frac{\omega_n R_{fd}}{L_{adu}} \cdot T_{fd} \tag{B.68}$$

$$K_{e\psi} = \frac{e_{do}}{e_o}\left(-bR_a + dX_{Tqi}\right) + \frac{e_{qo}}{e_o}\left(-dR_a - bX_{Tdi} + {L'_{adsi}}/{L_{fd}}\right) \quad \text{(B.69)}$$

$$K_{t\omega} = a \cdot i_{qo}\left(L_l + L_{aqsi} - L'_{adsi}\right) + c\left(e_{qo} + R_a \cdot i_{qo} + L_{qsi} \cdot i_{do}\right) \quad \text{(B.70)}$$

$$K_{f\omega} = \frac{L_{adu} \cdot L_{adsi} \cdot a}{L_{fd}} \quad \text{(B.71)}$$

$$K_{e\omega} = \frac{e_{do}}{e_o}\left(-aR_a - \psi_{qo} + cX_{Tqi}\right) + \frac{e_{qo}}{e_o}\left(-cR_a + \psi_{do} - aX_{Tdi}\right) \quad \text{(B.72)}$$

$$T_{fd} = \frac{\omega_n R_{fd}}{L_{fd}}\left[1 - L'_{adsi}\left(\frac{1}{L_{fd}} - b\right)\right]^{-1} \quad \text{(B.73)}$$

Table B- 1: Parameters for Model 2

Parameter	Active operating power (p.u.)				
	0.100	0.400	0.600	0.826	1.00
T_{fd}	6.231	5.399	4.651	3.893	3.423
$K_{t\psi}$	0.182	0.750	1.168	1.680	2.087
K_{fd}	0.598	0.519	0.447	0.374	0.329
$K_{e\psi}$	0.908	0.937	0.973	1.016	1.042
$K_{t\omega}$	0.098	0.459	0.730	1.003	1.167
$K_{f\omega}$	0.037	0.474	0.871	1.300	1.589
$K_{e\omega}$	1.014	1.139	1.199	1.212	1.193

Appendix C Implementation of plant model in DIgSILENT *PowerFactory*

The model that was implemented in DIgSILENT *PowerFactory* is presented below. An overview of the model is provided followed by the single-line diagram and controller block diagrams. The model was implemented in the per unit system.

Figure D-1 shows a single-line diagram of the generator, the connection to the external grid (via a transformer and transmission lines), and the SR. The SR consists of numerous stages that can be switched separately. Note that the modelling details of the transformer, lines and grid are important for the analyses presented in this thesis.

Figure D-2 shows the interconnection of the models for the generator, turbine, governor (or turbine control system), excitation system and SC. In DIgSILENT *PowerFactory* this figure is referred to as a 'frame'. The inputs to the generator are field voltage and mechanical power. The signal representing field voltage is calculated in the model for the excitation system. The signal representing mechanical power comes from the turbine model. The governor model calculates signals representing the valve positions, CVP and IVP. The SC model acts on the actual speeed wact. Its output is connected to the model of the excitation system.

The turbine model is shown in Figure D-3. It includes the non-linear characteristics of the turbine valves and the dynamics of the inlet chest, reheater and cross-over piping. Furthermore, it includes the modelling of critical flow through the intercept valve. The critical flow (or valve choking) is considered only in section 5.3.5.

Figure D-4 shows the model of the governor. This model includes the control gain, integration time constant, over-speed limitation and valve linearization. It also

includes the models of the valve motors – their minimum and maximum positions and rate limits.

Figure D-5 shows the excitation system model. The control error is developed from the difference between the set-point, the measured generator terminal voltage and the output of the stabilising controller.

Figure D-6 shows the stabilising controller model. It includes the washout function, the gain and the output limits.

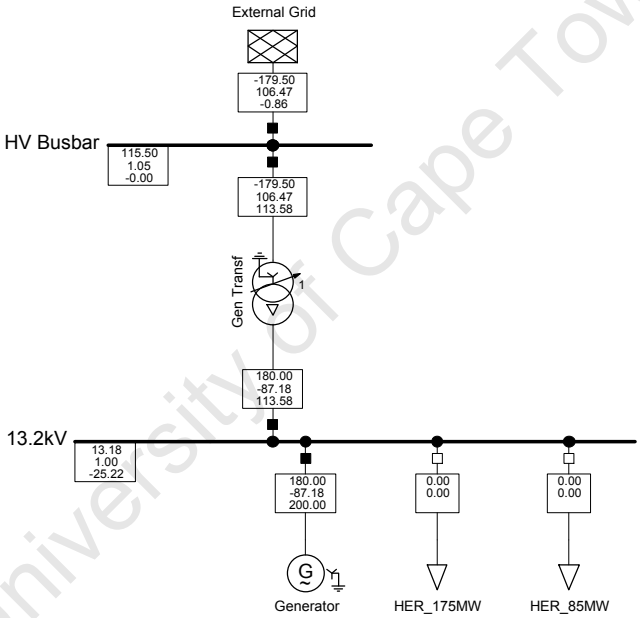

Load Flow Balanced			
Nodes	Branches	External Grid	Synchronous Machine
Line-Line Voltage, Magnitude [kV]	Active Power [MW]	Active Power [MW]	Active Power [MW]
Voltage, Magnitude [p.u.]	Reactive Power [Mvar]	Reactive Power [Mvar]	Reactive Power [Mvar]
Voltage, Angle [deg]	Loading [%]	Power Factor [-]	Apparent Power [MVA]

Figure D-1: Single line diagram in DIgSILENT *PowerFactory*

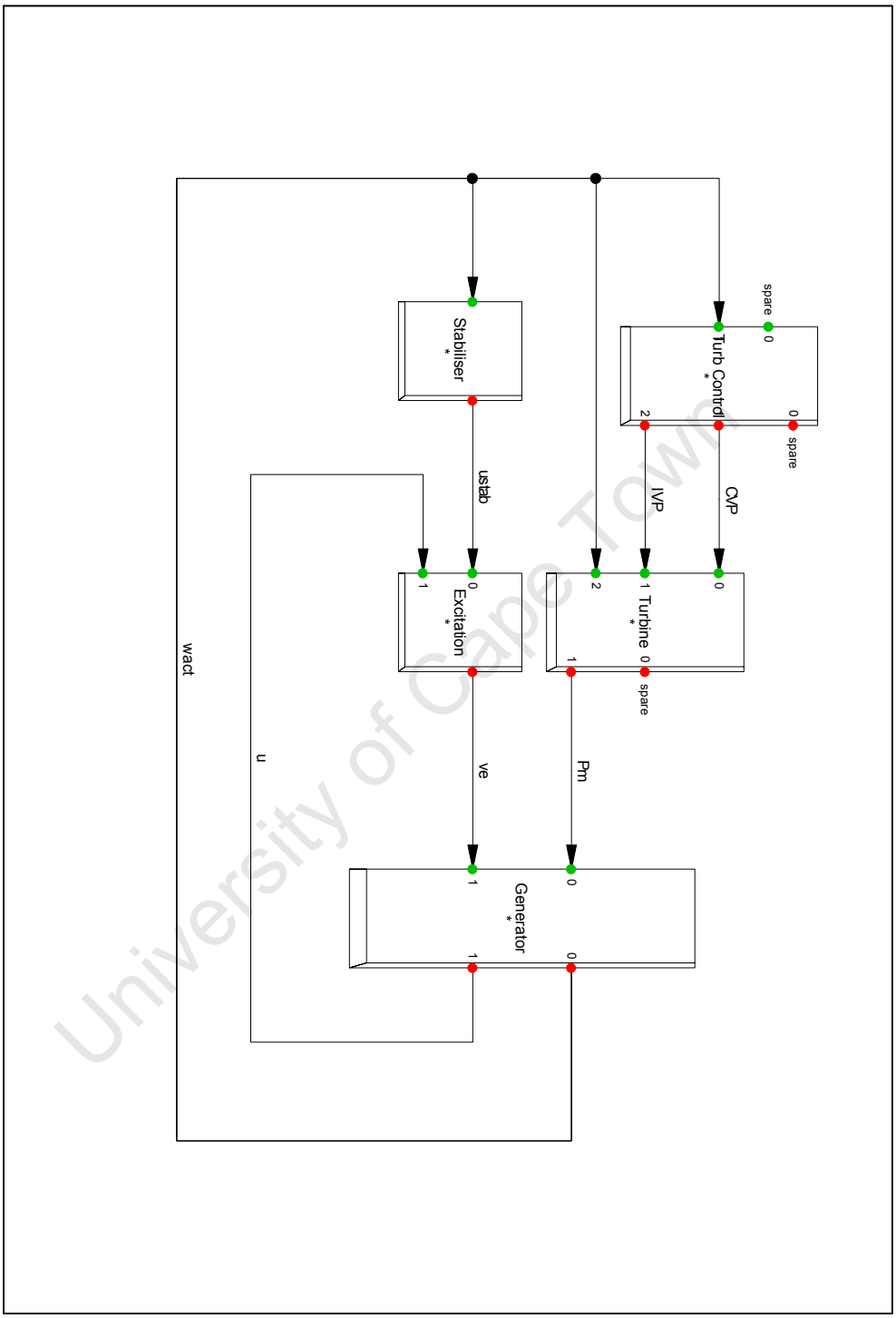

Figure D-2: Frame showing interconnection of models in DIgSILENT *PowerFactory*

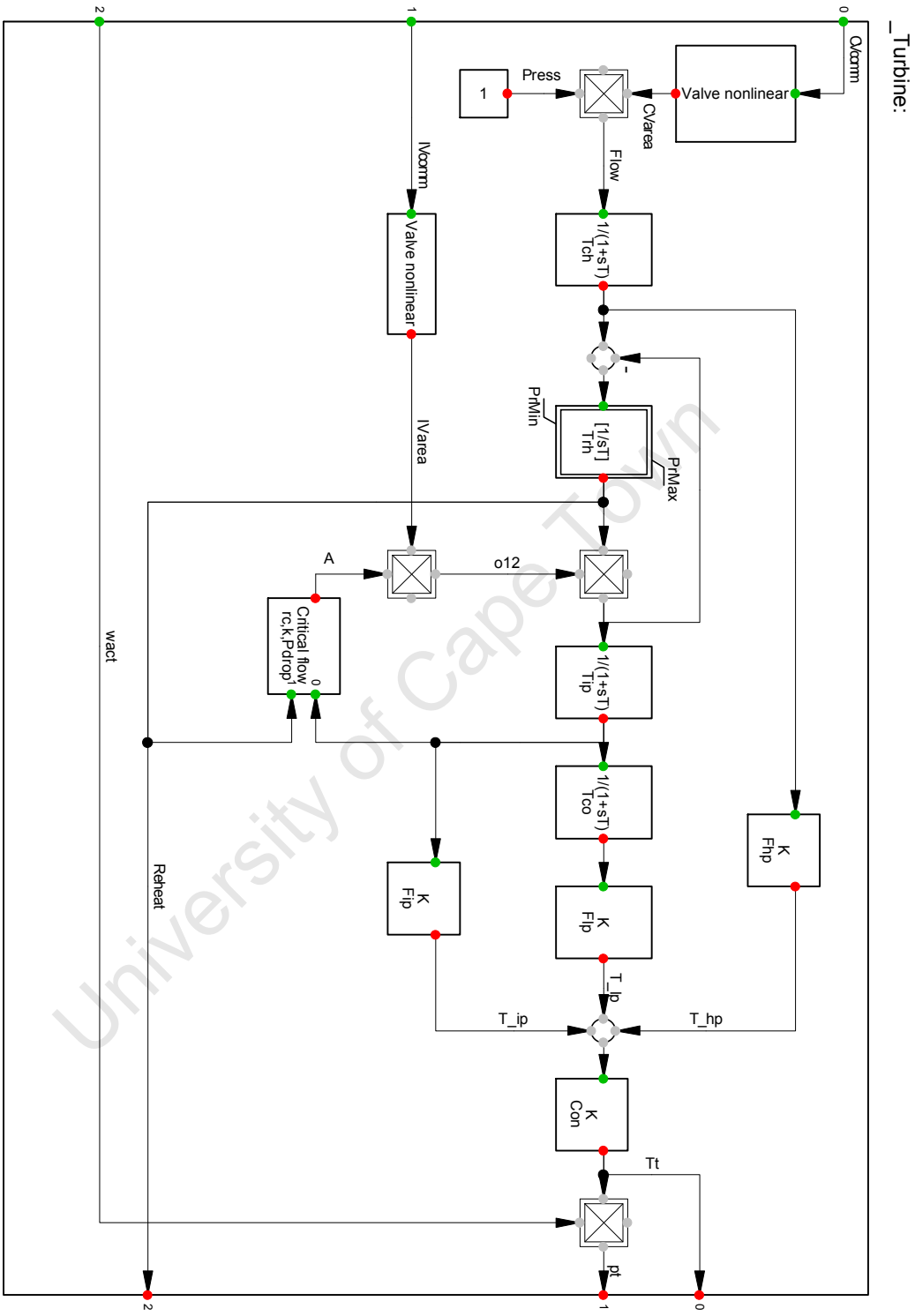

Figure D-3: Turbine model implemented in DIgSILENT *PowerFactory*

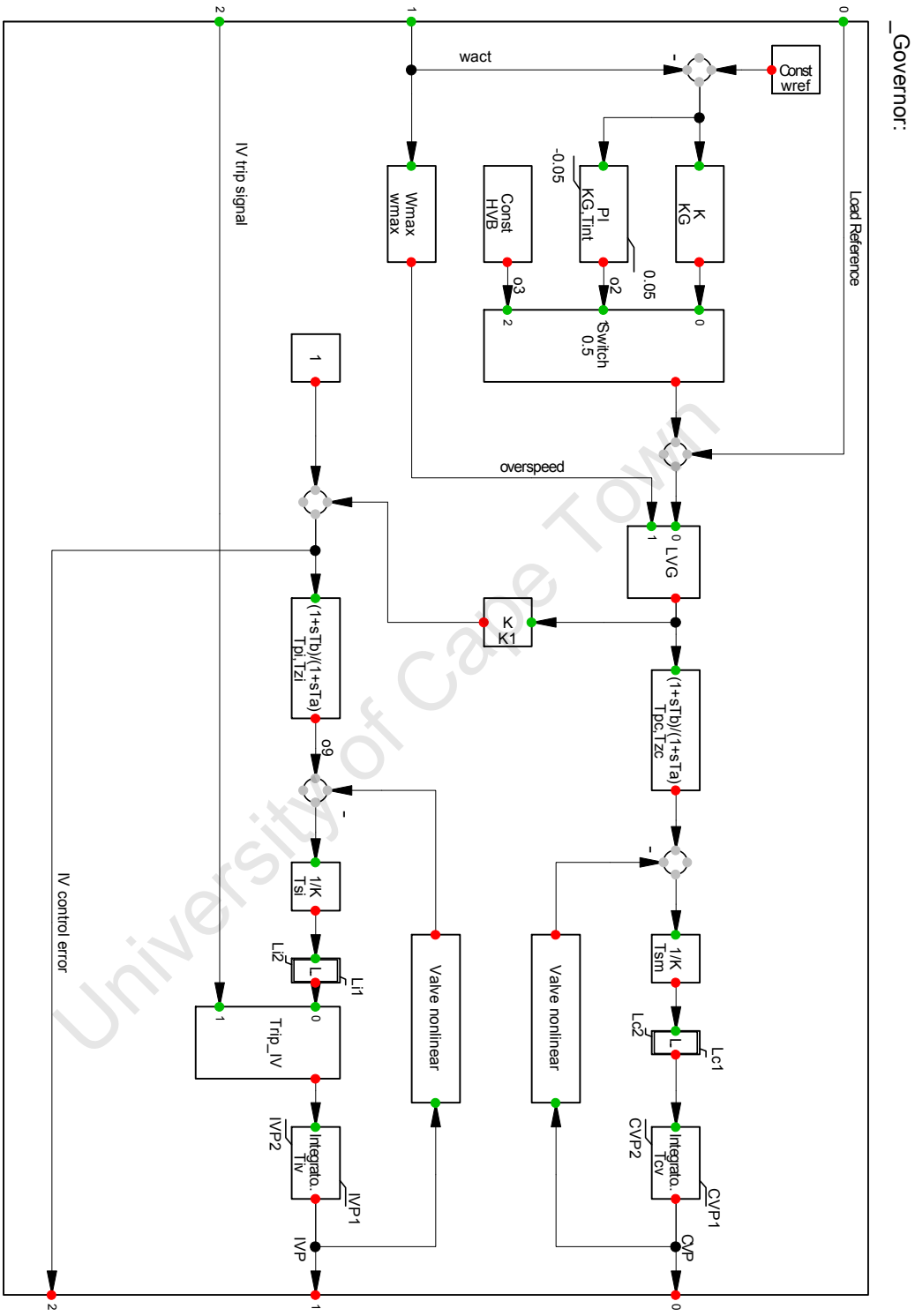

Figure D-4: Governor model implemented in DIgSILENT *PowerFactory*

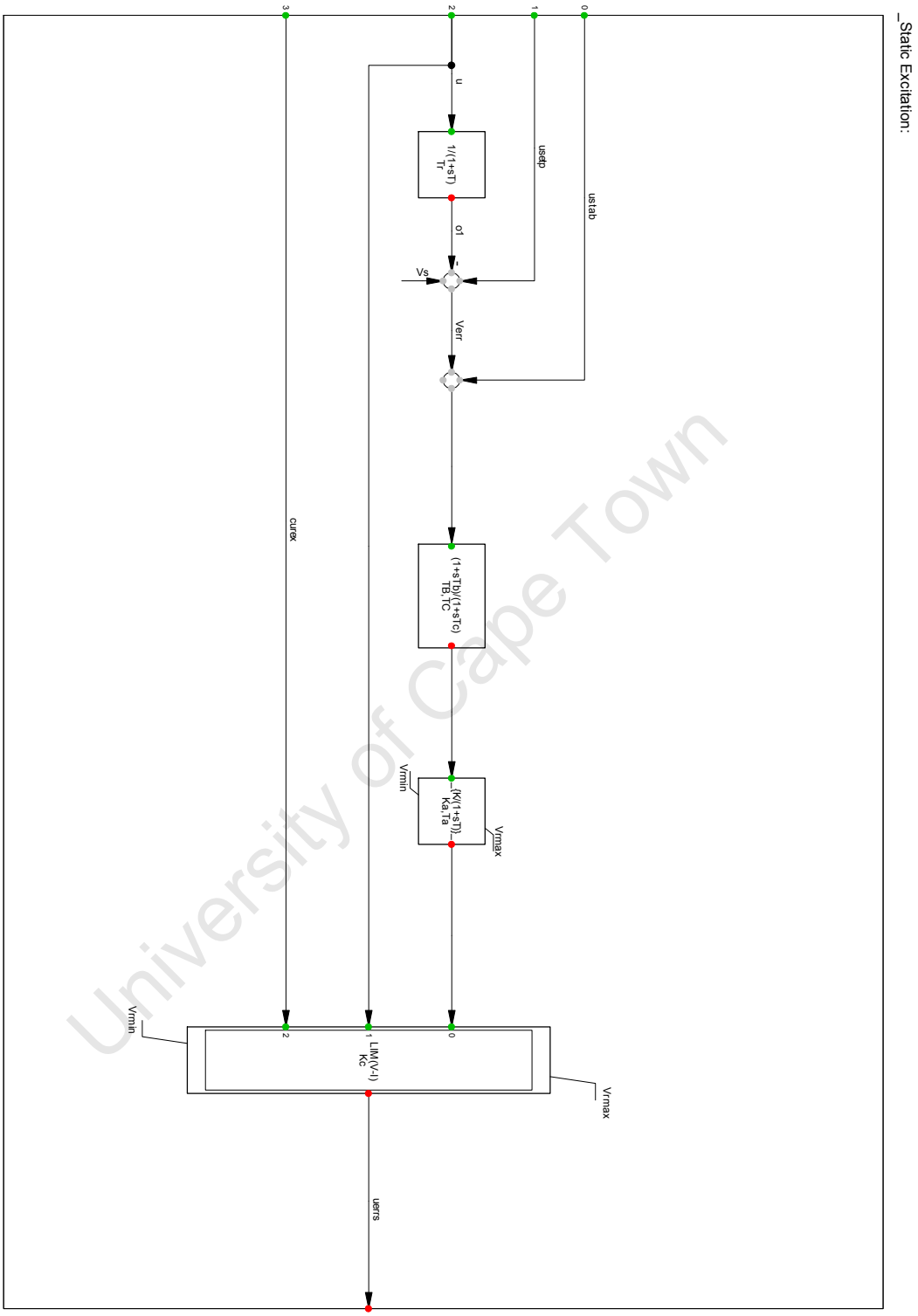

Figure D-5: Excitation system model implemented in DIgSILENT *PowerFactory*

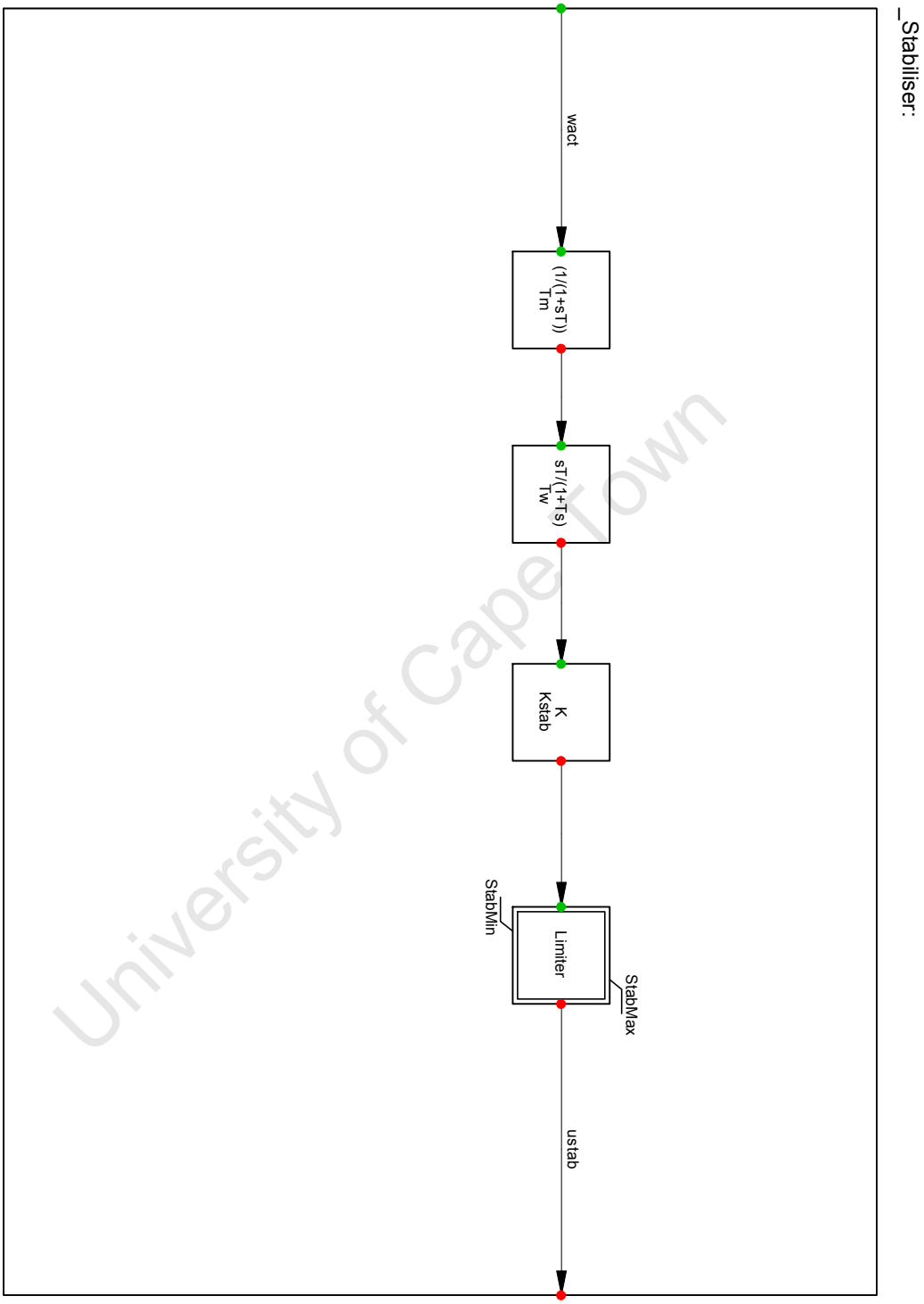

Figure D-6: Stabiliser model implemented in DIgSILENT *PowerFactory*

Appendix D Implementation of plant model in MATLAB SimPowerSystems

The model that was implemented in MATLAB SimPowerSystems is shown in Figure C-1. It is implemented in a per unit system. An overview of the model follows:

The output of the generator is connected to the SR. The inputs to the generator are field voltage Vf and mechanical power Pm.

The signal for field voltage comes from the excitation system. The gain Con converts the output of the excitation system to the per unit system of the generator- in MATLAB SimPowerSystems 1.0 p.u. field voltage is the voltage required for 1.0 p.u. generator terminal voltage on the saturation characteristic.

The stabiliser is represented by the transfer function 'Washout', the gain Ke and the output limits 'Stab lim'.

The signal representing mechanical power is obtained from the multiplication of the turbine output torque by the shaft speed, wm. The turbine model is contained in the block 'Turbine', which is shown in Figure C-2. The inputs to the turbine model are control valve position CVP, and intercept valve position IVP. These signals are obtained from the governor model shown in Figure C-3.

The turbine model includes the non-linear valve characteristics, and the dynamics of the inlet chest, reheater and cross-over piping. The total torque is sum of the contributions of the three high-pressure section, intermediate-pressure section and low-pressure section. The gain 'Per Unit' is used for the conversion from the turbine's per unit system to the generator's per unit system. In the former, 1.0 p.u. corresponds to 180 MW, but in the latter 1.0 p.u. power corresponds to 211.7 MW.

The governor model includes the control gain 'Gain', the integration time constant 'TI' and the intercept valve bias IVOB. Models of the valves and their motors are included in the governor model. These take into consideration the minimum and maximum valve positions and the limitations of the opening and closing rates.

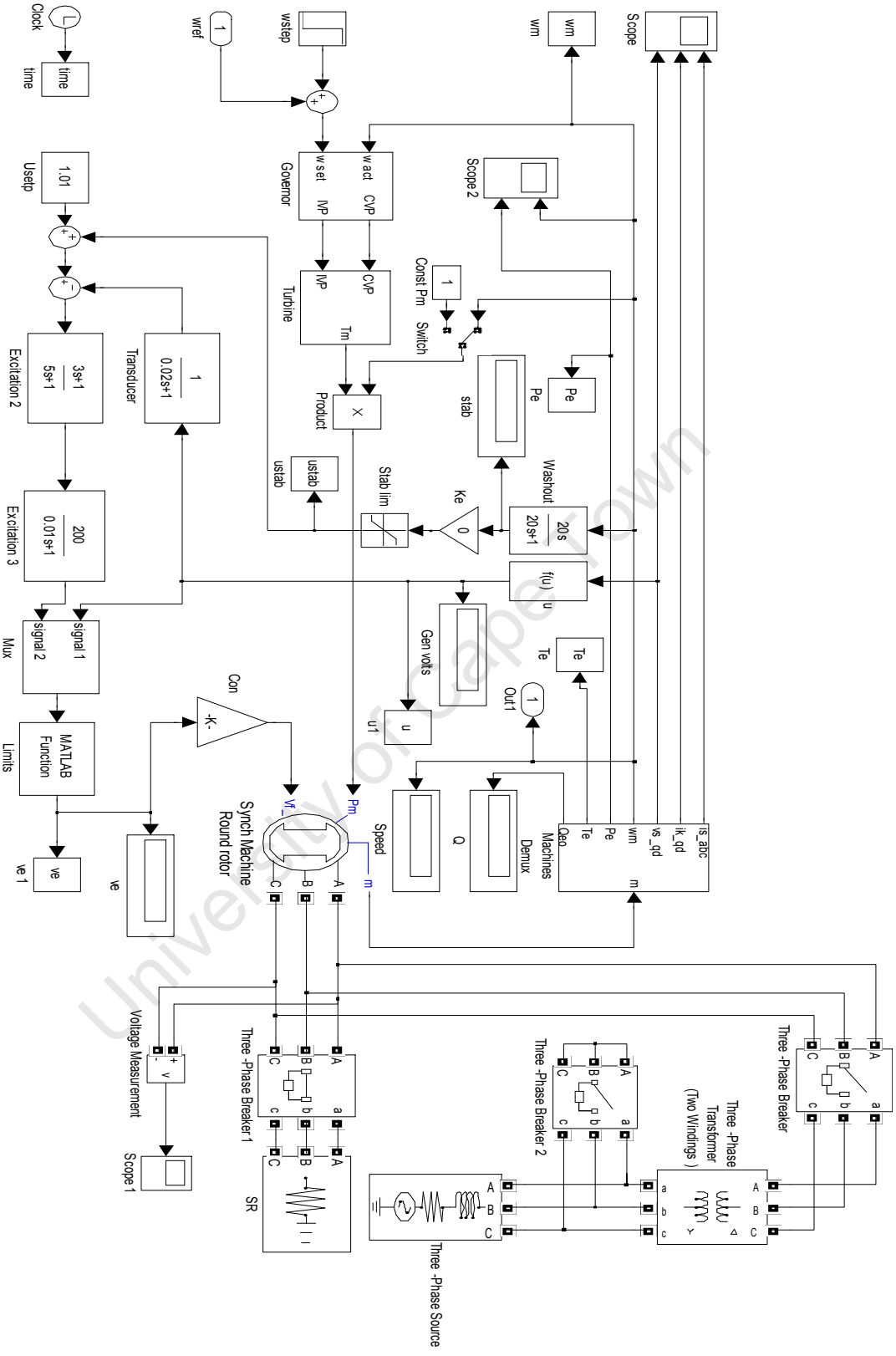

Figure C-1: Power plant model implemented in MATLAB SimPowerSystems

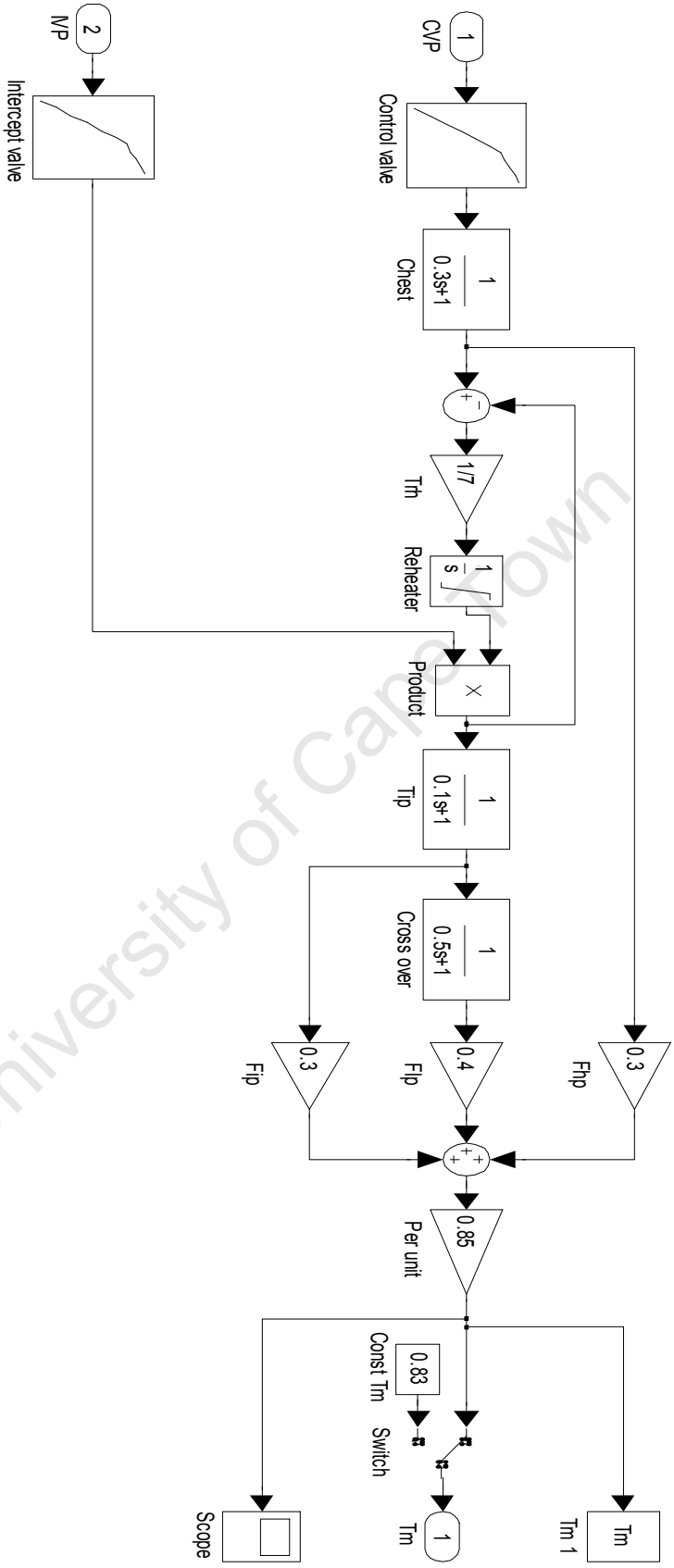

Figure C-2: Turbine model implemented MATLAB SimPowerSystems

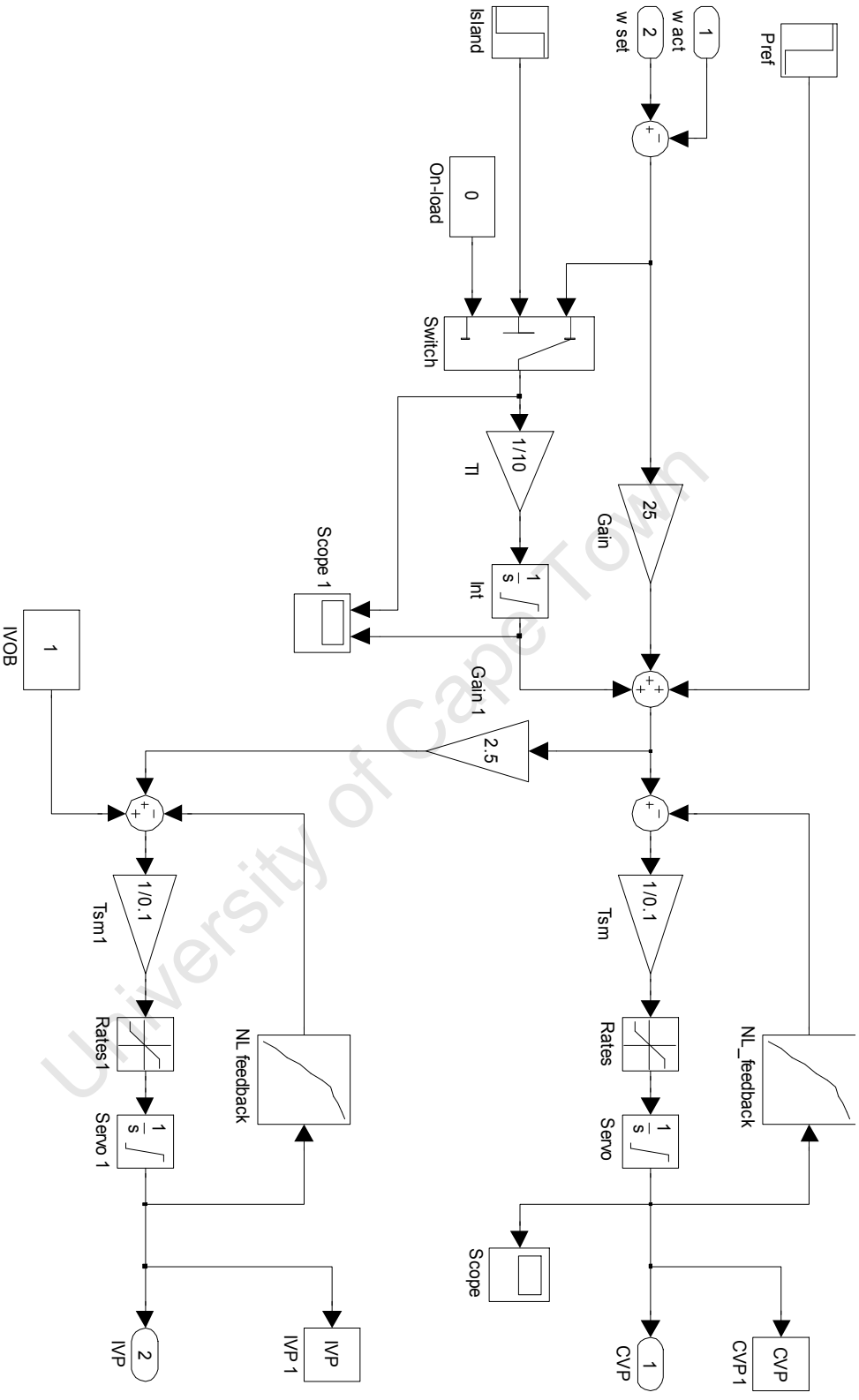

Figure C-3: Governor model implemented in MATLAB SimPowerSystems

Appendix E Annexure to Chapter 4

This appendix provides a complete list of eigenvalues of Model 2, for the case where the governor is included and the SC is excluded. Secondly, it includes a calculation of the damping from a time-domain analysis. Thirdly, it shows the response of the plant to a 2 MW change in active power.

E1: List of eigenvalues of Model 2

The following table shows the complete list of eigenvalues of Model 2. The eigenvalues apply to the analysis of islanded operation, a 175 MW SR, including the governor, bit excluding the SC (as in section 4.2.1). The table also shows the zeros of the transfer function $\Delta\omega/\Delta\omega_{ref}$.

Table E-1: Eigenvalues of Model 2 (including governor, excluding SC)

No.	Eigenvalues (s^{-1}) (Poles)	Zeros (s-1)
1,2	-0.4241 ± j0.7657	-1.661
3,4	-1.600 ± j0.6916	-0.5791
5	-5.262	-0.004
6	-109.1	-109.1
7	-100.0	-100.0
8	-50.00	-50.00
9	-20.67 ± j11.40	-20.515 ± j11.02
10	-10.00	-9.903
11	-0.3338	-0.3342
12	-0.2569	-0.2569
13	-0.2000	-0.200
14	-0.0012	

E2: Calculation of eigenvalue from time-domain analysis

The author checked whether the plant could be described by the transfer function in equation (E.1) in which τ = 1/0.1316 s. He calculated the time constant τ using four points on the curve in Figure 4-9, as explained below.

$$\frac{\Delta\omega}{\Delta T_d} = \frac{K}{s\tau - 1} \tag{E.1}$$

where

ΔT_d is a disturbance torque

K is a gain

τ is a time constant

The response of a system described by equation (E.1) to a step disturbance is given by:

$$\Delta\omega = \frac{|\Delta T_d|}{s}\frac{K}{s\tau - 1} \tag{E.2}$$

The speed response $\Delta\omega$, in the time domain, is given by the inverse Laplace transform of equation (E.2):

$$\Delta\omega = K|\Delta T_d| \cdot (1 - e^{t/\tau}) \tag{E.3}$$

If $(t_1, \Delta\omega_1)$ and $(t_2, \Delta\omega_2)$ are two points on the curve of Figure 4-9, then:

$$\frac{\Delta\omega_2}{\Delta\omega_1} = \frac{(1 - e^{t2/\tau})}{(1 - e^{t1/\tau})} \tag{E.4}$$

If the two points are chosen such that $t_2 = 2 \cdot t_1$ then equation (E.4) may be written as follows:

$$\frac{\Delta\omega_2}{\Delta\omega_1} = \frac{(1-e^{2t1/\tau})}{(1-e^{t1/\tau})} = \frac{(1-x^2)}{(1-x)} \tag{E.5}$$

where $x = e^{-t1/\tau}$.

Rearranging gives:

$$x^2 - (\Delta\omega_2 / \Delta\omega_1)\cdot x + (\Delta\omega_2 / \Delta\omega_1 - 1) = 0 \tag{E.6}$$

The above equation has the form $ax^2 + bx + c = 0$, from which x and hence the time constant τ may be calculated.

Table E- 1 shows the coordinates of the four points (two sets of points) on the curve of Figure 4-9, which the author used to calculate the damping. Both sets of points result in a τ of close to 1/0.1311 s^{-1}. Hence plant can be described by the transfer function in equation (E.1), and has a negative damping of approximately 0.133 s^{-1}.

Table E- 1: Coordinates of speed response used in calculating τ

$t1$ (s)	ω_1 (p.u.)	$t2$ (s)	ω_2 (p.u.)	$1/\tau$ (s^{-1})
1.000	1.00144	2.000	1.00309	0.1339
1.500	1.00224	3.000	1.00497	0.1328

E3: Response of plant to a 2 MW change in power

Figure E-1 shows the response of the plant, connected to a 175 MW SR, to a 2 MW increase in active power. In the case where the SC is excluded there is a period in which the control valves temporarily reach their maximum position. In this period the governor does not counteract the increasing electromagnetic torque effectively. The inclusion of the SC increases the damping significantly.

Figure E-2 shows the response of the plant, connected to a 175 MW SR, to a 2 MW increase in active power. In this case there is no saturation of the control valve. The SC increases the damping.

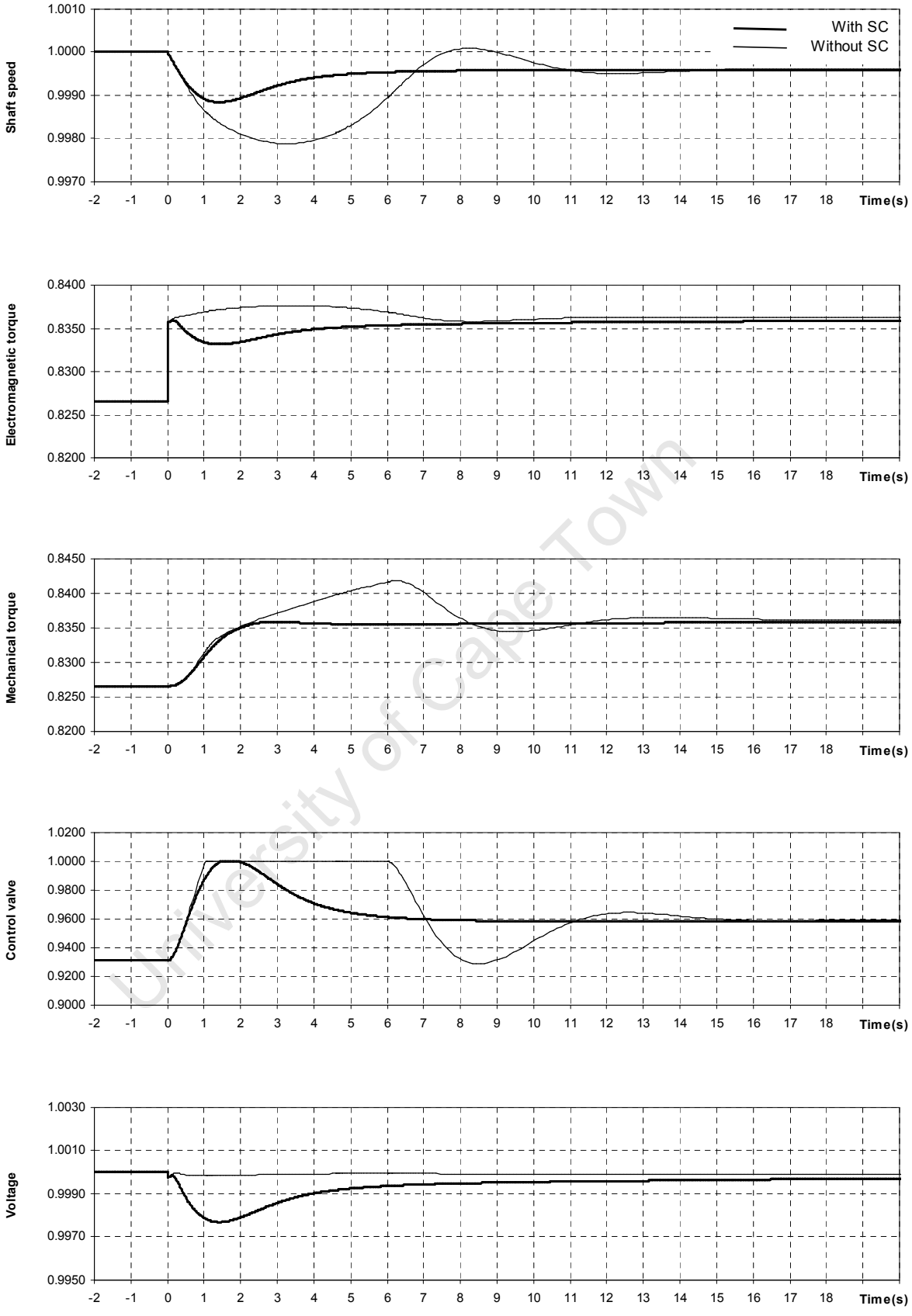

Figure E-1: Response of islanded plant to 2 MW increase in power (175 MW SR)

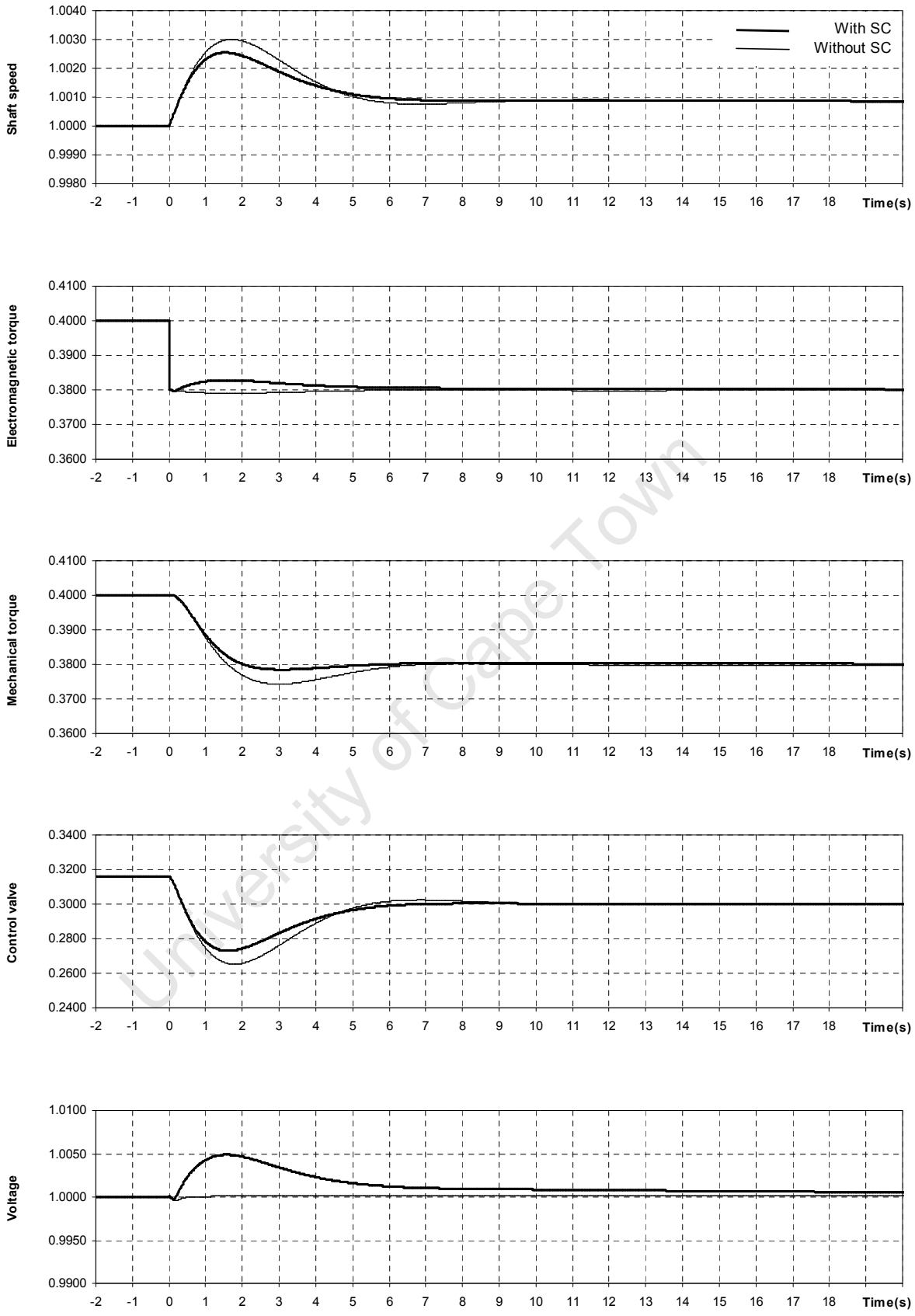

Figure E-2: Response of islanded plant to 2 MW increase in power (85 MW SR)

Appendix F Annexure to Chapter 5

Section 5.3 discusses the influence of the plant's stability of the turbine type, damper windings, reactive power prior to islanding, valve speed and valve choking. It refers to the following figures, which shows the response of the plant to the following events:

-A short-circuit on the high-voltage side of the transformer at time 0.00 s.

-The opening of the main breaker at the time 0.12 s.

-The closing of the SR breaker at the time 0.20 s.

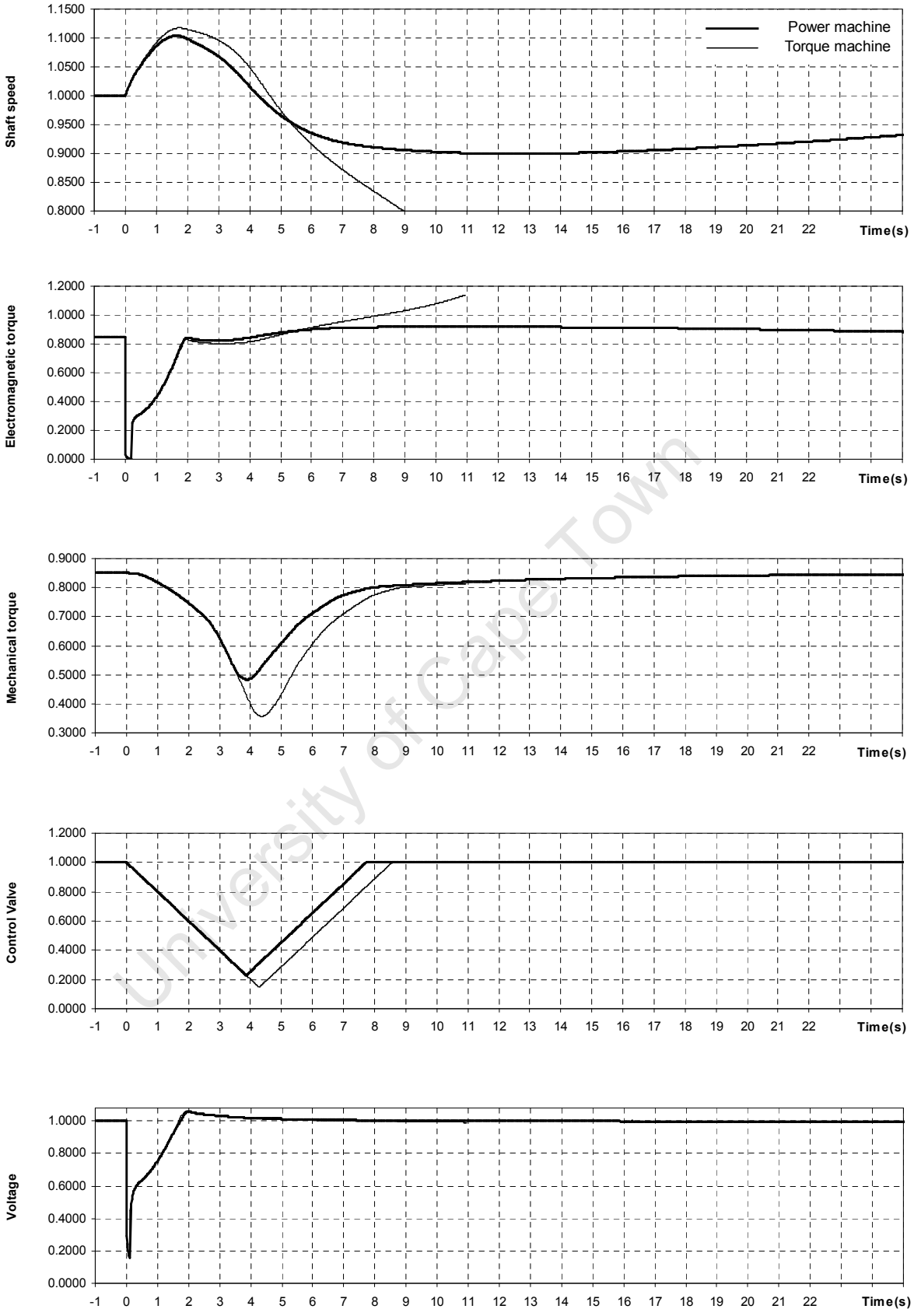

Figure F-1: Plant response after islanding, and effect of turbine type (175 MW SR, excluding SC)

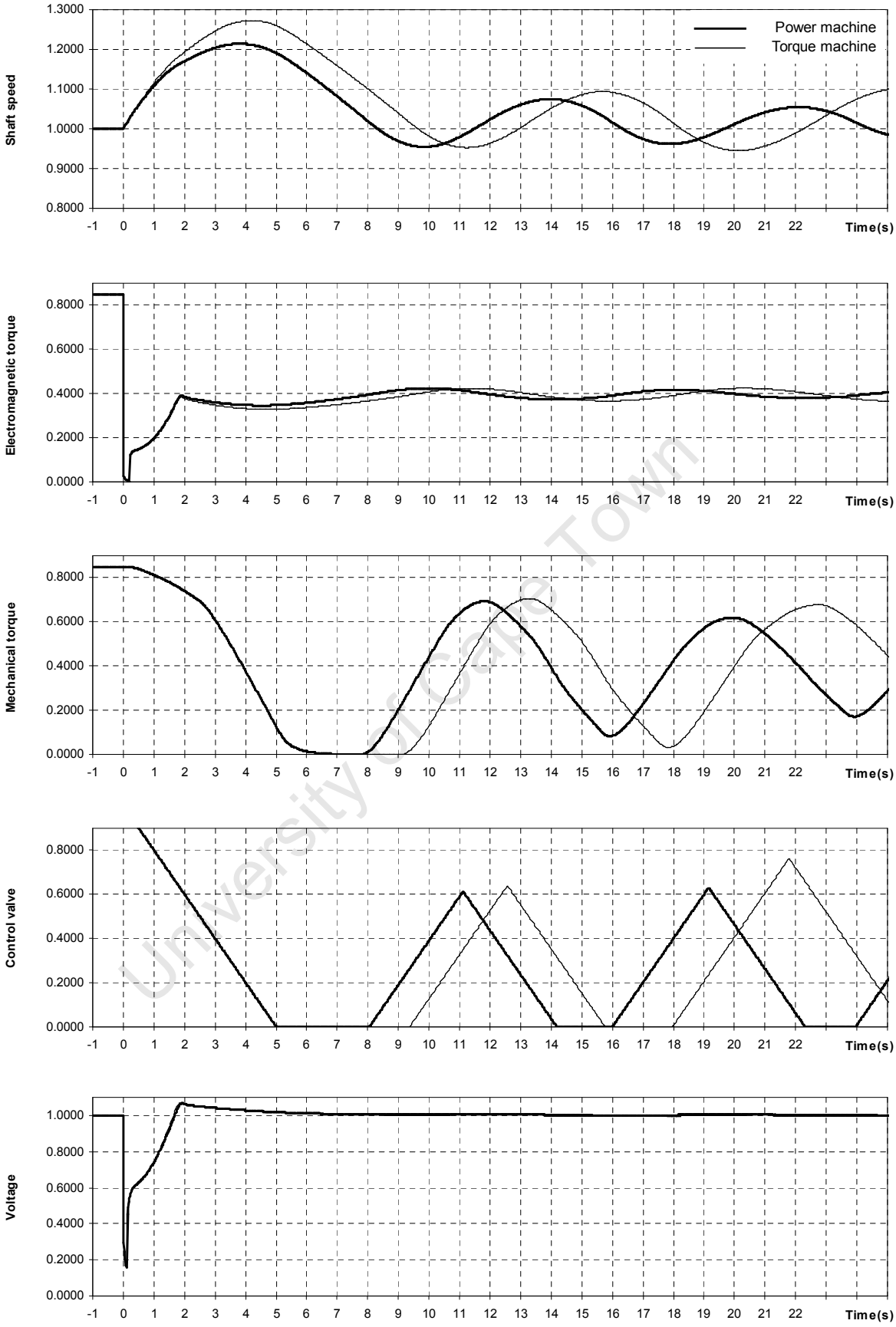

Figure F-2: Plant response after islanding, and effect of turbine type (85 MW SR, excluding SC)

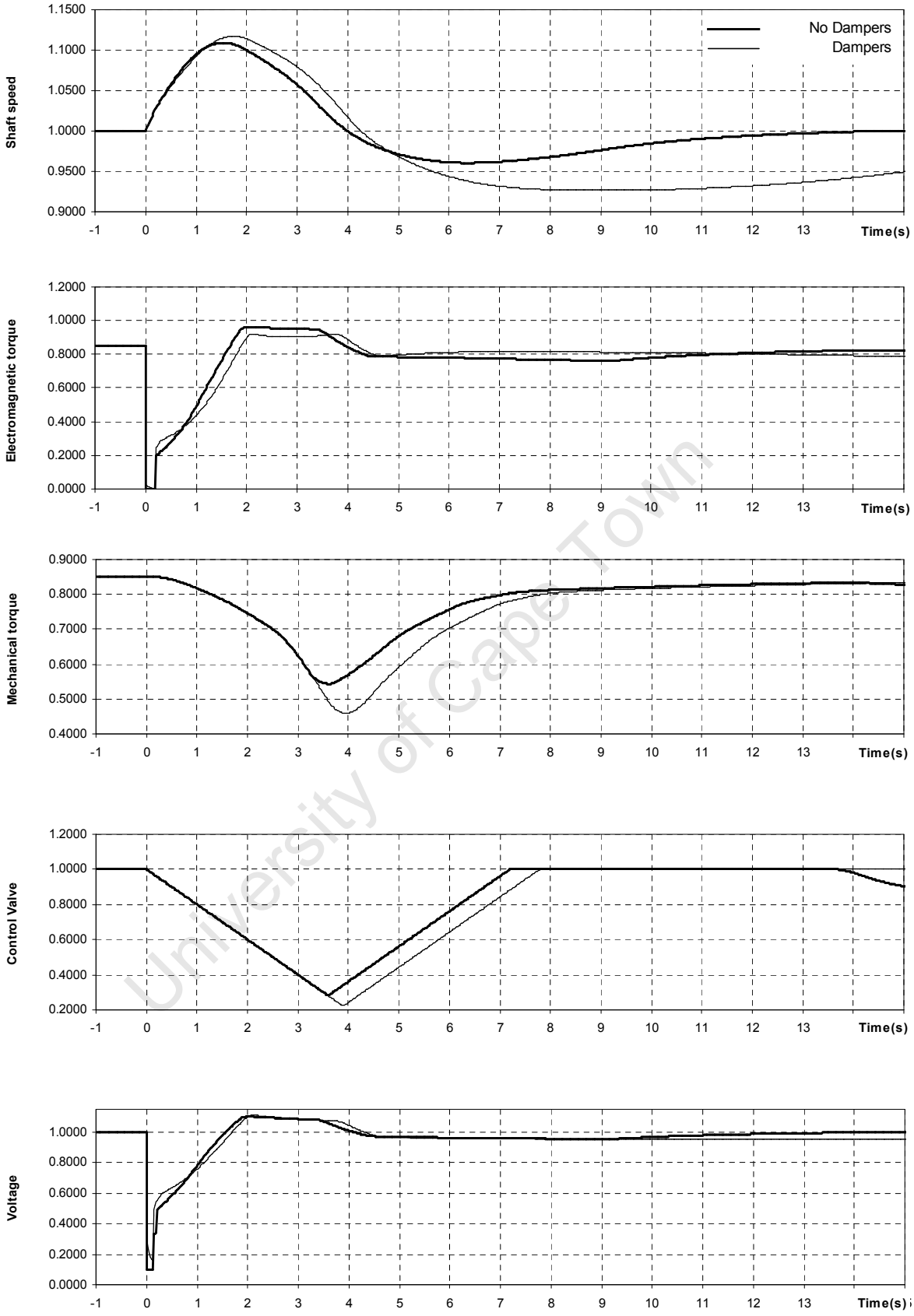

Figure F-3: Plant response after islanding, and effect of damper windings (including 175 MW SR and SC)

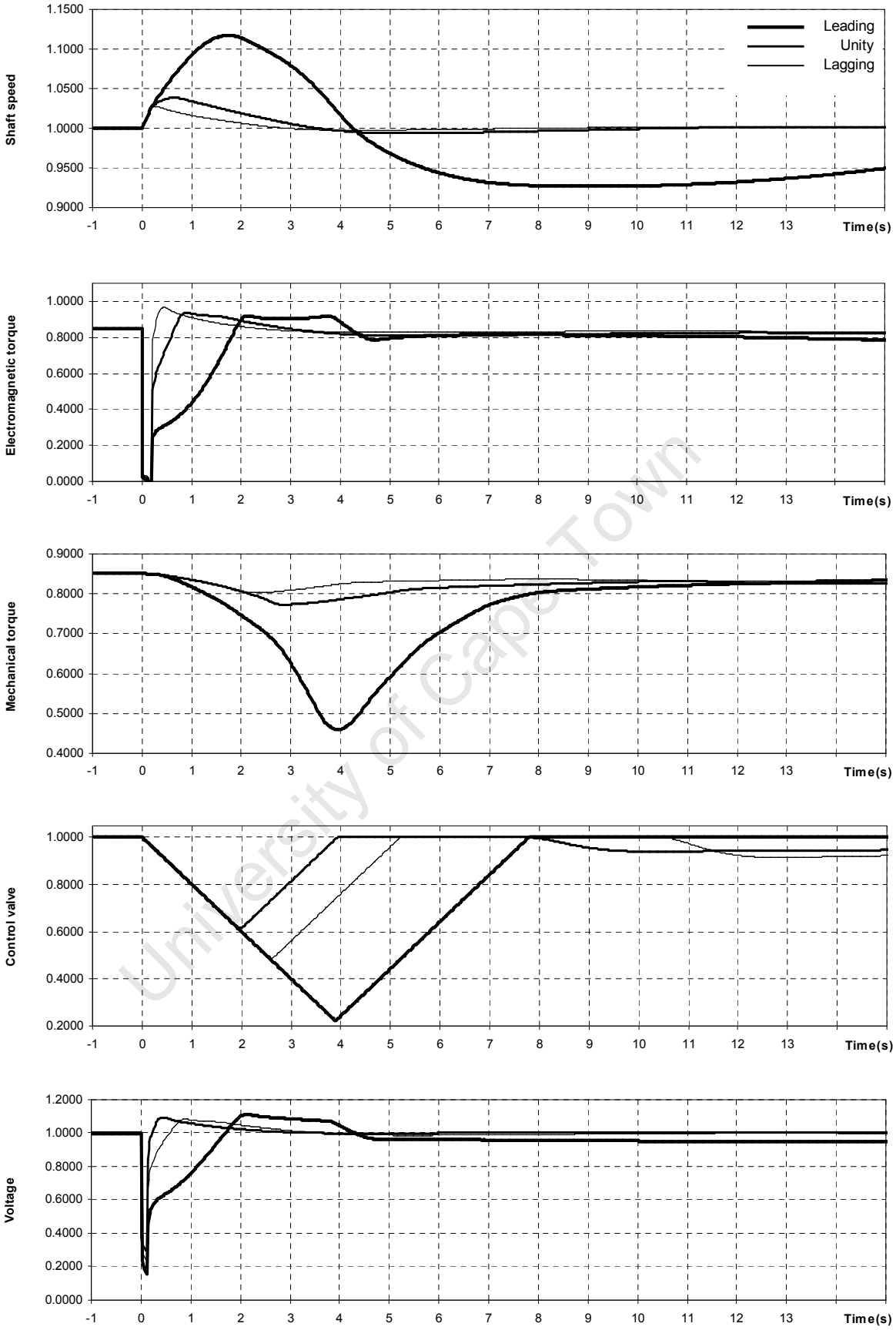

Figure F-4: Plant response after islanding, and effect of reactive power (including 175 MW SR and SC)

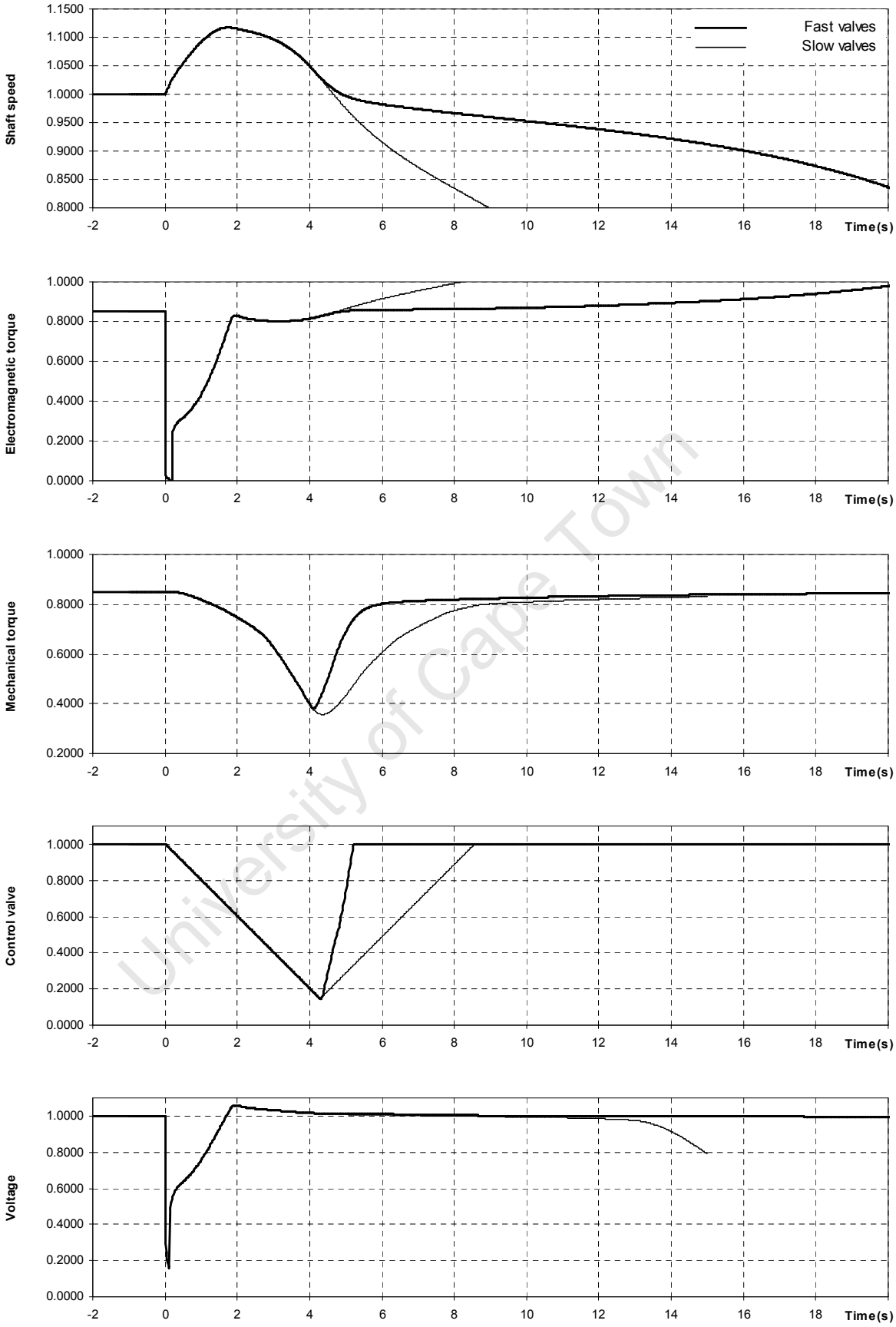

Figure F-5: Plant response after islanding (175 MW SR, no SC, fast valves)

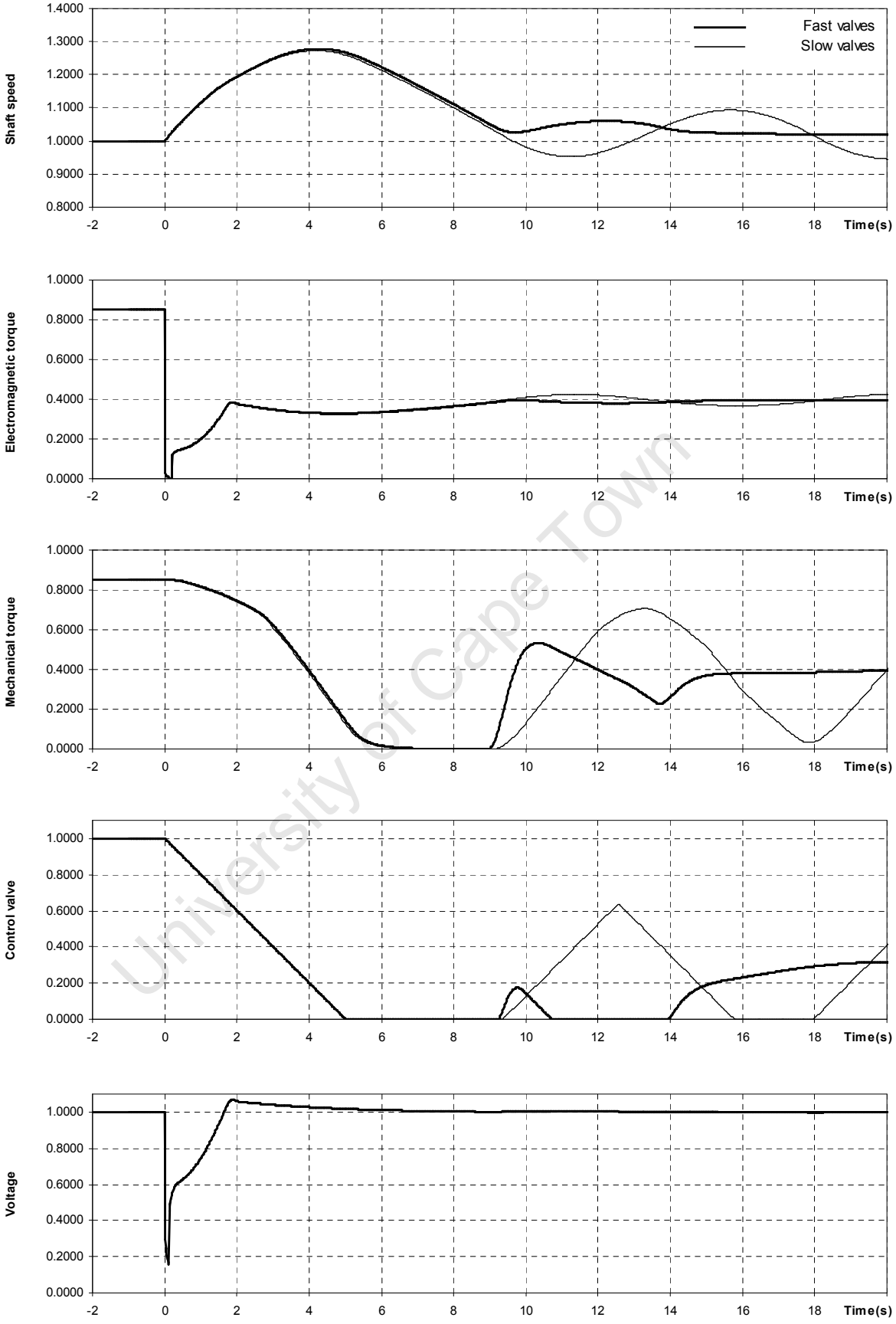

Figure F-6: Plant response after islanding (85 MW SR, no SC, fast valves)

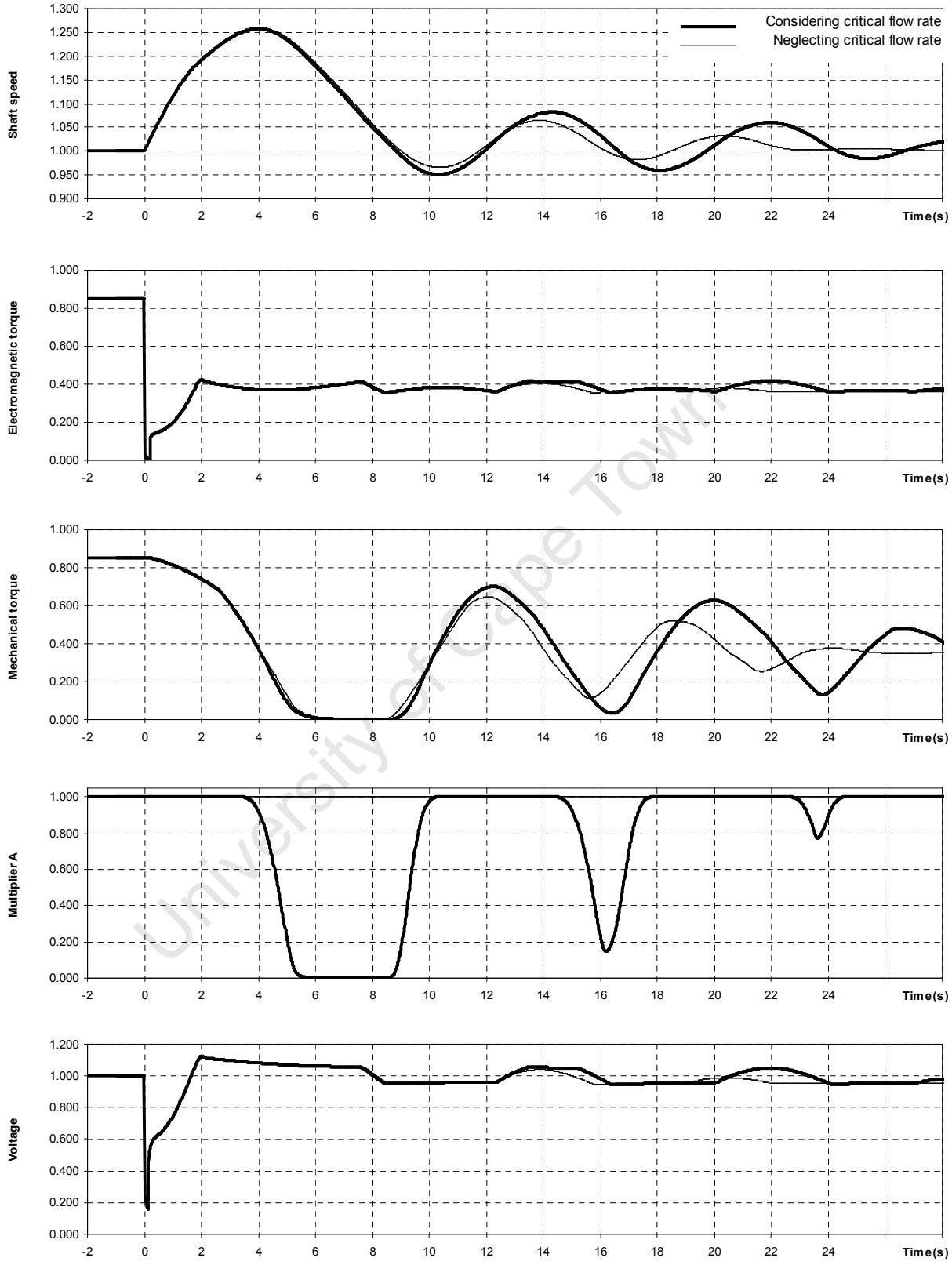

Figure F-7: Plant response after islanding (85 MW SR, SC, considering valve critical flow rate)